THE JOURNAL
OF
CHEMICAL PHYSICS

VOLUME 9 JUNE, 1941 NUMBER 6

# An X-Ray Study of Liquid Benzene, Cyclohexane and Their Mixtures

PAUL H. BELL AND WHEELER P. DAVEY
*The Pennsylvania State College, State College, Pennsylvania*

(Received August 6, 1940)

X-ray (Mo *K* alpha) studies were made of pure benzene, pure cyclohexane, and their mixtures, using a Geiger-Mueller counter with balanced filters. The benzene showed at 25°C a rather sharp intense peak at the customary 8°40′ and a new broader peak of about one-eighth intensity at 4°20′. The cyclohexane showed a similar pair of peaks at 8°0′ and 4°0′. The mixtures all showed a broad peak of low intensity reaching from 4°0′ to 4°20′ and three sharp peaks at 8°0′, 8°20′, and 8°40′ superimposed on a broad peak which reached from about 8°0′ to about 8°40′. The positions of the three sharp peaks were not affected by the proportions of the two components, and their relative intensities were independent of amount of stirring. The customary shift with temperature was observed on all peaks. The results are consistent with a cybotatic type of picture. Benzene is pictured as having short-lived highly organized groups of *-B-B-B-B-* floating in a chaotic sea of disorganized benzene molecules. The peak at 8°40′ is thought to be due to the presence of vibrating groups whose extreme positions simulate groups of *-B—B-B—B-B—B-* and *—B-B—B-B—B-B—*. Cyclohexane would contain similar groups of *-C-C-C-C-*. The mixtures are assumed to contain *-B-B-B-B-*, *-C-C-C-C-*, and *-B-C-B-C-*. The presence of any considerable amount of more complicated groupings is obviously highly improbable.

## INTRODUCTION

THE structure of liquids has been studied by many methods, including that of x-ray diffraction,[1,2] but their structure is not yet well understood. It is the purpose of this paper to give the results of an x-ray study of the mutual solutions of benzene and cyclohexane. These results, differing from those so far reported in the literature,[3–8] lead to a better understanding of the physical state of liquid structure. All authors, with the exception of H. K. Ward, seem to have obtained only one peak in their diffraction curves from liquid solutions. Ward,[8] working with benzene-cyclohexane solutions, obtained two peaks corresponding to those given by pure benzene and pure cyclohexane. Murray and Warren[6] repeated Ward's work and were unable to obtain two peaks. Since the experimental results conflicted with each other and with the thermodynamic data of Scatchard, Wood and Mochel,[9] a new x-ray investigation was made on the same system with an entirely different type of x-ray diffraction apparatus. The new data showed not one or two peaks, but four. Since the data were definitely reproducible, they seemed to warrant further study.

[1] G. W. Stewart, Chem. Rev. **6**, 483 (1929).
[2] G. W. Stewart, Rev. Mod. Phys. **2**, 116 (1930). For reviews of papers and theories see (a) J. T. Randall, *The Diffraction of X-rays and Electrons by Amorphous Solids, Liquids and Gases* (John Wiley and Sons, Inc., New York, 1934); (b) C. Drucker, Physik. Zeits. **29**, 273 (1928).
[3] P. Krishnamurti, Ind. J. Phys. **3**, 331 (1929); **3**, 507 (1929).
[4] A. W. Meyer, Phys. Rev. **38**, 1083 (1931).
[5] R. W. G. Wyckoff, Am. J. Sci. **5**, 455 (1923).
[6] G. E. Murray and B. E. Warren, J. Chem. Phys. **7**, 141 (1939).
[7] S. Parthasarathy, Phil. Mag. **18**, 90–7 (1934).
[8] H. K. Ward, J. Chem. Phys. **2**, 153 (1934.)
[9] G. Scatchard, S. E. Wood and J. M. Mochel, J. Phys. Chem. **43**, 119–130 (1939).

In the present work a Geiger-Mueller counter method was used with compensating filters. This method appears to be much more sensitive than the photographic method and less cumbersome than the ionization-chamber method.

## Apparatus

### A. X-ray radiation

A (G.E. X-Ray Corp.) molybdenum anode, Coolidge type tube was operated at 42 kilovolts (r.m.s.) and a tube current of 30 milliamperes. The voltage and tube current were maintained to within ±1.5 percent by use of voltage regulators on the transformer primary circuits (Raytheon Manufacturing Company).

To obtain a monochromatic beam of high intensity, the method of balanced filters was used.[10,11] A filter of filter paper saturated with $Sr(NO_3)_2$ was made such that its x-ray transmission was equal to a $ZrO_2$ filter (Patterson Screen Company) for all wave-lengths except the $K\alpha$ doublet of the tube. This was carefully balanced and checked over the entire x-ray spectrum using the (100) plane of NaCl.

### B. Spectrometer and slit system

A Spencer spectrometer (No. 818), on which angles could be read to one minute of arc, was mounted in a rigid frame in such a way that the movable arm moved in a vertical plane. Soller slits[12] were substituted for the slits and telescope. The slits for the collimator and Geiger-Mueller counter consisted of 6 parallel slits 20 cm long, 0.075 cm wide, by 1.0 cm high. The lead foil between slits was 0.0075 cm in thickness, the spreaders 0.075 cm.

The geometry of the incident beam was such that only three of the six collimating slits could be used. The thickness of liquid used in the specimen holder was such that all six of the slits could be used on the swinging spectrometer arm.

### C. Sample-holder and temperature control

To eliminate the possibility of any contamination the sample-holder was constructed entirely of glass. (See Fig. 1.) The cell windows were of Pyrex glass approximately 0.007 cm in thickness. The thickness of the liquid in the cell was 1.7 cm. This was large enough to insure a high intensity of diffracted beam. It was slightly less than the optimum thickness given by

$$t = 1/\mu,$$

where $t$ is the thickness and $\mu$ is the linear coefficient of absorption.

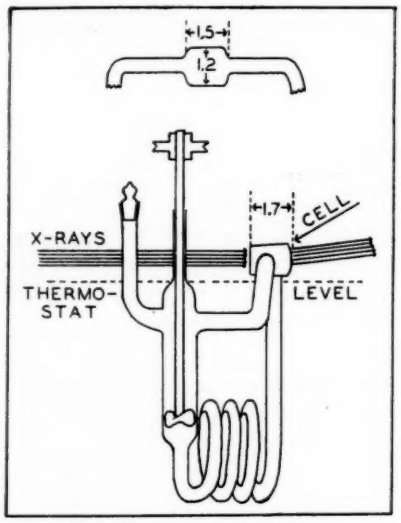


Fig. 1. Sample-holder.

The liquid under investigation was brought up to temperature, (±0.5°C), in a glass coil immersed in a thermostat. The liquid was circulated through the coil and the cell, by means of a Pyrex paddle, at a linear speed of approximately 3 cm per second. The temperature difference between the cell and the thermostat was therefore negligible. Temperatures between 5°C and 10°C were obtained by circulating ice water through a cooling coil immersed in the thermostat. For a temperature of −21°C a dry ice-acetone mixture was syphoned through the cooling coil, and a eutectic mixture of NaCl and water was used in the bath.

### D. Counting circuit

The Geiger-Mueller counter was argon-oxygen-filled. The cathode had a sufficiently large opening to allow all x-rays coming from the slits to enter the counter. The voltage supply was

[10] P. A. Ross, Phys. Rev. **28**, 425A (1926).
[11] W. C. Pierce, Phys. Rev. **38**, 1409 (1931).
[12] W. Soller, Phys. Rev. **24**, 158 (1924).

maintained at 850 volts by a voltage regulator of the Street and Johnson type.[13]

The amplifier circuit consisted of three stages of voltage amplification, using a 57 and finally two 56 tubes. The amplified pulse was fed into a modified Pickering[14] recording circuit, using a single 885 thyratron tube. The final counts were recorded by a Cenco counter in the plate circuit of the thyratron tube. With this circuit it was found necessary to shield the first stage of amplification. The time constants for the circuit were sufficiently small to allow the 60 cycle of the incident beam to be recorded. A small loudspeaker was also built in the circuit, powered by a 45 tube, so that the quality of sound from the speaker gave an indication of the proper operation of the G-M counter and of its circuit.

## Materials

The benzene was Baker's "C.P. Thiophene Free" with the following physical constants: B.P. 80°C; M.P.+5.5°C; index of refraction 1.5009 at 20°C.

The cyclohexane was obtained from Rohm and Haas Co. It was purified by a method somewhat similar to that used by other workers.[8,9] The material as received was shaken for 12 hr. with fuming $H_2SO_4$ (25 percent $SO_3$), washed with water, shaken with alkaline $KMnO_4$ and finally shaken with water again. It was then dried over metallic sodium and finally distilled at a high reflux ratio in a 15-plate column. Further purifications were carried out by fractional recrystallizations. The physical constants of the final material were: B.P. 80.5°C; M.P.+6.4°C; and index of refraction 1.4263 at 20°C.

The solutions, to be examined by diffraction methods, were prepared on a weight basis. They had weight compositions of (1) 74.5 percent benzene-25.5 percent cyclohexane; (2) 51.4 percent benzene-48.6 percent cyclohexane; (3) 25.4 percent benzene-74.6 percent cyclohexane. These corresponded to mole fraction compositions of (1) 0.76 benzene-0.24 cyclohexane; (2) 0.53 benzene-0.47 cyclohexane; (3) 0.27 benzene-0.73 cyclohexane. The exact percentages had no special significance, but were those obtained after measuring the approximate amounts by volume. The index of refraction was measured before and after each run and was found to be the same within 0.0001. This indicated that the composition did not change during the course of the experiments.

[13] J. C. Street and T. H. Johnson, J. Frank. Inst. **214**, 155 (1932).
[14] W. H. Pickering, Rev. Sci. Inst. **9**, 180 (1938).

## Experimental Procedure

To be certain that the apparatus was in a condition to operate uniformly over a long period, it was in every case allowed to warm up for one hour before making any measurements. The temperature of the G-M tube was always kept within one or two degrees of 25°C since these tubes have a marked decrease in efficiency with rising temperature.

The data reported are for the $K\alpha$ doublet lines of molybdenum, 0.710A. This was obtained by subtracting the "strontium filter" reading from the "zirconium filter" reading, the difference being the $K\alpha$ contribution to the diffracted beam intensity. The background correction due to cosmic rays need not be subtracted because its average intensity was eliminated by the two filter readings.

A blank run with the empty sample-holder gave a very small diffraction scattering with no peaks in the region used in this work. The counting rates were never higher than 300 per min., so that it was possible to detect failure of the mechanical counter by an audible method. The loudspeaker volume was adjusted so that it was not audible to the operator when the counter was operating. Any skipping of the counter made it possible to hear the loudspeaker pulse and thus to detect the failure of the counter.

The $ZrO_2$ and $Sr(NO_3)_2$ filters were changed after each minute interval, and all readings were thrown out for which any counter failure was detected.

Statistics of Geiger-Mueller counters have been developed by several authors.[15–17] Hughes[17] points out that

$$(n-x)_{Av}^2 = x,$$

[15] A. E. Ruark and F. E. Brammer, Phys. Rev. **52**, 322 (1937).
[16] L. Alaoglu and N. M. Smith, Jr., Phys. Rev. **53**, 832 (1938).
[17] A. L. Hughes, Am. Phys. T. **7**, 271–292 (1939).

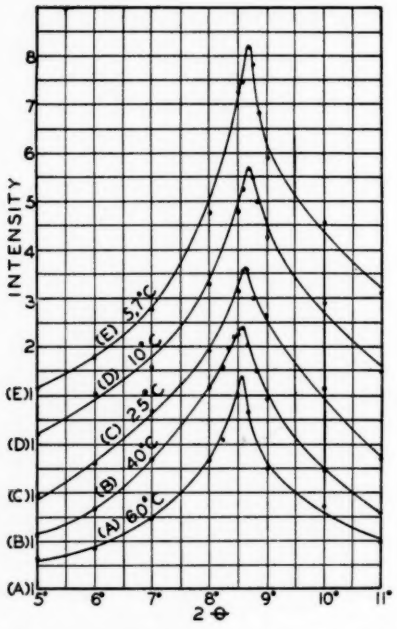


FIG. 2. X-ray diffraction curves; 100 percent benzene.

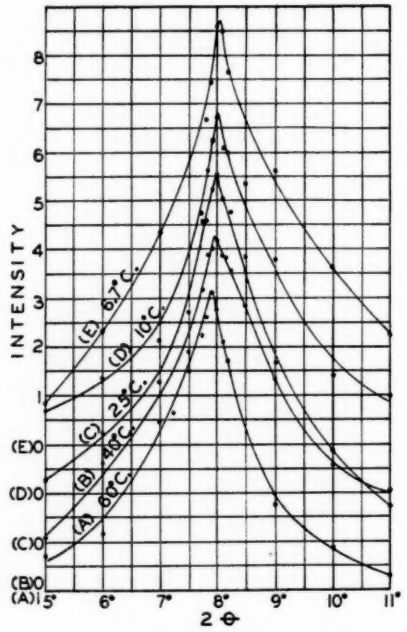


FIG. 3. X-ray diffraction curves; 100 percent cyclohexane.

where $n$ is the number of counts in a given time interval and $x$ the average number arriving in that time interval. The mean deviation is therefore equal to the square root of the counts recorded. Sufficient counts were taken to insure a valid graph over the range studied. In the region between 8°00′ and 8°40′ enough counts were made so that the differences between counts of the peaks and of the adjacent minima between the peaks were always greater than twice the mean deviation.

The shapes of the curves and peak positions were determined for each liquid sample at 40°C, 25°C, and in the case of pure benzene, pure cyclohexane and the 51.4-percent benzene mixture, additional curves were taken at 60°C, 10°C and as close as possible to the melting points. The melting points are +5.5°C, +6.4°C, and −22°C,[18] respectively.

The shapes of the curves were reproducible but the relative intensities varied from week to week. This was probably due to long time changes in the characteristics of the counter circuit. In order to put all curves on a common intensity scale, the following method was used: (1) Data on all the peaks of all the liquid samples studied were taken at each of the constant temperatures mentioned above, using a separate day for each temperature. (2) Measurements of the peaks of the 51.4-percent benzene mixture (M.P. −22°C) at −21°C, 10°C, 25°C, 40°C and 60°C, were made on the same day. (3) The data from (2) were used to correct the measurements of (1) so that the final results shown in Figs. 2–5, were what might have been expected if all the data could have been obtained on a single day.

[18] *Int. Crit. Tab.*, Vol. IV, p. 133.

## EXPERIMENTAL RESULTS

Diffraction curves for the pure liquids and mixtures at various temperatures are shown in Figs. 2–5. One unit on the intensity scale represents one hundred counts per five minutes. $2\theta$ is the angle of deviation from the incident beam made by the diffracted x-rays.

The range of $2\theta$ studied was from 2°00′ to 11°00′. This is not entirely reproduced in the curves shown, because of the size of graphs necessary. In all cases a small intensity peak was observed at a low angle of diffraction. The exact position of this peak was carefully checked in several cases. In the case of pure benzene and cyclohexane it was found, within the

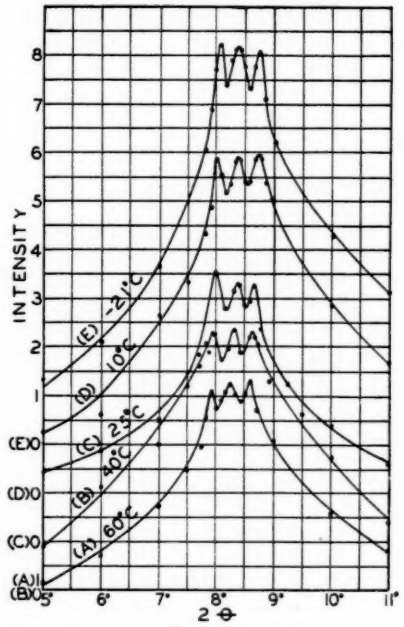


FIG. 4. X-ray diffraction curves; 51.4 percent benzene solution.

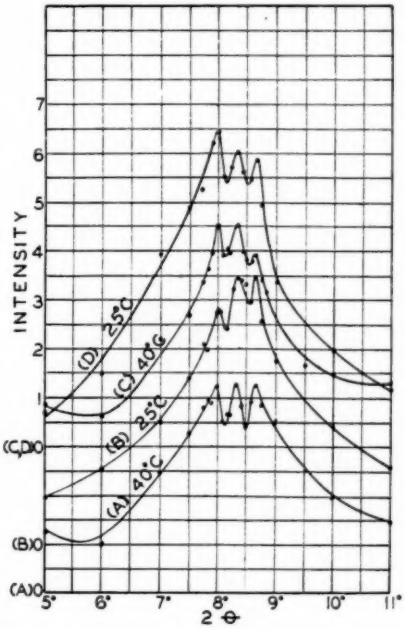


FIG. 5. X-ray diffraction curves; 74.5 percent benzene, 74.6 percent cyclohexane solutions.

accuracy of measurement, to be at one-half the angle of the high intensity peak (for small angles $\sin\theta=\theta$). For the mixtures no sharp peak was obtainable but a diffuse peak was found between $2\theta=40°00$ and $2\theta=4°20$. The intensities of these peaks were approximately one-eighth of the high intensity peaks.

The lowest temperature curves in the cases of Figs. 2–4 were taken to determine whether the liquid structure might change at a temperature just above the melting point.

## INTERPRETATION OF EXPERIMENTAL RESULTS

Several theories have been proposed to explain x-ray diffraction in liquids. The more important of these are those due to: Raman and Ramanathan,[19] Zernike and Prins,[20–22] Debye[23] and Stewart.[2] The approach of the first three is definitely mathematical in character, while that of Stewart is a nonmathematical picture of the state of the liquid. Raman and Ramanathan's function was able to predict only one peak in the diffraction curve and its exact position had to be obtained experimentally. Zernike and Prins used a distribution function evaluated in an empirical way. Debye used the experimental data to determine the distribution function.

These methods were applicable in the case of molecules having spherical symmetry, and many liquids have been worked out on the basis of the theories of Prins and Debye. The application of these theories to unsymmetrical molecules such as benzene or cyclohexane has not been so successful. Several distribution functions have been used for benzene.[24–27] All of these functions gave fair checks at high diffraction angles, but not at angles less than the principal peak. It seems that one must resort to the method of Stewart to explain the experimental facts in the cases of solutions.

It is well accepted that a liquid approximates a crystalline powder in the sense that the diffraction peak positions must be close to those given by Bragg's formula

$$n\lambda=2d\sin\theta. \qquad (1)$$

[19] C. V. Raman and K. R. Ramanathan, Proc. Ind. Assn. for Cultivation of Science, p. 127 (1923).
[20] F. Zernike and J. A. Prins, Zeits. f. Physik **41**, 184 (1927).
[21] J. A. Prins, Zeits. f. Physik **56**, 617 (1929).
[22] J. A. Prins, Naturwiss. **19**, 435 (1931).
[23] P. Debye, Physik. Zeits. **31**, 348 (1930).
[24] S. Katzoff, J. Chem. Phys. **2**, 841 (1934).
[25] L. Bewilogua, Physik. Zeits. **33**, 688–692 (1932).
[26] Gustav Thomer, Physik. Zeits. **38**, 48–57 (1937).
[27] C. M. Sogani, Ind. J. Phys. **1**, 357 (1927).

TABLE I. *Peak positions.*

| COMPOSITION | TEMPERATURE | $-C-C-C-$ $2\theta$ | $d$ | $-B-B-B-$ $2\theta$ | $d$ | $-B-C-B-C-$ $2\theta$ | $d$ |
|---|---|---|---|---|---|---|---|
| 100% $C_6H_{12}$ | 6.7°C | 8°03′ | 5.06A | | | | |
| " " | 10°C | 8°02′ | 5.07 | | | | |
| " " | 25°C | 8°00′ | 5.09 | | | | |
| " " | 40°C | 7°58′ | 5.11 | | | | |
| " " | 60°C | 7°55′ | 5.14 | | | | |
| 100% $C_6H_6$ | 5.7°C | | | 8°42′ | 4.68A | | |
| " " | 10°C | | | 8°41′ | 4.69 | | |
| " " | 25°C | | | 8°40′ | 4.70 | | |
| " " | 40°C | | | 8°38′ | 4.72 | | |
| " " | 60°C | | | 8°35′ | 4.74 | | |
| 51.4% $C_6H_6$ | −21°C | 8°04′ | 5.05A | 8°43′ | 4.67 | 8°24′ | 4.85A |
| " " | 10°C | 8°02′ | 5.07 | 8°42′ | 4.68 | 8°22′ | 4.87 |
| " " | 25°C | 8°00′ | 5.09 | 8°40′ | 4.70 | 8°20′ | 4.88 |
| " " | 40°C | 7°58′ | 5.11 | 8°38′ | 4.72 | 8 18′ | 4.90 |
| " " | 60°C | 7°56′ | 5.13 | 8°36′ | 4.73 | 8°15′ | 4.93 |
| 74.5% $C_6H_6$ | 25°C | 8°00′ | 5.09 | 8°40′ | 4.70 | 8°20′ | 4.88 |
| " " | 40°C | 7°58′ | 5.11 | 8°39′ | 4.71 | 8°19′ | 4.89 |
| 74.6% $C_6H_{12}$ | 25°C | 8°00′ | 5.09 | 8°40′ | 4.70 | 8°20′ | 4.88 |
| " " | 40°C | 7°59′ | 5.10 | 8°38′ | 4.72 | 8°18′ | 4.90 |
| 62.4% $C_6H_6$ | 25°C | 8°00′ | 5.09 | 8°40′ | 4.70 | 8°21′ | 4.88 |
| 62.8% $C_6H_{12}$ | 25°C | 8°00′ | 5.09 | 8°40′ | 4.70 | 8°19′ | 4.89 |

Applying this formula (1) to the data of Figs. 2 and 3, we obtain, for the x-ray radiation used ($\lambda=0.710$A), the following values of $d$ at 25°C: for 100 percent cyclohexane, $2\theta=8°00'$ and $d=5.09\pm0.01$A; for 100 percent benzene, $2\theta=8°40'$ and $d=4.70\pm0.01$A. Such values of $d$ have been interpreted by several authors as the effective thickness of the molecules in the liquid.[28]

It remains to explain, if possible, the low peaks at $2\theta=4°00'-4°20'$, and the three peaks shown by all the mixtures at $2\theta=8°00'$, 8°20′ and 8°40′. Let us consider the solution to be made up partly of randomly distributed molecules of benzene and cyclohexane, and partly of small groups, each existing temporarily, whose molecules have an almost orderly arrangement. This is consistent with Stewart's explanation[28] of x-ray diffraction in pure liquids. It is inherent in the theory of x-ray diffraction that sharp diffraction peaks require the diffracting material to have a periodic structure, with enough repetition of the fundamental structure to give a noticeable contribution to the diffraction pattern. For convenience of reference we shall use the symbol (*–B–B–B–*) to represent some definite grouping, composed entirely of pure benzene, the symbol (*–C–C–C–*) to represent a similar grouping of pure cyclohexane, and the symbols (*–B–C–B–C–*), (*–B–C–C–B–C–C–*), (*–B–C–B–C–C–B–*), etc., to represent groups composed of both benzene and cyclohexane. Obviously the groupings (*–B–B–B–*) and (*–C–C–C–*) show a repetitive structure with the single molecule as the fundamental unit. We should therefore expect definite diffraction peaks corresponding to the grating spaces given by adjacent molecules. Such peaks were observed experimentally in the present work. Since we are dealing with nonrigid liquids, instead of solid crystals, we must expect the pure liquid to show an equilibrium state between ($-B_k-B_l-B_m-B_n-$) and ($-B_k-B_l-B_m-B_n-$) or between ($-C_k-C_l-C_m-C_n-$) and ($-C_k-C_l-C_m-C_n-$). This should give a diffraction peak corresponding to the distance, $B_k-B_m$ (or $C_k-C_m$). This spacing is obviously not far from twice the mean spacing between adjacent molecules. Such peaks have been observed experimentally in every case. They are not shown in Figs. 2–4 for lack of space.

The groupings ($-B_d-C_e-B_f-C_g-$) show a slightly more complicated periodic structure. Such a grouping should show a diffraction peak corresponding to the fundamental spacing $-B_d-B_f-$ or $-C_e-C_f-$, but since the diffracting power of *B* and *C* are similar, this peak should be weak due to interference between *B* and *C*. Such peaks have been observed in the case of all the mixtures studied. The spacing $-B_d-C_e-$

[28] G. W. Stewart, Phys. Rev. **33**, 889 (1929).

obviously should be intermediate between the spacings $-B-B-$ and $-C-C-$ appearing in the $(-B-B-B-)$ and $(-C-C-C-)$ groupings, and this is found to be the actual case. Because of the similarity in diffracting power of $B$ and $C$, a definite diffraction peak should be found for all mixtures of $B$ and $C$ at a distance corresponding to $-B_d-C_e-$, (i.e., half the spacing $B_d-B_f$). Experimentally such peaks were found for all our mixtures. They are shown in Figs. 4 and 5, and in detail in Table I; within experimental error, these peaks fall half-way between the peaks of $(-B-B-B-)$ and $(-C-C-C-)$.

The next most complicated grouping can be represented by $(-B_e-C_f-C_g-B_h-C_i-C_j-)$. The basic repetitive distance for this grouping is $B_e-B_h$. This distance would have to be repeated several times to give a definite diffraction peak. The probability of many successive units of $(-B-C-C-)$ occurring in a single group is so small that any diffraction peak would necessarily be weak. Even if such a definite peak were strong enough to be detected, it would lie at too small a diffracting angle to be observed on our apparatus with Mo $K\alpha$ rays. A similar argument could be used for still more complicated molecular groups.

It might be argued that the shapes of the experimental curves are due to addition of two complete curves for $(-C-C-C-)$ and $(-B-B-B-)$. Figure 6 shows, by dotted lines, the curves for $(-B-B-B-)$ and for $(-C-C-C-)$ obtained by multiplying the experimental curves (at 25°C) of Figs. 2 and 3 by the mole fractions 0.534 and 0.466, respectively. This composition corresponds to the weight fractions 0.514 and 0.486 shown in Fig. 4. Figure 6 shows that the sum of the two dotted line curves does not even approximate the experimental curve.

Considering the diffraction effects of such groups as $(-B_e-C_f-C_g-B_h-C_i-C_j-)$ mentioned above, we see that scattering over an angular range ought, however, to occur due to spacings, $B_e-C_f$, $C_f-C_g$, $C_g-B_h$, etc., because of the similarity of diffracting power of $B$ and $C$, and the close similarity of the distances, $B_e-C_f$, $C_f-C_g$, $C_g-B_h$, etc. The same argument applies also to more disordered groups, such as $(-B-C-B-C-C-B-)$, and to molecules which may be in such a chaotic configuration as not to show even a definite molecular orientation. The contribution to the diffraction curve due to all such groupings should be a diffuse peak, with its maximum between $2\theta=8°00'$ and $8°40'$.

To summarize the above, we may consider that the total x-ray diffraction curve is made up of the following:—(1) sharp peaks due to the order states $(-B-B-B-)$, $(-C-C-C-)$, and $(-B-C-B-C-)$ and (2) a diffuse peak, superimposed on the peaks of (1), due to more complicated groupings and randomly distributed molecules.

It remains to determine the relative magnitude of the order and disorder contributions to the diffraction curve, both in the case of the pure liquids and in the case of the solutions. This may be done as follows:—(1) A smooth curve was drawn on the curves of Figs. 2–5, connecting the points on both sides of the main peak, where the slope seemed to change most rapidly. This was entirely arbitrary but is apparently justified by the end results. It is similar to the method of Stewart in obtaining half-peak width.[28] The area under this curve was considered to represent the contribution due to all the disorder states. (2) The area above the smooth curve of (1) was considered to be due to the x-ray diffraction of the order states $(-B-B-B-)$, $(-C-C-C-)$ for pure benzene and pure cyclohexane, respectively, and of the order states

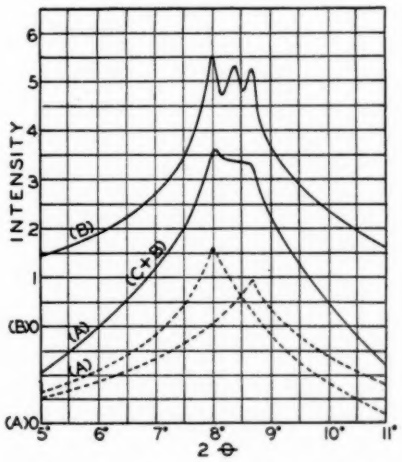


FIG. 6. Theoretical curve due to addition of curves for benzene and cyclohexane. Dotted line curves from pure benzene and cyclohexane curves of Figs. 2 and 3. $(C+B)$: Addition of dotted line curves. Upper curves: Actual experimental curve.

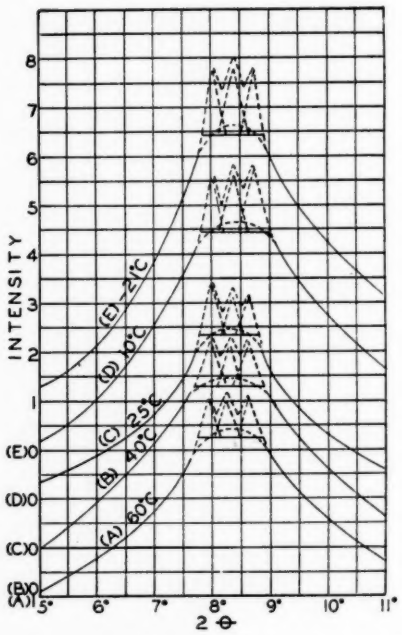


FIG. 7. Theoretical diffraction curves for 51.4 percent benzene solution.

(–*B*–*B*–*B*–), (–*C*–*C*–*C*–) and (–*B*–*C*–*B*–*C*–) of the mixtures. If we assume that the (–*B*–*B*–*B*–) and (–*C*–*C*–*C*–) groupings in the mixtures are in every way the same as in the pure liquids, then the amounts of (–*B*–*B*–*B*–) and (–*C*–*C*–*C*–) present in a given mixture should be proportional to the mole fraction of each in that mixture. In other words, the intensity due to (–*C*–*C*–*C*–) in the pure cyclohexane times the mole fraction of *C* in the solution should equal the intensity due to (–*C*–*C*–*C*–) in the solution. A similar argument should hold for benzene. Using the (–*B*–*B*–*B*–) and (–*C*–*C*–*C*–) values of Figs. 2 and 3 placed on an arbitrary base line, as shown, the theoretical curves of Figs. 7 and 8 were obtained. The (–*B*–*C*–*B*–*C*–) peak intensity was made such that the addition of all curves would give the experimental peaks of Figs. 4 and 5.

Using the method of (1) and (2) the peak intensities were determined and tabulated in Table II. The intensities are expressed in terms of counts per 5 minutes, as before. Those given in parenthesis are the theoretical values from Figs. 7 and 8. The others are from Figs. 2–5. The half-peak widths are for the order state curves for the pure liquids, and over the entire three-order peaks for the solutions.

The complete theoretical curves are shown in Figs. 7 and 8. The top dotted line is the addition of all the curves contributing to the x-ray diffraction. Curves of Figs. 7 and 8 and those of Figs. 4 and 5 are in good agreement. The data for absolute intensities in the case of the 51.4 percent benzene mixture are better than for the other mixtures since they were very carefully checked. The other mixtures were studied more to prove whether all the peaks could be detected than to ascertain their absolute heights. The theory did not give very good agreement in the case of the −21°C curve of the 51.4 percent benzene mixture, since it was necessary to use the data for the pure liquids, approximately 15 degrees higher.

A few possible objections to this present work must be met and, if possible, satisfied. The matter of peak resolution, which was first considered by Meyer,[29] and later by Murray and Warren,[6] seems to be adequately answered, if the interpretation given in Figs. 7 and 8 is correct. It is true that these separate peaks have not been observed by other workers, but most

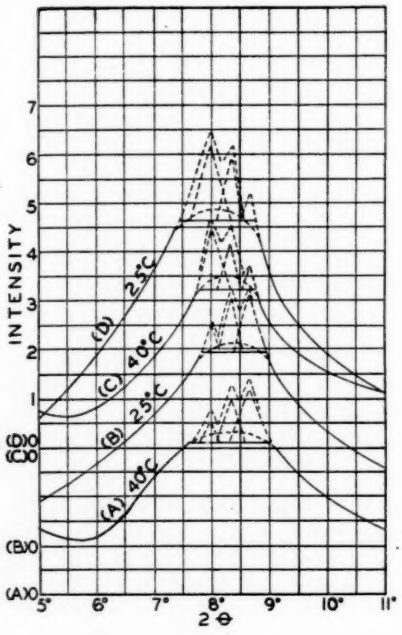


FIG. 8. Theoretical diffraction curves for *A*, *B*—74.5 percent benzene; *C*, *D*—74.6 percent cyclohexane solutions.

[29] A. W. Meyer, Phys. Rev. **38**, 1083–1093 (1931).

TABLE II. *Relative peak intensities. Values in parentheses are from Figs. 7 and 8. All other values are experimental data shown in Figs. 2–5.*

| COMPOSITION | TEMPERATURE | RELATIVE PEAK INTENSITY –C–C–C– | | –B–B–B– | | –C–B–C–B– | HALF-PEAK WIDTH |
|---|---|---|---|---|---|---|---|
| 100% $C_6H_{12}$ | 6.7°C | 290 | | | | | 30′ |
| " " | 10°C | 240 | | | | | 35′ |
| " " | 25°C | 200 | | | | | 35′ |
| " " | 40°C | 170 | | | | | 35′ |
| " " | 60°C | 150 | | | | | 25′ |
| 100% $C_6H_6$ | 5.7°C | | | 240 | | | 20′ |
| " " | 10°C | | | 200 | | | 30′ |
| " " | 25°C | | | 150 | | | 30′ |
| " " | 40°C | | | 130 | | | 30′ |
| " " | 60°C | | | 110 | | | 30′ |
| 51.4% $C_6H_6$ | −21°C | 160 | (135) | 150 | (130) | (140) | 55′ |
| " " | 10°C | 120 | (110) | 110 | (110) | (110) | 1°05′ |
| " " | 25°C | 110 | (100) | 90 | (85) | (90) | 1°00′ |
| " " | 40°C | 85 | (80) | 80 | (70) | (80) | 1°05′ |
| " " | 60°C | 80 | (70) | 70 | (60) | (60) | 1°05′ |
| 74.5% $C_6H_6$ | 25°C | 60 | (50) | 110 | (110) | (100) | 55′ |
| " " | 40°C | 80 | (40) | 90 | (100) | (90) | 1°05′ |
| 74.6% $C_6H_{12}$ | 25°C | 140 | (145) | 100 | (40) | (130) | 1°00′ |
| " " | 40°C | 110 | (120) | 40 | (35) | (100) | 1°00′ |
| 62.4% $C_6H_6$ | 25°C | 70 | (70) | 130 | (90) | (130) | 55′ |
| 62.8% $C_6H_{12}$ | 25°C | 180 | (120) | 90 | (60) | (110) | 1°00′ |

of them except Ward[8] used a photographic method. It seems questionable that a photographic method would ever resolve peaks of such intensities as those obtained, because of the high background density of the film, and the small distance on the film between peaks. The experimental peaks, it is true, as pointed out by Murray and Warren, should not be sharp but slightly rounded. The data of the present work, taken at small angular intervals show a definite rounding, although the scale of Figs. 2–5 does not bring this out clearly. Also one might ask whether the (–*B*–*B*–*B*–) and (–*C*–*C*–*C*–) groupings found in the mixtures were due to insufficient mixing of the components. Experimentally, the x-ray diffraction results were independent of the amount of stirring. The effects observed could not have been caused by a streaming effect in the liquid, for curves run at room temperature, with and without stirring, were identical.

The results reported here may be discussed with relation to other data from the literature. The data for the unit diffracting distance in a given group, ($d=n\lambda/2\sin\theta$), read off a graph of *d versus T*, over a temperature range from 10°C to 60°C (see Table I), show that the increase in *d* is more than 6 percent and less than 18 percent, with a probable value of 12 percent. This is consistent with the results now in the literature[24,30–32] on x-ray diffraction of liquids. The fact that the I.C.T. tables show, for both benzene and cyclohexane, a volume expansion of only 6 percent, indicates strongly that only a small fraction of the liquid can be in an order state at any one time. This conclusion is consistent with thermodynamic data on liquids in general,[33,34] and on the benzene-cyclohexane system.[9] The positions of the (–*B*–*B*–*B*–) and (–*C*–*C*–*C*–) peaks at the freezing points of the pure liquids strongly indicate that the order state is nearly that of the solid, in one dimension at least. The two strong lines of the solid benzene arising from the (111) and (020) planes give an average *d* of 4.65A,[35] the experimental value from the liquid peak at 5.7°C gives $d=4.68$A. Two very strong lines for solid cyclohexane gave an average *d* of 5.04A[36] compared to a value at 6.7°C of 5.06A for the liquid cyclohexane.

The positive deviation of the benzene-cyclohexane system from Raoult's law[9] and the increase in molal volume on mixing[9,37] would

[30] E. W. Skinner, Phys. Rev. **36**, 1625–30 (1930).
[31] S. S. Ramasubramanyan, Ind. J. Phys. **3**, 137–49 (1928).
[32] V. I. Vaidynathan, Ind. J. Phys. **5**, 501–524 (1930).
[33] J. G. Kirkwood, J. Phys. Chem. **43**, 97 (1939).
[34] G. Scatchard and W. J. Hamer, J. Am. Chem. Soc. **57**, 1805 (1935).
[35] E. G. Cox, Proc. Roy. Soc. **A135**, 491 (1932).
[36] K. Lonsdale and H. Smith, Phil. Mag. **28**, 614 (1939).
[37] H. Poltz, Zeits. f. physik. Chemie **B32**, 243–273 (1936).

lead to the conclusion that the intermolecular forces between benzene and cyclohexane molecules were less than those between benzene-benzene or cyclohexane-cyclohexane molecules. Therefore, the probability of the (–*B*–*C*–*B*–*C*–) array appearing in the liquid should be less than that predicted on the basis of mole fractions. If the forces had been all equal, the (–*B*–*C*–*B*–*C*–) peak intensity should have been between the (–*B*–*B*–*B*–) and (–*C*–*C*–*C*–) intensities. In the case of the carefully studied 51.4-percent benzene mixture, Table II shows that not only is the (–*B*–*C*–*B*–*C*–) peak intensity lower than the average intensity of the benzene and cyclohexane peaks, but also that it is almost always lower than the benzene peak itself. This is consistent with the above prediction based on Raoult's law.


## Summary

(1) A low intensity peak at half the diffraction angle of the main peaks has been detected and a plausible explanation has been given for its existence.

(2) The main peak from x-ray diffraction measurements of benzene-cyclohexane solutions has been resolved experimentally into three peaks.

(3) The observed diffraction peaks in the liquid mixtures are explained on an order-disorder basis, which is consistent with existing thermodynamic data.

(4) Theoretical curves are shown to give intensities comparable to measured values, for the most probable order states in the solutions.

(5) The usefulness of Geiger-Mueller counters for liquid x-ray diffraction studies has been demonstrated.


---

JUNE, 1941 JOURNAL OF CHEMICAL PHYSICS VOLUME 9

# Atomic Distributions in Liquid Elements

CARL GAMERTSFELDER
*University of Missouri, Columbia, Missouri*

(Received March 27, 1941)

Monochromatic x-ray diffraction patterns of liquid chlorine, tin, indium, zinc, cadmium, aluminum, and lithium were obtained, using Mo $K\alpha$ radiation. The effect of temperature change on the patterns was determined for tin and indium. Fourier analyses of these patterns led to the determination of atomic distribution curves for each element. Each atom in liquid chlorine has one nearest neighbor, which means that chlorine is diatomic in the liquid state. The distribution curves for liquid tin, zinc and aluminum agree very well with the distributions in the corresponding crystals. The distribution curves for indium, cadmium, and lithium do not agree very well with distributions in the corresponding crystals.

## Introduction

ATOMIC distributions in liquids are obtainable from x-ray diffraction patterns by a method of analysis based on the theories of Zernike and Prins[1] and of Debye and Menke.[2] Such determinations have been made for the elements mercury,[2,3] gallium,[4] sodium,[5,6] potassium,[7] phosphorus,[8] sulfur,[9] and argon,[10,11] all in the liquid state. In the present work the diffraction patterns of liquid chlorine, tin, indium, zinc, cadmium, aluminum, and lithium have been obtained and their atomic distribution curves have been determined. The chlorine was liquid under its own vapor pressure at room temperature, the

[1] F. Zernike and J. Prins, Zeits. f. Physik **41**, 184 (1927).
[2] P. Debye and H. Menke, *Erg. d. Tech. Röntgenkunde II* (1931).
[3] R. N. Boyd and H. R. R. Wakeham, J. Chem. Phys. **7**, 958 (1939).
[4] H. Menke, Physik. Zeits. **33**, 593 (1932).
[5] L. P. Tarasov and B. E. Warren, J. Chem. Phys. **4**, 236 (1936).
[6] F. H. Trimble and N. S. Gingrich, Phys. Rev. **53**, 278 (1938).
[7] C. D. Thomas and N. S. Gingrich, J. Chem. Phys. **6**, 411 (1938).
[8] C. D. Thomas and N. S. Gingrich, J. Chem. Phys. **6**, 659 (1938).
[9] N. S. Gingrich, J. Chem. Phys. **8**, 29 (1940).
[10] A. Eisenstein and N. S. Gingrich, Phys. Rev. **58**, 307 (1940).
[11] K. Lark-Horovitz and E. P. Miller, Nature **146**, 459 (1940).

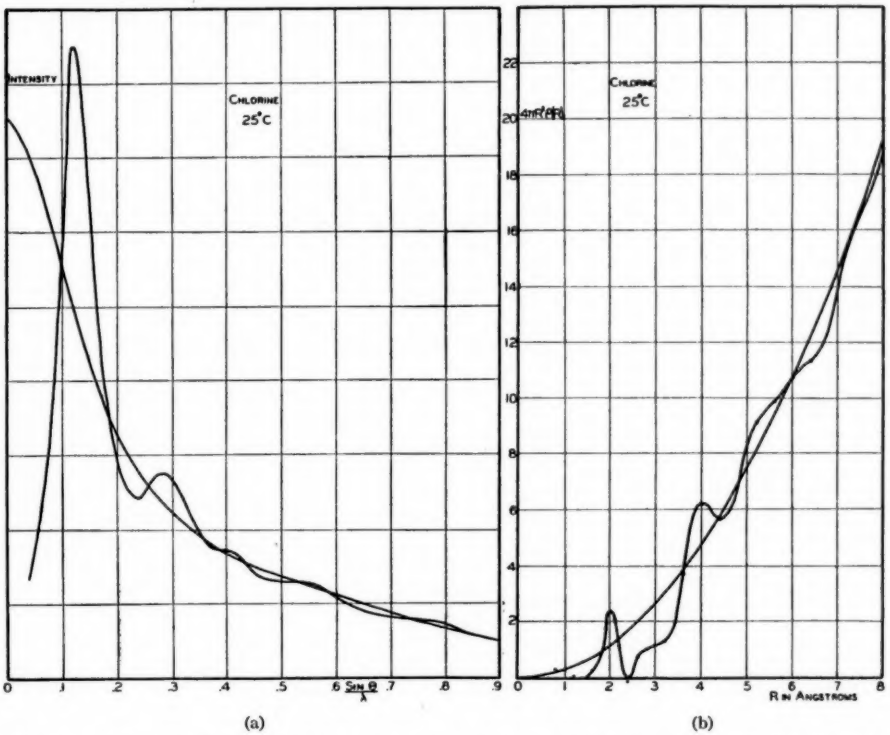


(a) (b)

FIG. 1. (a) Corrected experimental intensity curve for liquid chlorine at 25°C. (b) Radial density distribution of atoms about any one atom in liquid chlorine at 25°C.

metals were just above their melting points, and in the cases of tin and indium, temperatures above the melting points were also used.

## EXPERIMENTAL

Two cylindrical cameras were used in obtaining the diffraction patterns, one with a radius of 8.85 cm and the other with a radius of 9.20 cm. Both radii were mechanically measured and they were also checked by calculations from the diffraction patterns of powdered rocksalt. Mo $K\alpha$ radiation monochromatized by reflection from a rocksalt crystal outside the camera was directed through a pair of collimating slits before being scattered by the sample at the center of the camera. Each camera was provided with a sample-holder which could be heated while the rest of the camera was water-cooled to protect the photographic film used to detect the scattered x-rays. The liquid chlorine was contained in a thin-walled glass capillary, 0.15 cm in diameter, under its own vapor pressure of about 7.7 atmospheres at 25°C. Tin (at 250°C and 390°C), indium (at 160° and 390°C), zinc (at 460°C), and cadmium (at 350°C) were flat samples, about 0.008 cm thick, clamped between mica sheets 0.0005 cm thick. The aluminum (at about 700°C) in the form of a wire 0.17 cm in diameter was heated in a small Bunsen flame which kept the aluminum liquid inside its very thin but tough oxide coat. The lithium sample (at 200°C) was shaped with its horizontal cross section as a right isosceles triangle, and the x-ray beam was incident perpendicular to the hypotenuse. The length of path of the x-rays in the lithium was 1.8 cm. The lithium was contained in a special brass holder and was prevented from reacting with the brass by means of a thin coat of carbon applied with a thin shellac binder and then baked. Mica windows were used with this holder.

The intensity of scattered x-rays at various angles was determined from the blackening of the photographic film by means of a microphotometer. The intensity in each case was then plotted as a function of $\sin\theta/\lambda$, where $\theta$ is half the angle

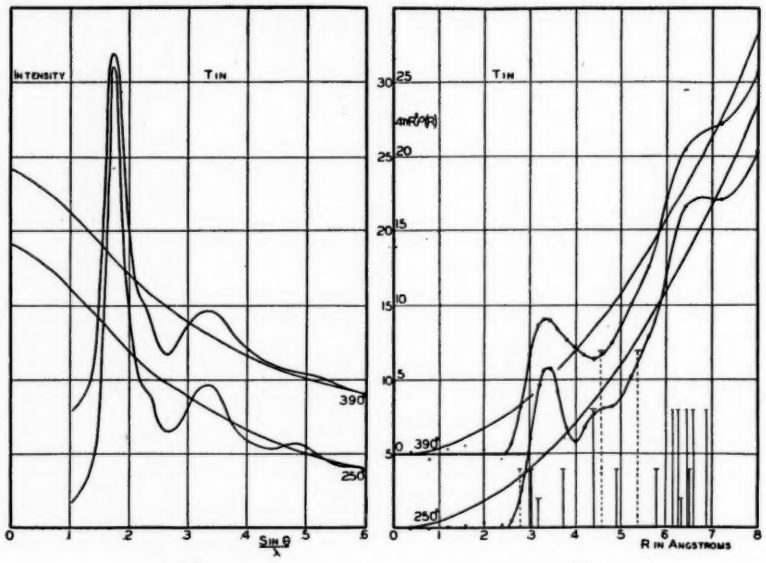


(a) (b)

FIG. 2. (a) Corrected experimental intensity curves for liquid tin at 250°C and 390°C. (b) Radial density distributions of atoms about any one atom in liquid tin at 250°C and 390°C.

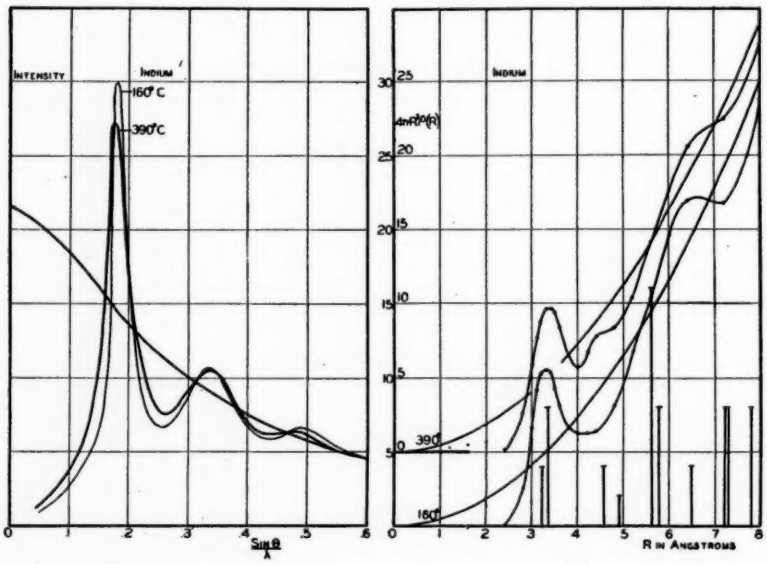


(a) (b)

FIG. 3. (a) Corrected experimental intensity curves for liquid indium at 160°C and 390°C. (b) Radial density distributions of atoms about any one atom in liquid indium at 160°C and 390°C.

of scattering and $\lambda$ is 0.710A. The experimental intensity curves have been corrected and are given as the (a) parts of Figs. 1 to 7. The nature of the corrections is given in the next section. Table I gives the positions, in $\sin\theta/\lambda$ units, of the intensity maxima of the various patterns. Prins,[12] and Danilov and Radchenko[13] have obtained the first maximum in the intensity pattern of tin and their results agree very well with the

[12] J. Prins, Trans. Faraday Soc. **33**, 110 (1937).
[13] J. V. Danilov and V. J. Radchenko, Physik. Zeits. der Sowjetunion **12**, 313 (1937).

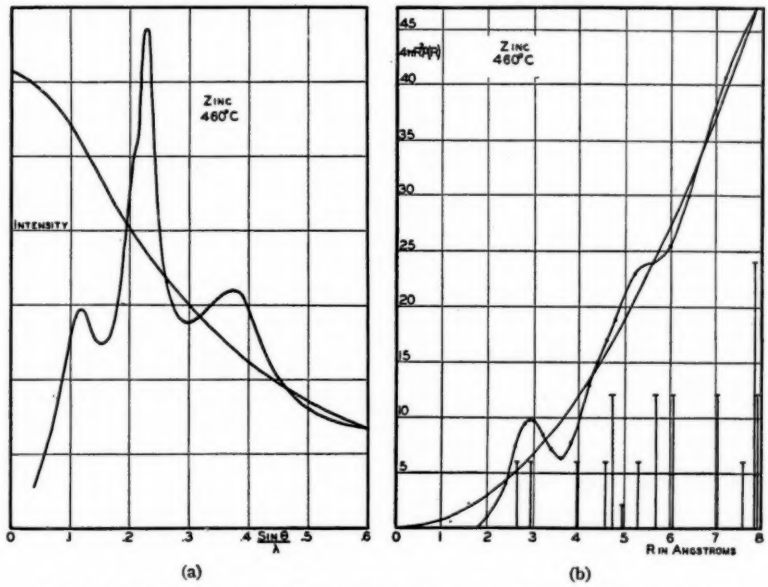


FIG. 4. (a) Corrected experimental intensity curve for liquid zinc at 460°C. (b) Radial density distribution of atoms about any one atom in liquid zinc at 460°C.

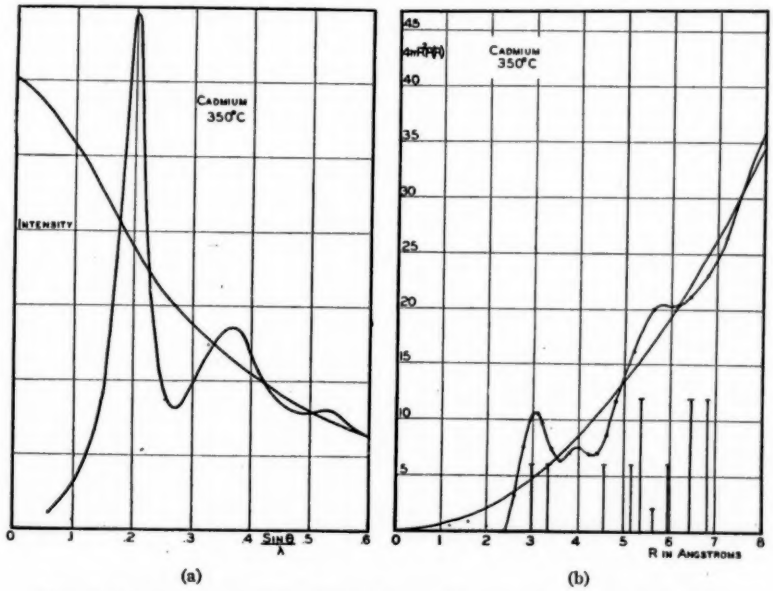


FIG. 5. (a) Corrected experimental intensity curve for liquid cadmium at 350°C. (b) Radial density distribution of atoms about any atom in liquid cadmium at 350°C.

ones given here, while Sauerwalde and Teske[14] report a value which is much larger. Randall[15] reports that the diffraction maximum of liquid aluminum corresponds to that of the (111) planes of the solid, but no exact data are given. The spacing of the (111) planes in aluminum is 2.33A and this corresponds to a diffraction maximum, using Bragg's law, at $\sin\theta/\lambda = 0.214$

[14] F. Sauerwalde and W. Teske, Zeits. f. anorg. Chemie 210, 247 (1933).

[15] F. R. Randall, *The Diffraction of X-Rays and Electrons by Amorphous Solids, Liquids and Gases* (John Wiley and Sons, Inc., New York, 1934), p. 134.

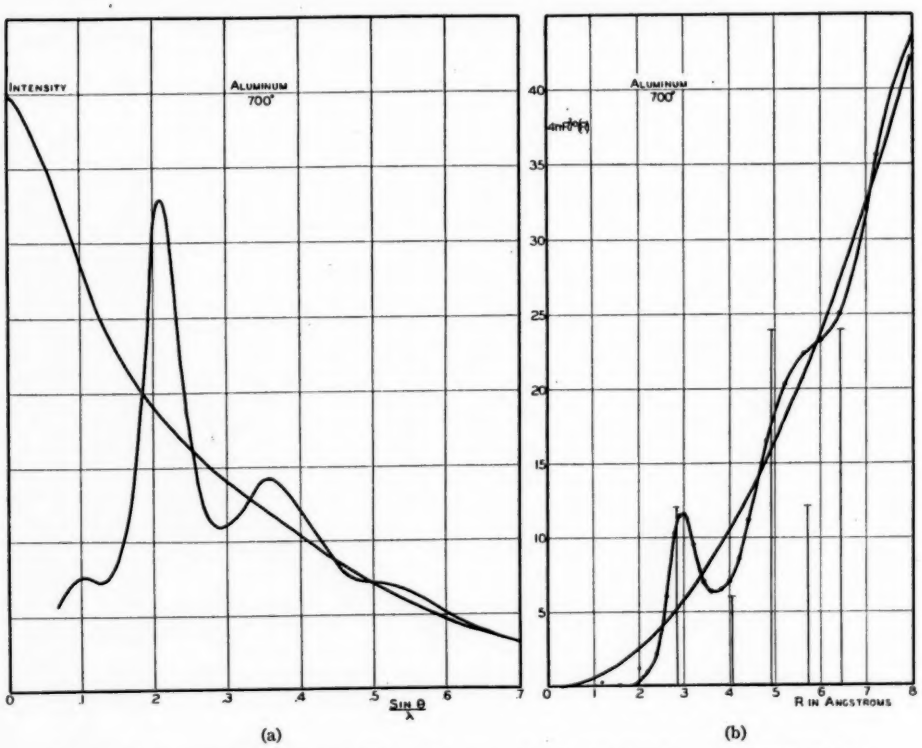


FIG. 6. (a) Corrected experimental intensity curve for liquid aluminum at 700°C. (b) Radial density distribution of atoms about any one atom in liquid aluminum at 700°C.

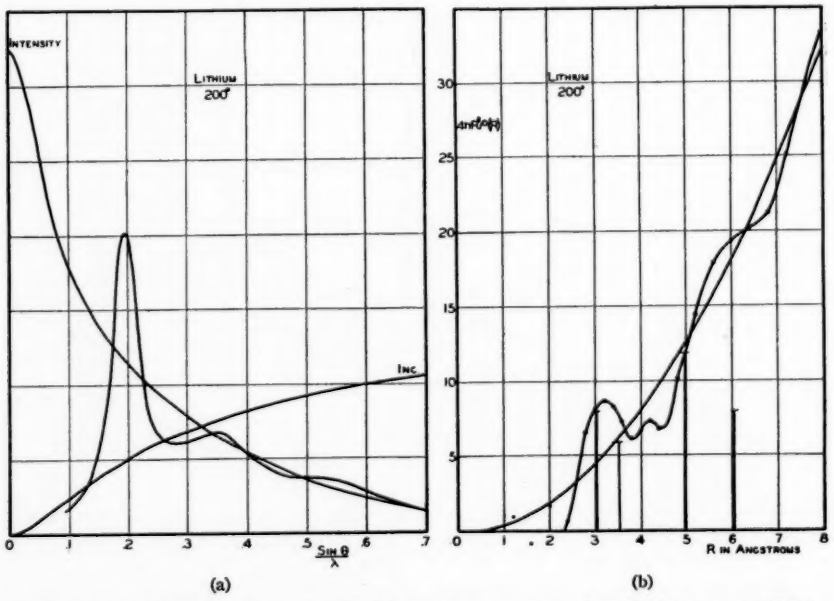


FIG. 7. (a) Corrected experimental intensity curve for liquid lithium at 200°C. (b) Radial density distribution of atoms about any one atom in liquid lithium at 200°C.

which is in good agreement with the main peak reported here.

In the course of this investigation it was necessary to determine the densities of liquid indium and liquid lithium. The density of indium at various temperatures was determined by filling a bulb on the end of a capillary tube with indium. The volume of the indium was measured by calibrating the bulb and tube with mercury the density of which is very well known. The density of liquid indium at its melting point of 155°C is 7.03±0.01 g/cm³ and the coefficient of volume expansion is 0.00013 per degree C. The density of liquid lithium was found by means of a pyknometer filled with oil in which the lithium was placed. The density of liquid lithium at 195°C is 0.46±0.01 g/cm³.

## The Fourier Method

The theory, upon which the analyses of these diffraction patterns are based, is given elsewhere,[16] and the equation used here is

$$4\pi R^2\rho(R)=4\pi R^2\rho_0+\frac{2R}{\pi}\int_0^\infty Si(S)\sin RSdS, \quad (1)$$

where $R$ is the distance in angstroms from any arbitrary atom taken as the origin. $\rho(R)$ is the actual density in atoms per cubic angstrom, $\rho_0$ is average density in atoms per cubic angstrom, and $S=4\pi\sin\theta/\lambda$. The function $i(S)$ is defined as $(I/N-F^2)/F^2$ where $I/N$ is the intensity of the coherent scattered radiation per atom from a sample having no absorption and with corrections for polarization of the scattered x-rays, and $F$ is the structure factor of the atom. The values of $4\pi R^2\rho(R)dR$ give, then, the number of atoms in a spherical shell of thickness $dR$ and radius $R$ about any one atom of the liquid. The experimentally determined diffraction patterns were corrected for polarization[17] and absorption. Absorption corrections for samples with flat sides were easily calculated and corrections for cylindrical samples are given by Blake.[18] Correction was also made for the incoherent radiation by means of the $F$ and $\Sigma f_n^2$ tables given by Compton and Allison[19] or interpolations from their values, except in the case of lithium whose values were not given accurately enough. The $F$ values for lithium were calculated from the electron distribution as given by Fock and Petrashen.[20] Table II gives the values of the $F=\Sigma f_n$ and $\Sigma f_n^2$ terms as calculated for various $\sin\theta/\lambda$ values.

Table I.

| | First Peak | Second Peak | Third Peak | Fourth Peak | Fifth Peak |
|---|---|---|---|---|---|
| Cl 25° | 0.122 | 0.285 | 0.41 | 0.55 | 0.8 |
| Sn 250° | .174 | .335 | .49 | — | — |
| Sn 390° | .175 | .330 | .50 | — | — |
| In 160° | .179 | .335 | .50 | — | — |
| In 390° | .177 | .335 | .49 | — | — |
| Zn 460° | .115 | .228 | .38 | — | — |
| Cd 350° | .203 | .360 | .55 | — | — |
| Al 700° | .10 | .210 | .36 | .55 | — |
| Li 200° | .195 | .340 | .55 | — | — |

Table II.

| $\sin\theta/\lambda$ | $F=\Sigma f_n$ | $\Sigma f_n^2$ |
|---|---|---|
| 0.0 | 3.00 | 3.00 |
| .1 | 2.20 | 1.99 |
| .2 | 1.77 | 1.57 |
| .3 | 1.47 | 1.08 |
| .4 | 1.24 | .768 |
| .5 | 1.007 | .508 |
| .6 | .803 | .322 |
| .7 | .634 | .200 |
| .8 | .510 | .130 |

The ratio between the coherent and incoherent radiation was determined at a large angle of scattering where no effects due to interferences appear and then the complete incoherent curve was drawn in and subtracted from the intensity curve. The $F^2$ curve was then drawn in and the $i(S)$ values calculated. The values of the integral in Eq. (1) were determined by graphical integration and the values of $4\pi R^2\rho(R)$ thus determined were plotted against $R$.

The results for the various elements are shown in the (b) parts of Figs. 1 to 7. The positions and numbers of the atoms in the crystal lattices are given by the straight lines located at various abscissae of the graphs, the height of each line representing the number of atoms at that particular distance. The dotted lines with the tin curve give the atoms for gray tin, the solid

[16] B. E. Warren, J. App. Phys. **8**, 645 (1937).

[17] S. Katzoff, J. Chem. Phys. **2**, 841 (1934).

[18] F. C. Blake, Rev. Mod. Phys. **5**, 169 (1933).

[19] A. H. Compton and S. K. Allison, *X-Rays in Theory and Experiment* (D. Van Nostrand, 1935), p. 139 and 781.

[20] V. Fock and M. J. Petrashen, Physik. Zeits. der Sowjetunion **8**, 547 (1936).

TABLE III.

| ELEMENT | LIQUID DIST. | NO. | SOLID DIST. | NO. | | ATOMS/A³ | DENSITY LIQUID | SOLID (20°C) |
|---|---|---|---|---|---|---|---|---|
| Cl 25° | 2.01 | 0.97 | — | — | | 0.0238 | 1.40 g/cm³ | — |
| Sn 250° | 3.38 | 10.0 | 3.02 | 4 | | | | |
| | | | 3.16 | 2 | white tin | 0.0356 | 6.97 | 7.31 g/cm³ |
| | | | 3.75 | 4 | | | | |
| | | | 2.79 | 4 | | | | |
| | | | 4.56 | 8 | gray tin | | | |
| Sn 390° | 3.36 | 8.9 | — | — | | 0.0350 | 6.86 | — |
| In 160° | 3.30 | 8.5 | 3.24 | 4 | | 0.0371 | 7.03 | 7.28 |
| | | | 3.36 | 8 | | | | |
| In 390° | 3.36 | 8.4 | — | — | | 0.0361 | 6.84 | — |
| Zn 460° | 2.94 | 10.8 | 2.66 | 6 | | 0.0604 | 6.51 | 7.14 |
| | | | 2.94 | 6 | | | | |
| Cd 350° | 3.06 | 8.3 | 2.98 | 6 | | 0.0430 | 7.98 | 8.65 |
| | | | 3.34 | 6 | | | | |
| Al 700° | 2.96 | 10.6 | 2.86 | 12 | | 0.0530 | 2.36 | 2.70 |
| Li 200° | 3.24 | 9.8 | 3.03 | 8 | | 0.0402 | 0.46 | 0.534 |
| | | | 3.50 | 6 | | | | |

lines for white tin. Table III gives the positions of the first maxima in the distribution curves for the liquids and the number of atoms at these distances as determined by drawing in symmetrical peaks and measuring the areas under them. In addition some data are given on the crystalline forms and the densities of the liquids and solids.

## DISCUSSION OF RESULTS

The diffraction pattern of liquid chlorine has two distinct maxima and three more fluctuations about the $F^2$ curve. The distribution curve shows definitely that the chlorine is diatomic in the liquid state and the interatomic distance of 2.01A agrees very well with the value of 2.009A given by Pauling and Brockway[21] as determined from electron diffraction patterns of the gas. The rest of the distribution curve is not easy to interpret quantitatively, though it seems that on the average, one atom of one of the neighboring molecules is approximately 3A from the reference atom while the rest of the neighboring molecules are located at a distance of about 4A. The number of neighboring molecules at these distances is difficult to determine. The values of the distribution function at small values of $R$ are very sensitive to the shape of the diffraction pattern at large angles of scattering, which is the most difficult to measure accurately. This effect was noticed in the case of chlorine where an incomplete diffraction pattern, without the last two maxima, was analyzed. The results in this case gave a distribution curve very much like the one reported here except in the vicinity of the peak at 2.01A. The area under the peak was the same but it was broader and moved in to about 1.8A. In the case of argon[22] the introduction of a fourth peak in the intensity curve did not cause any appreciable effect in the first maximum of the distribution curve. The effect in this case is not the same however, because the first maximum for argon is at a larger value (about 3.9A) of $R$ than in the case of chlorine.

Both diffraction patterns of tin have three maxima. In the 390°C case the maxima are not so high but are broader than in the 250°C case. The distribution curve for liquid tin shows that there are 10.0 nearest neighbors at 3.38A, which is in excellent agreement with crystalline white tin where there are 10 nearest neighbors at an average distance of 3.34A. There is no such correlation with the gray tin structure. The distribution curve at the high temperature does not have as definite maxima as at the lower temperature because of the increased heat motion of the atoms. The distance to the nearest neighbors is not changed but the number is decreased. The atoms which leave the first concentration join with the secondary concentration which moves in to a shorter distance.

The diffraction patterns of liquid indium at 160°C and 390°C are very much alike except for

[21] L. Pauling and L. O. Brockway, J. Chem. Phys. **2**, 867 (1934).

[22] N. S. Gingrich, Phys. Rev. **59**, 290 (1941).

the main peak which is narrower and higher for the 160°C case. The third maximum is also much stronger for the lower temperature. Liquid indium at 160°C has, on the average, 8.5 nearest neighbors at 3.30A, which is quite different from the 4 atoms at 3.24A and 8 atoms at 3.36A or 12 atoms at an average distance of 3.32A in the crystal. The distribution curve does not change much at the higher temperature except for the appearance of a slight secondary maximum which did not show at the low temperature, presumably because it was too close to the first concentration.

Zinc and cadmium have very similar hexagonal crystal structures, but the diffraction patterns of the liquids are not very much alike. The diffraction pattern of zinc is very unusual in that a small maximum occurs at a value of sin $\theta/\lambda$ which is much smaller than that for the main peak. The pattern for cadmium is very much like that of indium except that the first maximum is at a larger value of sin $\theta/\lambda$. Liquid zinc has 10.8 nearest neighbors at 2.94A as compared with 6 atoms at 2.66A and 6 atoms at 2.94A or 12 atoms at an average of 2.80A in the crystal. Cadmium has only 8.3 nearest neighbors at 3.06A as compared with 6 atoms at 2.98A and 6 atoms at 3.34A or 12 atoms at an average of 3.16A in the crystal.

The diffraction pattern of aluminum is like that of zinc in that it has a small maximum inside the main peak, so that there are four maxima altogether. The distribution curve for aluminum shows that there are 10.6 atoms at 2.96A while in the crystal there are 12 atoms at 2.86A.

The diffraction pattern of liquid lithium is not known as accurately as for the other elements because the sample used was not small compared to the radius of the camera used to obtain it. Another source of error might be in the very large incoherent correction for which the recoil factor[19] could not be neglected. The analysis shows that liquid lithium has 9.8 nearest neighbors at 3.24A as compared with 8 atoms at 3.03A and 6 atoms at 3.50A in the crystal.

Prins[23] has attempted to express the atomic distribution in a liquid by making a comparison with the corresponding crystal, where the atomic distribution in the liquid is produced by blurring the crystalline distribution. Prins has calculated diffraction patterns for atomic distributions obtained in this way which give good agreement with experimentally observed patterns. The agreement between the liquid distributions reported here and the corresponding crystal structures is good in the cases of tin, zinc, and aluminum. In the cases of indium, cadmium, and lithium the agreement is not at all good. Coulson and Rushbrooke[24] have suggested that there are likely to be greater structural changes on melting in cases where the volume change is large. However, zinc and aluminum both have larger volume changes than cadmium, and it is cadmium which has the largest structural change. Lithium also has a very large volume change on melting but the number of nearest neighbors is increased rather than decreased.

The author wishes to thank Professor N. S. Gingrich, under whose guidance this work was done, for his very helpful criticism and advice and for making available certain equipment obtained through grants in aid of research from the American Academy of Arts and Science and from the American Association for the Advancement of Science.

---

[23] J. Prins, Physica [3], **3**, 147 (1936).
[24] C. A. Coulson and G. S. Rushbrooke, Phys. Rev. **56**, 1216 (1939).

# The Infra-Red Bands of Hydrogen Peroxide at λ9720 and the Structure and Torsional Oscillation of Hydrogen Peroxide

LLOYD R. ZUMWALT* AND PAUL A. GIGUÈRE†
*Gates and Crellin Laboratories of Chemistry, California Institute of Technology, Pasadena, California*
(Received March 18, 1941)

A high dispersion study of the OH bands of hydrogen peroxide in the photographic infra-red is described. The rotational structure of the two hybrid bands at 10,283.68 $cm^{-1}$ and 10,291.08 $cm^{-1}$ is analyzed. The small moment of inertia of hydrogen peroxide is found to be $2.78_6\times10^{-40}$ g $cm^2$ while the harmonic mean of the two larger moments of inertia is found to be approximately $33.9\times10^{-40}$ g $cm^2$. The planar *cis*-configuration is ruled out spectroscopically and it is concluded that hydrogen peroxide exists in a non-planar form. It is tentatively decided that the vibrational levels of hydrogen peroxide are doubled and that the double minimum potential associated with the internal rotation of the OH groups has a high and a low barrier.

## INTRODUCTION

THE position of the OH groups with respect to their relative rotation about the O—O bond in hydrogen peroxide is of some interest. The OH groups can be imagined as preferring to assume the planar *cis*- or *trans*-configurations or some intermediate non-planar configuration. In the third case the molecule will have two equivalent enantiomorphic forms and the hindering potential for internal rotation will have two minima of equal depth and, in general, two barriers of unequal height. The OH groups undergo free rotation, hindered rotation or torsional oscillation depending on the heights of the barriers of the hindering potential.

Penney and Sutherland[1] have proposed a non-planar structure for hydrogen peroxide where the azimuthal angle[2] is 100°. Both barriers are given as being fairly high. These deductions are based on theoretical considerations and are shown to give a calculated value of the electric moment which agrees well with that obtained from measurements of the dielectric constants of dilute solutions of hydrogen peroxide in dioxane.[3]

Evidence of hindered rotation or torsional oscillation should appear in the rotational fine structure of the infra-red bands. In the hope of obtaining such evidence we have recently studied the absorption spectrum of hydrogen peroxide vapor in the photographic infra-red. The result has been the discovery of an unusual pair of bands at λ9720 which give some information regarding the structure and torsional motion of hydrogen peroxide.

## EXPERIMENTAL

The hydrogen peroxide used in these experiments had a strength which ranged from 95 to 98 percent. It was prepared from the commercial 30 percent solution by distillation under reduced pressure. The absorption cell was a six-meter Pyrex tube (22 mm diam.) which was heated to 100°C and through which hydrogen peroxide was continuously distilled at a pressure of 90 mm. Hydrogen peroxide which had been carefully purified was found to decompose very little on boiling. It was important to keep the all-Pyrex system very clean. Contact of the vapor with dirt or even a rough spot on the glass was found to cause violent decomposition.

When a tungsten lamp was used as a light source, the exposure time required for the high dispersion spectrogram was found to be excessive, consequently a carbon arc was employed as a light source. It was found necessary to run the carbon arc in an atmosphere of carbon dioxide to eliminate emission lines of the red CN bands. This light source reduced the required time of exposure by a factor of four; thus the spectroscopic plate was amply exposed in eight hours. During this time approximately two liters of the concentrated hydrogen peroxide were dis-

* Arthur A. Noyes Fellow in Chemistry.
† Provincial Government of Quebec Fellow in Chemistry.
[1] W. G. Penney and G. B. B. M. Sutherland, J. Chem. Phys. **2**, 492 (1934).
[2] The angle between the OH groups as seen projected on a plane normal to the O—O bond.
[3] E. P. Linton and O. Maass, Can. J. Research **7**, 81 (1932).

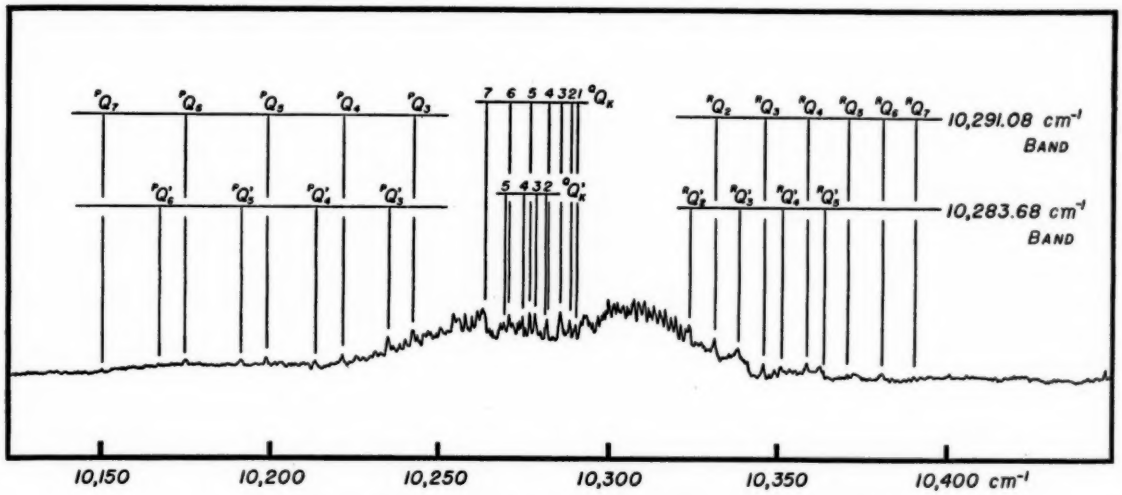


FIG. 1. Microphotometer trace of hydrogen peroxide bands at λ9720.

tilled over. The decomposition was only about 2 percent.

Exploration spectrograms were taken on Eastman 1Z plates with a glass Littrow spectrograph which covered the region between 7500 and 12,000A. Only one band at 9720A was found and this was then photographed in the first order of a twenty-one-foot concave grating spectrograph using Eastman 144Q plates. Measurements of the high dispersion plates were made with reference to third-order iron arc lines.

**Rotational structure of band**

An examination of the high dispersion spectrogram shows that a hybrid band is present which has the $Q$ branches characteristic of both the parallel and the perpendicular bands of a symmetrical rotator molecule. The appearance of this band is analogous to that of the 10,477A band of hydrazoic acid.[4] In the case of hydrogen peroxide, as in the case of hydrazoic acid, there is a strong dependence of the small moment of inertia upon the vibrational state, thus the parallel sub-bands are separated and an unusually marked convergence is present in the perpendicular component. A second hybrid band occurring at a slightly lower frequency also appears. This band is similar to the first but is a little less intense. The ${}^{Q}Q_K$ branches[5] of the parallel component and the ${}^{P}Q_K$ and ${}^{R}Q_K$ branches of the perpendicular component of the two bands have been identified. The branches of the lower frequency band which occur at a displacement of 7.40 cm$^{-1}$ have been given primed symbols.

A careful scrutiny reveals that at least a part of the band system appears to have a quadruplet character rather than a doublet character. Thus in the instances where $K''=3, 4, 5, 6$ a satellite of ${}^{P}Q_K'$ occurs at a shift of about minus 3.8 cm$^{-1}$ and also a satellite of ${}^{P}Q_K$ occurs at a shift of about plus 3.8 cm$^{-1}$. These attendant lines are weak and somewhat difficult to measure; never-

TABLE 1. *Frequency and identification of lines in the absorption spectrum of hydrogen peroxide at* λ9720.

| IDENTIFICATION | FREQUENCY cm$^{-1}$ | IDENTIFICATION | FREQUENCY cm$^{-1}$ |
|---|---|---|---|
| ${}^{P}Q_7$ | 10,151.49 | ${}^{Q}Q_4'$ | 10,274.76 |
| $a_6$ | 164.69 | ${}^{Q}Q_5$ | 276.95 |
| ${}^{P}Q_6'$ | 168.21 | ${}^{Q}Q_3'$ | 278.55 |
| ${}^{P}Q_6$ | 175.94 | ${}^{Q}Q_2'$ | 281.39 |
| $b_6$ | 179.65 | ${}^{Q}Q_4$ | 282.12 |
| $a_5$ | 188.24 | ${}^{Q}Q_3$ | 286.06 |
| ${}^{P}Q_5'$ | 191.94 | ${}^{Q}Q_2$ | 288.82 |
| ${}^{P}Q_5$ | 199.25 | ${}^{Q}Q_1$ | 290.40 |
| $b_5$ | 203.23 | ${}^{R}Q_3'$ | 339.21 |
| $a_4$ | 210.28 | ${}^{R}Q_3$ | 346.51 |
| ${}^{P}Q_4'$ | 213.96 | ${}^{R}Q_4'$ | 351.86 |
| ${}^{P}Q_4$ | 221.49 | ${}^{R}Q_4$ | 359.56 |
| $b_4$ | 225.51 | ${}^{R}Q_5'$ | 364.44 |
| $a_3$ | 231.10 | ${}^{R}Q_5$ | 371.71 |
| ${}^{P}Q_3'$ | 235.06 | ${}^{R}Q_6$ | 382.27 |
| ${}^{P}Q_3$ | 242.41 | ${}^{R}Q_7$ | 391.82 |
| ${}^{Q}Q_7$ | 263.44 | | |
| ${}^{Q}Q_5'$ | 269.37 | | |
| ${}^{Q}Q_6$ | 270.72 | | |

[4] E. H. Eyster, J. Chem. Phys. **8**, 135 (1940).

[5] In this nomenclature the large letter describes the behavior of $J$ in transition, the left-hand superscript gives the behavior of $K$, and the right-hand subscript gives the value of $K$ in the lower state.

# The Infra-Red Bands of Hydrogen Peroxide at λ9720 and the Structure and Torsional Oscillation of Hydrogen Peroxide

LLOYD R. ZUMWALT* AND PAUL A. GIGUÈRE†
*Gates and Crellin Laboratories of Chemistry, California Institute of Technology, Pasadena, California*
(Received March 18, 1941)

A high dispersion study of the OH bands of hydrogen peroxide in the photographic infra-red is described. The rotational structure of the two hybrid bands at 10,283.68 $cm^{-1}$ and 10,291.08 $cm^{-1}$ is analyzed. The small moment of inertia of hydrogen peroxide is found to be $2.78_6 \times 10^{-40}$ g $cm^2$ while the harmonic mean of the two larger moments of inertia is found to be approximately $33.9 \times 10^{-40}$ g $cm^2$. The planar *cis*-configuration is ruled out spectroscopically and it is concluded that hydrogen peroxide exists in a non-planar form. It is tentatively decided that the vibrational levels of hydrogen peroxide are doubled and that the double minimum potential associated with the internal rotation of the OH groups has a high and a low barrier.

## INTRODUCTION

THE position of the OH groups with respect to their relative rotation about the O—O bond in hydrogen peroxide is of some interest. The OH groups can be imagined as preferring to assume the planar *cis*- or *trans*-configurations or some intermediate non-planar configuration. In the third case the molecule will have two equivalent enantiomorphic forms and the hindering potential for internal rotation will have two minima of equal depth and, in general, two barriers of unequal height. The OH groups undergo free rotation, hindered rotation or torsional oscillation depending on the heights of the barriers of the hindering potential.

Penney and Sutherland[1] have proposed a non-planar structure for hydrogen peroxide where the azimuthal angle[2] is 100°. Both barriers are given as being fairly high. These deductions are based on theoretical considerations and are shown to give a calculated value of the electric moment which agrees well with that obtained from measurements of the dielectric constants of dilute solutions of hydrogen peroxide in dioxane.[3]

Evidence of hindered rotation or torsional oscillation should appear in the rotational fine structure of the infra-red bands. In the hope of obtaining such evidence we have recently studied the absorption spectrum of hydrogen peroxide vapor in the photographic infra-red. The result has been the discovery of an unusual pair of bands at λ9720 which give some information regarding the structure and torsional motion of hydrogen peroxide.

## EXPERIMENTAL

The hydrogen peroxide used in these experiments had a strength which ranged from 95 to 98 percent. It was prepared from the commercial 30 percent solution by distillation under reduced pressure. The absorption cell was a six-meter Pyrex tube (22 mm diam.) which was heated to 100°C and through which hydrogen peroxide was continuously distilled at a pressure of 90 mm. Hydrogen peroxide which had been carefully purified was found to decompose very little on boiling. It was important to keep the all-Pyrex system very clean. Contact of the vapor with dirt or even a rough spot on the glass was found to cause violent decomposition.

When a tungsten lamp was used as a light source, the exposure time required for the high dispersion spectrogram was found to be excessive, consequently a carbon arc was employed as a light source. It was found necessary to run the carbon arc in an atmosphere of carbon dioxide to eliminate emission lines of the red CN bands. This light source reduced the required time of exposure by a factor of four; thus the spectroscopic plate was amply exposed in eight hours. During this time approximately two liters of the concentrated hydrogen peroxide were dis-

* Arthur A. Noyes Fellow in Chemistry.
† Provincial Government of Quebec Fellow in Chemistry.
[1] W. G. Penney and G. B. B. M. Sutherland, J. Chem. Phys. **2**, 492 (1934).
[2] The angle between the OH groups as seen projected on a plane normal to the O—O bond.
[3] E. P. Linton and O. Maass, Can. J. Research **7**, 81 (1932).

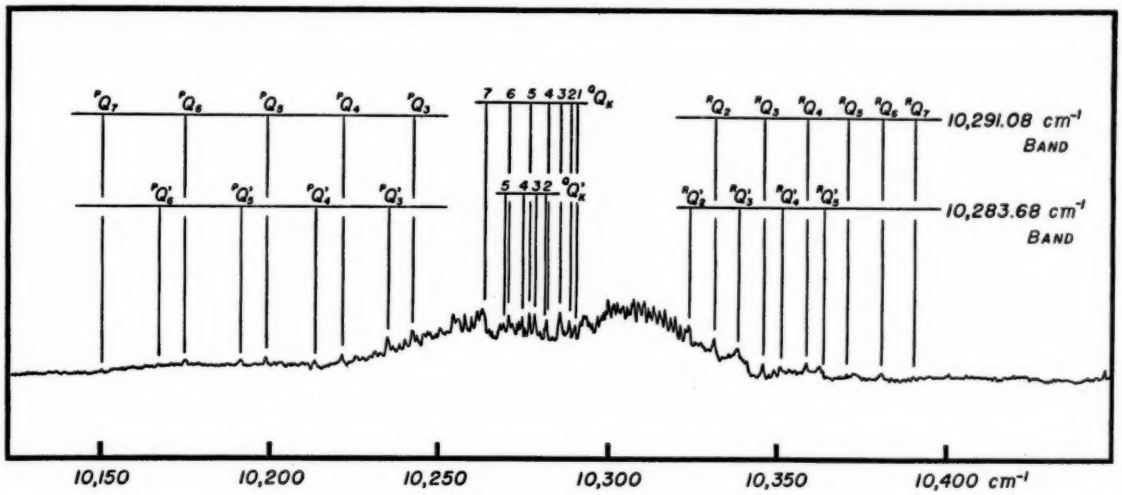


FIG. 1. Microphotometer trace of hydrogen peroxide bands at λ9720.

tilled over. The decomposition was only about 2 percent.

Exploration spectrograms were taken on Eastman 1Z plates with a glass Littrow spectrograph which covered the region between 7500 and 12,000A. Only one band at 9720A was found and this was then photographed in the first order of a twenty-one-foot concave grating spectrograph using Eastman 144Q plates. Measurements of the high dispersion plates were made with reference to third-order iron arc lines.

**Rotational structure of band**

An examination of the high dispersion spectrogram shows that a hybrid band is present which has the $Q$ branches characteristic of both the parallel and the perpendicular bands of a symmetrical rotator molecule. The appearance of this band is analogous to that of the 10,477A band of hydrazoic acid.[4] In the case of hydrogen peroxide, as in the case of hydrazoic acid, there is a strong dependence of the small moment of inertia upon the vibrational state, thus the parallel sub-bands are separated and an unusually marked convergence is present in the perpendicular component. A second hybrid band occurring at a slightly lower frequency also appears. This band is similar to the first but is a little less intense. The ${}^{Q}Q_K$ branches[5] of the parallel component and the ${}^{P}Q_K$ and ${}^{R}Q_K$ branches of the perpendicular component of the two bands have been identified. The branches of the lower frequency band which occur at a displacement of 7.40 cm$^{-1}$ have been given primed symbols.

A careful scrutiny reveals that at least a part of the band system appears to have a quadruplet character rather than a doublet character. Thus in the instances where $K''=3, 4, 5, 6$ a satellite of ${}^{P}Q_{K'}$ occurs at a shift of about minus 3.8 cm$^{-1}$ and also a satellite of ${}^{P}Q_K$ occurs at a shift of about plus 3.8 cm$^{-1}$. These attendant lines are weak and somewhat difficult to measure; never-

TABLE 1. *Frequency and identification of lines in the absorption spectrum of hydrogen peroxide at* λ9720.

| IDENTIFICATION | FREQUENCY cm$^{-1}$ | IDENTIFICATION | FREQUENCY cm$^{-1}$ |
|---|---|---|---|
| ${}^{P}Q_7$ | 10,151.49 | ${}^{Q}Q_4'$ | 10,274.76 |
| $a_6$ | 164.69 | ${}^{Q}Q_5$ | 276.95 |
| ${}^{P}Q_6'$ | 168.21 | ${}^{Q}Q_3'$ | 278.55 |
| ${}^{P}Q_6$ | 175.94 | ${}^{Q}Q_2'$ | 281.39 |
| $b_6$ | 179.65 | ${}^{Q}Q_4$ | 282.12 |
| $a_5$ | 188.24 | ${}^{Q}Q_3$ | 286.06 |
| ${}^{P}Q_5'$ | 191.94 | ${}^{Q}Q_2$ | 288.82 |
| ${}^{P}Q_5$ | 199.25 | ${}^{Q}Q_1$ | 290.40 |
| $b_5$ | 203.23 | ${}^{R}Q_3'$ | 339.21 |
| $a_4$ | 210.28 | ${}^{R}Q_3$ | 346.51 |
| ${}^{P}Q_4'$ | 213.96 | ${}^{R}Q_4'$ | 351.86 |
| ${}^{P}Q_4$ | 221.49 | ${}^{R}Q_4$ | 359.56 |
| $b_4$ | 225.51 | ${}^{R}Q_5'$ | 364.44 |
| $a_3$ | 231.10 | ${}^{R}Q_5$ | 371.71 |
| ${}^{P}Q_3'$ | 235.06 | ${}^{R}Q_6$ | 382.27 |
| ${}^{P}Q_3$ | 242.41 | ${}^{R}Q_7$ | 391.82 |
| ${}^{Q}Q_7$ | 263.44 | | |
| ${}^{Q}Q_5'$ | 269.37 | | |
| ${}^{Q}Q_6$ | 270.72 | | |

[4] E. H. Eyster, J. Chem. Phys. **8**, 135 (1940).

[5] In this nomenclature the large letter describes the behavior of $J$ in transition, the left-hand superscript gives the behavior of $K$, and the right-hand subscript gives the value of $K$ in the lower state.

theless, they do seem to be real. The satellites have been named $a_K$ and $b_K$, respectively. Corresponding branches are not seen on the high frequency side of the band centers.

Figure 1 gives a reproduction of the microphotometer trace of the grating spectrogram while Table I lists the frequencies[6] and identifications of all lines which are assigned as $Q$ branches and also of the satellites mentioned above.

It is to be noted that the ${}^{P}Q_2$, ${}^{P}Q_1$, ${}^{R}Q_0$ and ${}^{R}Q_1$ branches are not identified. There is no clear evidence of these branches although they are the strongest branches in the perpendicular band of the symmetrical rotator. This is probably due to the fact that the hydrogen peroxide molecule is a slightly asymmetric top and consequently the $Q$ branches involving the levels where $K=0$ or 1 are considerably broadened. The ${}^{Q}Q_1$ branch involving transitions between levels where $K=1$, however, is observed. One, indeed, might expect the perpendicular band $Q$ branches to be smeared out before the corresponding parallel band $Q$ branches because in the limiting case of the symmetric rotator[7] we know that the transitions involving the lowest $J$ levels contribute most of the intensity to the latter branches while the higher levels contribute most of the intensity to the perpendicular band $Q$ branches. When transitions between slightly perturbed levels of low $J$ value are the principal contributors to the intensity of a $Q$ branch then the branch is sharp and well defined. On the other hand when transitions between strongly perturbed levels of higher $J$ value substantially contribute to a $Q$ branch then the branch becomes greatly broadened and loses its identity.

The observed spectrum is characterized by multifold overlapping of sub-bands so that the fine structure is considerably confused and it is impossible to analyze the $J$ structure of the sub-bands. Regular fine spacing is observed only on the high frequency side of the band centers. The fine spacing shows convergence towards high frequencies, and it falls off from 1.65 $cm^{-1}$ to 1.59 $cm^{-1}$.

[6] The frequencies are based on two independent sets of measurements on each of two high dispersion spectrograms.

[7] See the expressions for the intensities of the branches of the symmetric rotator bands given by D. M. Dennison, Rev. Mod. Phys. **3**, 313 (1931).

**Analysis of band structure**

The rotational energy of a symmetric rotator may be written:

$$F(J,K,v)=\sum_{ij}{}' X_{ij}{}^{v}\{J(J+1)\}^{i}\{K^2\}^{j}. \quad (1)$$

The constant term $X_{00}{}^{v}$ is omitted in the summation, and $v$ represents the set of quantum numbers required to specify the vibrational state. The first coefficients are related to the effective moments of inertia as follows:

$$X_{01}{}^{v}=A_v-\tfrac{1}{2}(B_v+C_v), \quad X_{10}{}^{v}=\tfrac{1}{2}(B_v+C_v), \quad (2)$$

$$A_v=h/8\pi^2cI_A{}^{v}, \quad B_v=h/8\pi^2cI_B{}^{v}, \quad C_v=h/8\pi^2cI_C{}^{v}, \quad A_v\gg B_v=C_v. \quad (3)$$

Hydrogen peroxide seems to be a slightly asymmetric rotator with $B_v$ almost equal to $C_v$ so that Eq. (1) very closely represents the characteristic energy values of the rotating molecule.

The constants $X_{01}{}^{0}$ and $X_{02}{}^{0}$ are evaluated by employing the following relations:

$$\frac{\Delta F''(K)}{2K+1}=X_{01}{}^{0}+2X_{02}{}^{0}M+\cdots;\ M=(K+\tfrac{1}{2})^2+\tfrac{1}{4}$$

and

$$\frac{\Delta_2 F''(K)}{4K}=X_{01}{}^{0}+2X_{02}{}^{0}M+\cdots;\ M=K^2+1,$$

where the term differences are given by:

$$\Delta F''(K)={}^{Q}Q_K-{}^{P}Q_{K+1}={}^{R}Q_K-{}^{Q}Q_{K+1}$$

and

$$\Delta_2 F''(K)={}^{R}Q_{K-1}-{}^{P}Q_{K+1}.$$

The frequencies of the assigned lines were found to be compatible with the above relations within experimental error. The best values for the constants of the equations were found to be:

$$X_{01}{}^{0}=9.23_1\ cm^{-1}, \quad X_{02}{}^{0}=-0.0008_5\ cm^{-1}.$$

Similarly the rotational constants for the excited state, which we will denote by $v=3$, were found to be:

$$X_{01}{}^{3}=8.66_8\ cm^{-1}, \quad X_{02}{}^{3}=-0.0008_6\ cm^{-1}.$$

An identical treatment of the frequencies of the $Q$ branches which are denoted by primed symbols gave rotational constants which, within

experimental error, were exactly the same as the above. The two hybrid bands thus seem to have precisely the same rotational structure.

Since it was impossible to analyze the $J$ structure of the bands we were obliged to obtain an estimate of the rotational constant $X_{10}^0$ (which must be very nearly equal to $X_{10}^3$) from the regular fine spacing which is clearly resolved only on the high frequency side of the band centers. We took 1.65 $cm^{-1}$ as the best average value of the fine spacing. This is related to the rotational constant as follows:

$$2X_{10}^0 \approx 1.65 \text{ cm}^{-1}$$

thus

$$X_{10}^0 \approx 0.82_5 \text{ cm}^{-1}.$$

We believe that the observed fine spacing arises from $R$ branches of the parallel sub-bands. This being the case the convergence is such that the above estimated value of $X_{10}^0$ may be a little low.

The center of the band denoted by unprimed $Q$ branches is given by:

$$G(3)-G(0)={}^QQ_K+K^2(X_{01}^0-X_{01}^3)+K^4(X_{02}^0-X_{02}^3)+\cdots.$$

The best value for this was found to be 10,291.08 $cm^{-1}$. Similarly the center of the band denoted by primed $Q$ branches was found to be 10,283.68 $cm^{-1}$.

The rotational constants $X_{01}^0=9.23_1$ $cm^{-1}$ and $X_{10}^0 \approx 0.82_5$ $cm^{-1}$ correspond, respectively, to the values of $I_A^0=2.78_6\times10^{-40}$ g $cm^2$ for the small moment of inertia and $2I_B^0I_C^0/(I_B^0+I_C^0) \approx 33.9\times10^{-40}$ g $cm^2$ for the harmonic mean of the two larger moments of inertia of hydrogen peroxide.

### Structure of hydrogen peroxide

The harmonic mean of the two larger moments of inertia is principally dependent on the length of the O—O bond in hydrogen peroxide. Calculation shows that the value given above corresponds to an O—O distance of about 1.48A.

The fact that the observed bands are of the hybrid type shows that the OH groups of hydrogen peroxide are not in the planar *cis*-configuration. If these groups were so situated, the molecule would have a point group symmetry $C_{2v}$ and one would only observe pure perpendicular or parallel type bands. Incidentally, we also know that the OH stretching vibration involved in the observed bands is antisymmetric. A symmetric stretching frequency would give a pure perpendicular band.

As shown by Linton and Maass[3] the hydrogen peroxide molecule has a fairly large electric dipole moment. This rules out the *trans*-configuration and, thus, since the *cis*-form is ruled out spectroscopically, the hydrogen peroxide molecule must have a non-planar structure.

We are unable to give an estimate of the azimuthal angle[2] of the OH groups from our spectroscopic data although it appears that this angle cannot be between 85° and 95°. We conclude this because the absence of the ${}^PQ_2$, ${}^PQ_1$, ${}^RQ_0$ and ${}^RQ_1$ branches indicates the molecule is actually an asymmetric top while a calculation of the moments of inertia shows that a hydrogen peroxide molecule with an azimuthal angle of around 90° is not significantly asymmetric.

It is interesting to note that Lu, Hughes and Giguère[8] in their recent x-ray studies of the "hyperol" crystal in these laboratories have found the hydrogen peroxide molecule to have an azimuthal angle of about 106°.

### Discussion of the band structure

The bands which have been described and analyzed correspond closely to the type of band which is characteristic of a spindle-shaped symmetrical top molecule that is fairly rigid. The complete rotation of the OH groups about the O—O bond in hydrogen peroxide must be strongly hindered. A very different band structure would appear if there were a free or a weakly hindered internal rotation. In this case the band would have a more extended structure, a larger $Q$ spacing and, in the event of a weakly hindered rotation, an irregular $Q$ spacing.

The occurrence of two hybrid bands separated by 7.40 $cm^{-1}$ must be explained. A visual examination of the spectrogram and the microphotometer trace shows that the low frequency band must be more than one-half as intense as the other band. The ${}^PQ_6$ and ${}^PQ_5'$ branches which

[8] Chia-Si Lu, E. W. Hughes, and P. A. Giguère, "Crystal structure of the urea-hydrogen peroxide addition compound, $CO(NH_2)\cdot H_2O_2$," to be published in J. Am. Chem. Soc.

occur where the background absorption is weak seem to have just about the same intensity. Assuming relative intensities of the $Q$ branches are given by the matrix elements of the electric moment for the symmetric rotator given by Dennison,[7] we calculate that the perpendicular component of the low frequency band is about two-thirds as intense as the same component of the other band.

Three possible explanations for the hybrid bands occur to us. The two bands may be thought to originate from two entirely different vibrational transitions. As they both have to be antisymmetric OH stretching frequencies, one might be the third harmonic of the antisymmetric frequency, and the other the combination frequency of the antisymmetric stretching frequency and the second harmonic of the symmetric stretching frequency. This explanation seems improbable, however, since the expected frequency difference is much larger than the observed doublet separation.

The two bands may be imagined to be members of a sequence of bands all of which involve the same vibrational transition but which involve absorption from different excited states. Thus the strongest band may originate in a transition from the ground state while the band displaced 7.40 $cm^{-1}$ to lower frequencies originates in a vibrational transition that is different in that the torsion oscillation is excited in the lower and upper levels. In this case, however, there should appear a third member of the band sequence which is displaced about 7.40 $cm^{-1}$ from the low frequency band and which is about two-thirds as strong as this band. Actually one is unable to discern a trace of a third member of the imagined band sequence; consequently we have decided that the two observed bands are not members of a sequence of bands involving absorption from different excited states of the torsion vibration.

According to theory the vibrational levels of non-planar hydrogen peroxide are doubled. There will be a sizable doublet splitting if one of the barriers of the potential hindering the internal rotation of the OH groups is low. We are inclined to believe that this situation most plausibly accounts for the two bands of nearly equal intensity and identical rotational structure; hence we have tentatively decided that the bands arise from transitions between well-split doublet levels. The separation of 7.40 $cm^{-1}$ of the observed bands probably represents the difference in the splitting of the ground state and the upper vibrational state. The doublet splitting which results from the double minimum and the one low barrier in the torsion potential may be expected to be different in the ground state from that in the excited vibrational state since there should be a rather strong interaction between the OH stretching motion and the torsional motion. Stretching of the OH bonds changes the moments of inertia of the torsionally oscillating OH groups and also changes the hindering potential.

At present we are unable to give an explanation of the apparent quadruplet character of part of the observed rotational structure.

In order that our decision concerning the origin of the bands may be confirmed a further spectroscopic study of hydrogen peroxide should be made. We hope to undertake soon the study of the fundamental bands and thereby obtain some additional information regarding the spectroscopic behavior and the nature of hydrogen peroxide.

In conclusion the authors would like to express their appreciation to Professor Richard M. Badger for his helpful advice and continued interest in this study.

# Note on Diamagnetic Anisotropy and the Method of Molecular Orbitals

HARVEY BROOKS
*Harvard University, Cambridge, Massachusetts*
(Received March 21, 1941)

The simple London theory of the diamagnetic anisotropy of organic molecules containing benzene rings is modified to include the effect of a non-orthogonality of 25 percent between atomic wave functions on adjacent atoms. Except in the case of diphenyl the effect of such a modification is surprisingly small; that is, although the contributions to the anisotropy from individual electronic orbits is materially changed the resultant contribution of all the electrons is hardly altered. The significance of this result is discussed.

## INTRODUCTION

RECENTLY a theory has been developed by F. London[1] to explain the large diamagnetic anisotropy of certain aromatic molecules. Considering the crudeness of the model the results are in remarkably good agreement with experiment, especially in view of the fact that the diamagnetism is far more sensitive than the energy to the form of the approximate wave functions. The purpose of the present note is to examine the effects of a certain improvement in the model, secured by taking into consideration the large non-orthogonality between the atomic wave functions.

## GENERAL FORMULAE

The present discussion follows closely the notation and procedure of London's paper.[1] The method used is the "approximation of tight binding" as applied to aromatic molecules, for example, in the work of E. Hueckel.[2] Each atomic function satisfies the wave equation in a magnetic field with the origin of the vector potential chosen at the given atom, but in setting up the molecular orbitals the atomic functions are subject to a gauge transformation which transfers the vector potential to which they refer to a common origin at the center of the molecule. To make the discussion definite we consider the secular equation for naphthalene.[3] When this equation is revised to take account of the overlap integral $\delta$ between adjacent atomic wave functions, it has the form:

$$\begin{vmatrix}
-x & m\epsilon_2 & 0 & 0 & 0 & 0 & 0 & 0 & 0 & m\epsilon_3^* \\
m\epsilon_2^* & -x & m\epsilon_1 & 0 & 0 & 0 & 0 & 0 & 0 & 0 \\
0 & m\epsilon_1^* & -x & m\epsilon_1 & 0 & 0 & 0 & m & 0 & 0 \\
0 & 0 & m\epsilon_1^* & -x & m\epsilon_2 & 0 & 0 & 0 & 0 & 0 \\
0 & 0 & 0 & m\epsilon_2^* & -x & m\epsilon_3 & 0 & 0 & 0 & 0 \\
0 & 0 & 0 & 0 & m\epsilon_3^* & -x & m\epsilon_2 & 0 & 0 & 0 \\
0 & 0 & 0 & 0 & 0 & m\epsilon_2^* & -x & m\epsilon_1 & 0 & 0 \\
0 & 0 & m & 0 & 0 & 0 & m\epsilon_1^* & -x & m\epsilon_1 & 0 \\
0 & 0 & 0 & 0 & 0 & 0 & 0 & m\epsilon_1^* & -x & m\epsilon_2 \\
m\epsilon_3 & 0 & 0 & 0 & 0 & 0 & 0 & 0 & m\epsilon_2^* & -x
\end{vmatrix} = 0 \quad (1)$$

where

$$m=1-\delta(x+\alpha), \quad x=(E-E_0)/W_1, \quad \alpha=E_0/W_1,$$

$$E_0=\int u_K V u_K d\tau, \quad W_1=\int u_K V u_{K+1}\delta\tau, \quad (2)$$

$$\epsilon_1=\exp(2\pi i f_{12}), \quad f_{12}=(e/hc)\tfrac{1}{2}H(x_1y_2-x_2y_1).$$

($x_K$, $y_K$ coordinates of atom $K$).

If we divide each row or column of this determinant by $1-\delta(x+\alpha)$, we obtain a secular equation which is formally identical with London's, except that the energy variable is replaced by

$$y=\frac{x}{1-\delta(x+\alpha)}. \quad (3)$$

This secular equation we shall hereafter designate by $P$. Let $y_1$ be a root of $P$; then from (3) we obtain immediately that

$$x=(1-\delta\alpha)(1+\delta y_1)^{-1}y_1 \quad (4)$$

or

$$E=E_0+\frac{W_1-\delta E_0}{1+\delta y_1}y_1. \quad (4')$$

[1] F. London, J. de phys. et rad. **8**, 397 (1937), designated as I. H. Brooks, J. Chem. Phys. **8**, 939 (1940).
[2] E. Hueckel, Zeits. f. Physik **70**, 204 (1931).
[3] Reference 1, p. 403.

TABLE I. *Comparison of anisotropy with and without non-orthogonality.*

| $y'$ | $y''$ | $y'''$ | $x'''$ |
|---|---|---|---|
| | *Benzene* | | |
| 2 | 0 | −0.0278 | −0.0123 |
| 1 | $1/(2\sqrt{3})$ | −0.0139 | −0.0195 |
| | $-1/(2\sqrt{3})$ | −0.0139 | −0.0195 |
| | Sum = | −0.0555 | −0.0513 |
| | *Naphthalene* | | |
| 2.3028 | | −0.0322 | −0.0134 |
| 1.6181 | | 0.1382 | 0.0700 |
| 1.3028 | | −0.1985 | −0.1135 |
| 0.6181 | | −0.3615 | −0.2710 |
| 1.0 | | 0.3333 | 0.2135 |
| | Sum = | −0.1207 | −0.1144 |
| | *Anthracene* | | |
| 0.414 | | −0.289 | −0.237 |
| 1.414 | | 0.194 | 0.105 |
| | | −0.092 | −0.050 |
| 2.0 | | 0.036 | 0.016 |
| 2.414 | | −0.041 | −0.016 |
| | Sum = | −0.192 | −0.182 |

| $y'$ | $y'''$ | $x'''$ |
|---|---|---|
| | *Phenanthrene* | |
| 0.605 | −0.779 | −0.586 |
| 0.770 | 0.617 | 0.434 |
| 1.14 | 0.014 | 0.0085 |
| 1.26 | −0.001 | −0.0006 |
| 1.52 | −0.033 | −0.0173 |
| 1.95 | 0.038 | 0.0172 |
| 2.44 | −0.033 | −0.0127 |
| Sum = | −0.177 | −0.1569 |
| | *Pyrene* | |
| 0.4450 | −0.483 | −0.389 |
| 0.8794 | 0.492 | 0.330 |
| 1.0 | −0.333 | −0.213 |
| 1.2470 | −0.913 | −0.531 |
| 1.3743 | 1.169 | 0.646 |
| 1.8019 | −0.386 | −0.183 |
| 2.0 | 0.254 | 0.113 |
| 2.532 | −0.048 | −0.018 |
| Sum = | −0.248 | −0.245 |
| | *Diphenyl* | |
| 2.28 | −0.020 | −0.0081 |
| 1.89 | −0.025 | −0.0115 |
| 1.33 | 0.201 | 0.113 |
| 0.0705 | −0.279 | −0.269 |
| Sum = | −0.123 | −0.176 |

Thus the eigenvalues of Eq. (1) are immediately expressible in terms of the eigenvalues of $P$, which have already been obtained by London in I, provided we make the usual approximation of disregarding integrals between all but nearest neighbors. From Eq. (4′) we see that $(W_1-\delta E_0)$ actually plays the same role as $W_1$ in London's theory, i.e., it is the analog of the "hopping" integral. The denominator $1+\delta y_1$ is just a renormalization factor.

In the presence of a magnetic field the eigenvalues $y_1$ depend in general on the flux $2\pi f=2\pi eS/hc$, and so also does $x$, so that we have

$$y=y'+y''(2\pi f)+y'''(2\pi f)^2,$$
$$x=x'+x''(2\pi f)+x'''(2\pi f)^2. \tag{5}$$

Making these substitutions in Eq. (4) and equating the coefficients of successive powers of $(2\pi f)$, we obtain the following results

$$x'=(1-\delta\alpha)(1+\delta y')^{-1}y', \tag{6a}$$

$$x''=(1-\delta\alpha)(1+\delta y')^{-2}y'', \tag{6b}$$

$$x'''=\frac{1-\delta\alpha}{(1+\delta y')^2}y'''-\frac{1-\delta\alpha}{(1+\delta y')^3}y''^2. \tag{6c}$$

For the anisotropic part of the susceptibility it is readily shown that

$$\chi_p=-2|W_1|x'''(2\pi eS/hc)^2, \tag{7}$$

where $\chi_p$ is the contribution of a single electron and the summation is carried out over all the occupied orbitals, $x'''$ being taken from Eq. (6c).

This general theory is applicable to each of the six aromatic compounds considered by London. In formula (6c) the quantities $y'$, $y''$, and $y'''$ have already been obtained in London's paper, since they are simply the roots of a secular equation of type $P$, which is identical with London's. Formula (6c) is a good illustration of the statement in the introduction that changes in the wave function affect the diamagnetism much more significantly than the energy, for the renormalization factor occurs squared and cubed in the field dependent parts of the energy.

## NUMERICAL RESULTS

In Table I the calculations have been made with formula (7), assuming $\delta=\frac{1}{4}$.[4] All the numerical values given are measured in units of $(1-\delta\alpha)$. The column headed $y'$ gives the non-magnetic part of the energy of the given orbital, while the columns headed $y'''$ and $x'''$ are proportional to the contributions to the anisotropy from this orbital without and with non-orthogonality taken into account, respectively. Table II shows the anisotropies of the various aromatic molecules relative to benzene as determined with and without non-orthogonality.

The notable feature of these results is the small extent to which even quite a large non-orthogonality alters the total anisotropy even though the contributions from the individual electrons are materially changed. The alteration of the relative anisotropies of different molecules is even smaller. The satisfactory result is probably to be ascribed in all cases to the fact that

TABLE II. *Relative anisotropies with and without non-orthogonality.*

| | $(\Delta\chi/\Delta\chi_{benz})$ LONDON | CORRECTED | EXPERIMENT |
|---|---|---|---|
| Naphthalene | 2.19 | 2.23 | 2.11 |
| Anthracene | 3.45 | 3.54 | 3.38 |
| Phenanthrene | 3.19 | 3.06 | 3.07 |
| Pyrene | 4.46 | 4.75 | 4.31 |
| Diphenyl | 2.21 | 3.42 | 2.20 |

[4] A. L. Sklar and M. Goeppert Mayer, J. Chem. Phys. **6**, 645 (1938).

we are dealing in effect with a half-filled shell, for which the properties of the whole half-shell may often be expected to be invariant of the particular form of the individual wave functions. The one exception to this rule seems to be diphenyl, for which the simple and corrected theories give widely divergent results, experiment being definitely in favor of the simpler theory.

Such refinements of the simple molecular orbital treatment should not be taken too seriously, but they do serve to illustrate the very provisional and crude nature of the approximations used in describing the structure of polyatomic molecules. The neglected effects are by no means small. The surprising thing is, indeed, that the crude theories give such good results. In the case of magnetic anisotropy the good results of the London theory, as pointed out by London, are probably to be ascribed to geometrical considerations which are invariant of the model, but which are well represented in the crude molecular orbital picture.

---

JUNE, 1941 JOURNAL OF CHEMICAL PHYSICS VOLUME 9

# Tables of Thermodynamic Functions of Paramagnetic Substances and Harmonic Oscillators

J. R. AND R. A. HULL
*Clarendon Laboratory, Oxford, England*
(Received March 5, 1941)

Numerical values of the partition function, magnetic moment, entropy, and temperature derivative of the entropy are tabulated for free paramagnetic ions with $j=\frac{1}{2}$, $\frac{3}{2}$, and $\frac{5}{2}$. These tables are needed in connection with experiments on adiabatic demagnetization. As a by-product, the thermodynamic functions for an Einstein oscillator are computed numerically to a higher degree of accuracy than in the tables available in the literature.

## INTRODUCTION

THE calculations shown in this paper have as their principal object the evaluation of the entropy and its derivative for ideal paramagnetic substances in terms of $H/T$. Such theoretical values are necessary in interpreting the results of magnetic experiments, particularly at low temperatures, and these applications are dealt with more fully below.

The starting point for the calculation of entropy $S$ is the partition function $Q$, in this case $\sum e^{mx}$. The summation over $m$ is from $-j$ to $+j$ where $j$ is the angular momentum quantum number appropriate to the substance considered, and $x$ is proportional to $H/T$. $S$ and its derivative can then be obtained in terms of $Q$ and its derivative, as is done in the first half of this paper. It is also possible to obtain $S$ in a more indirect (though actually briefer) way; for $Q$ can be rewritten as the ratio of the partition functions for two Einstein oscillators, and so $S$ and its derivative are obtained as the differences between the corresponding quantities for these Einstein oscillators. This method is used in the second part of the paper.

It was felt advisable to do the calculations by both methods as a check on accuracy. Incidentally several other useful thermodynamic quantities were evaluated as intermediate steps, and these have also been tabulated. They include either explicitly or else implicitly (as quantities obtainable simply by addition) the magnetization, total energy and free energy of a paramagnetic substance, and the total energy and free energy of an Einstein oscillator. Some of these quantities have already been tabulated in the literature, e.g., the Einstein functions in Landolt-Bornstein, but not in sufficient accuracy to be always useful.

TABLE I.

| $x$ | $Q$ | $\ln Q$ | $M/N\mu$ | $(M/N\mu)^2$ | $S/R$ | $(-xdS/dx)/R$ |
|---|---|---|---|---|---|---|
| | | | j=1/2 | | | |
| 0 | 2 | 0.69315 | 0 | 0 | 0.69315 | 0 |
| 0.02 | 2.0001 | 0.69320 | 0.01000 | 0.00010 | 0.69310 | 0.00010 |
| 0.04 | 2.0004 | 0.69335 | 0.02000 | 0.00040 | 0.69294 | 0.00040 |
| 0.06 | 2.0009 | 0.69360 | 0.02999 | 0.00090 | 0.69270 | 0.00090 |
| 0.08 | 2.0016 | 0.69395 | 0.03998 | 0.00160 | 0.69235 | 0.00160 |
| 0.10 | 2.0025 | 0.69440 | 0.04996 | 0.00250 | 0.69190 | 0.00249 |
| 0.12 | 2.0036 | 0.69495 | 0.05993 | 0.00359 | 0.69135 | 0.00359 |
| 0.14 | 2.0049 | 0.69560 | 0.06989 | 0.00488 | 0.69070 | 0.00488 |
| 0.16 | 2.0064 | 0.69634 | 0.07983 | 0.00637 | 0.68996 | 0.00636 |
| 0.18 | 2.0081 | 0.69719 | 0.08976 | 0.00806 | 0.68911 | 0.00804 |
| 0.20 | 2.0100 | 0.69814 | 0.09967 | 0.00993 | 0.68817 | 0.00990 |
| 0.24 | 2.0144 | 0.70033 | 0.11943 | 0.01426 | 0.68600 | 0.01420 |
| 0.28 | 2.0196 | 0.70292 | 0.13909 | 0.01935 | 0.68344 | 0.01922 |
| 0.30 | 2.0225 | 0.70436 | 0.14889 | 0.02217 | 0.68202 | 0.02200 |
| 0.32 | 2.0257 | 0.70589 | 0.15865 | 0.02517 | 0.68051 | 0.02496 |
| 0.36 | 2.0325 | 0.70926 | 0.17808 | 0.03171 | 0.67721 | 0.03137 |
| 0.40 | 2.0401 | 0.71302 | 0.19738 | 0.03896 | 0.67354 | 0.03844 |
| 0.50 | 2.0628 | 0.72408 | 0.24492 | 0.05999 | 0.66285 | 0.05875 |
| 0.60 | 2.0907 | 0.73749 | 0.29131 | 0.08486 | 0.65009 | 0.08236 |
| 0.70 | 2.1238 | 0.75319 | 0.33638 | 0.11315 | 0.63546 | 0.10864 |
| 0.80 | 2.1621 | 0.77110 | 0.37995 | 0.14436 | 0.61912 | 0.13690 |
| 0.90 | 2.2059 | 0.79115 | 0.42190 | 0.17800 | 0.60130 | 0.16646 |
| 1.0 | 2.2553 | 0.81326 | 0.46212 | 0.21355 | 0.58220 | 0.19661 |
| 1.1 | 2.3102 | 0.83734 | 0.50052 | 0.25052 | 0.56205 | 0.22672 |
| 1.2 | 2.3709 | 0.86328 | 0.53705 | 0.28842 | 0.54105 | 0.25617 |
| 1.3 | 2.4376 | 0.89100 | 0.57167 | 0.32681 | 0.51942 | 0.28442 |
| 1.4 | 2.5103 | 0.92041 | 0.60437 | 0.36526 | 0.49735 | 0.31102 |
| 1.5 | 2.5894 | 0.95141 | 0.63515 | 0.40341 | 0.47505 | 0.33558 |
| 1.6 | 2.6749 | 0.98390 | 0.66404 | 0.44095 | 0.45267 | 0.35780 |
| 1.7 | 2.7671 | 1.01779 | 0.69107 | 0.47758 | 0.43038 | 0.37745 |
| 1.8 | 2.8662 | 1.05298 | 0.71630 | 0.51308 | 0.40831 | 0.39440 |
| 1.9 | 2.9725 | 1.08939 | 0.73978 | 0.54728 | 0.38659 | 0.40858 |
| 2.0 | 3.0862 | 1.12693 | 0.76159 | 0.58003 | 0.36533 | 0.41998 |
| 2.1 | 3.2076 | 1.16552 | 0.78181 | | 0.34462 | |
| 2.2 | 3.3370 | 1.20508 | 0.80050 | | 0.32453 | 0.43463 |
| 2.3 | 3.4748 | 1.24555 | 0.81775 | | 0.30513 | |
| 2.4 | 3.6213 | 1.28684 | 0.83366 | | 0.28645 | 0.43923 |
| 2.5 | 3.7768 | 1.32889 | 0.84828 | | 0.26854 | |
| 2.6 | 3.9418 | 1.37165 | 0.86172 | | 0.25141 | 0.43506 |
| 2.7 | 4.1167 | 1.41505 | 0.87405 | | 0.23507 | |
| 2.8 | 4.3018 | 1.45903 | 0.88535 | | 0.21954 | 0.42366 |
| 2.9 | 4.4977 | 1.50356 | 0.89569 | | 0.20481 | |
| 3.0 | 4.7048 | 1.54859 | 0.90515 | | 0.19087 | 0.40660 |
| 3.1 | 4.9237 | 1.59407 | 0.91379 | | 0.17769 | |
| 3.2 | 5.1549 | 1.63995 | 0.92167 | | 0.16528 | 0.38535 |
| 3.3 | 5.3990 | 1.68622 | 0.92886 | | 0.15361 | |
| 3.4 | 5.6566 | 1.73283 | 0.93541 | | 0.14263 | 0.36128 |
| 3.5 | 5.9284 | 1.77975 | 0.94138 | | 0.13234 | |
| 3.6 | 6.2149 | 1.82696 | 0.94681 | | 0.12271 | 0.33553 |
| 3.7 | 6.5171 | 1.87442 | 0.95175 | | 0.11369 | |
| 3.8 | 6.8355 | 1.92212 | 0.95624 | | 0.10527 | 0.31304 |
| 3.9 | 7.1710 | 1.97004 | 0.96032 | | 0.09742 | |
| 4.0 | 7.5244 | 2.01815 | 0.96403 | | 0.09009 | 0.28260 |
| 4.2 | 8.2886 | 2.11488 | 0.97045 | | 0.07694 | 0.25676 |
| 4.4 | 9.1358 | 2.21220 | 0.97574 | | 0.06557 | |
| 4.6 | 10.074 | 2.31000 | 0.98010 | | 0.05578 | |
| 4.8 | 11.114 | 2.40820 | 0.98368 | | 0.04738 | 0.18653 |
| 5.0 | 12.265 | 2.50672 | 0.98661 | | 0.04018 | |
| 5.2 | 13.538 | 2.60550 | 0.98903 | | 0.03403 | |
| 5.4 | 14.947 | 2.70451 | 0.99101 | | 0.02879 | 0.13054 |
| 5.6 | 16.505 | 2.80369 | 0.99263 | | 0.02432 | |
| 5.8 | 18.229 | 2.90302 | 0.99396 | | 0.02053 | |
| 6.0 | 20.135 | 3.00248 | 0.99506 | | 0.01731 | 0.08879 |

| $x$ | $Q$ | $\ln Q$ | $M/N\mu$ | $(M/N\mu)^2$ | $S/R$ | $(-xdS/dx)/R$ |
|---|---|---|---|---|---|---|
| | | | j=3/2 | | | |
| 0 | 4 | 1.38629 | 0 | 0 | 1.38629 | 0 |
| 0.02 | 4.0010 | 1.38654 | 0.04999 | 0.00250 | 1.38604 | 0.00050 |
| 0.04 | 4.0040 | 1.38729 | 0.09995 | 0.00999 | 1.38530 | 0.00200 |
| 0.06 | 4.0090 | 1.38854 | 0.14984 | 0.02245 | 1.38405 | 0.00449 |
| 0.08 | 4.0160 | 1.39029 | 0.19964 | 0.03986 | 1.38231 | 0.00796 |
| 0.10 | 4.0250 | 1.39254 | 0.24929 | 0.06215 | 1.38007 | 0.01239 |
| 0.12 | 4.0361 | 1.39528 | 0.29878 | 0.08927 | 1.37735 | 0.01778 |
| 0.14 | 4.0492 | 1.39851 | 0.34807 | 0.12115 | 1.37415 | 0.02410 |
| 0.16 | 4.0643 | 1.40224 | 0.39713 | 0.15771 | 1.37047 | 0.03132 |
| 0.18 | 4.0814 | 1.40645 | 0.44592 | 0.19884 | 1.36632 | 0.03941 |
| 0.20 | 4.1007 | 1.41115 | 0.49442 | 0.24445 | 1.36171 | 0.04834 |
| 0.24 | 4.1454 | 1.42200 | 0.59042 | 0.34860 | 1.35115 | 0.06860 |
| 0.28 | 4.1986 | 1.43476 | 0.68490 | 0.46909 | 1.33887 | 0.09178 |
| 0.30 | 4.2285 | 1.44184 | 0.73151 | 0.53511 | 1.33212 | 0.10436 |
| 0.32 | 4.2605 | 1.44939 | 0.77766 | 0.60476 | 1.32496 | 0.11755 |
| 0.36 | 4.3312 | 1.46585 | 0.86851 | 0.75431 | 1.30952 | 0.14553 |
| 0.40 | 4.4111 | 1.48412 | 0.95727 | 0.91637 | 1.29266 | 0.17534 |
| 0.50 | 4.6522 | 1.53734 | 1.1692 | 1.3669 | 1.24505 | 0.25536 |
| 0.60 | 4.9568 | 1.60077 | 1.3654 | 1.8643 | 1.19115 | 0.33853 |
| 0.70 | 5.3313 | 1.67360 | 1.5451 | 2.3874 | 1.13282 | 0.41966 |
| 0.80 | 5.7835 | 1.75500 | 1.7080 | 2.9173 | 1.07179 | 0.49470 |
| 0.90 | 6.3226 | 1.84413 | 1.8545 | 3.4392 | 1.00961 | 0.56086 |
| 1.0 | 6.9601 | 1.94019 | 1.9853 | 3.9414 | 0.94754 | 0.61659 |
| 1.1 | 7.7092 | 2.04242 | 2.1015 | 4.4164 | 0.88658 | 0.66135 |
| 1.2 | 8.5859 | 2.15012 | 2.2044 | 4.8592 | 0.82750 | 0.69540 |
| 1.3 | 9.6085 | 2.26265 | 2.2951 | 5.2676 | 0.77083 | 0.71948 |
| 1.4 | 10.799 | 2.37945 | 2.3751 | 5.6410 | 0.71690 | 0.73468 |
| 1.5 | 12.183 | 2.50001 | 2.4454 | 5.9802 | 0.66591 | 0.74218 |
| 1.6 | 13.789 | 2.62385 | 2.5074 | 6.2869 | 0.61796 | 0.74315 |
| 1.7 | 15.652 | 2.75062 | 2.5619 | 6.5632 | 0.57303 | 0.73874 |
| 1.8 | 17.813 | 2.87993 | 2.6099 | 6.8116 | 0.53102 | 0.72993 |
| 1.9 | 20.318 | 3.01151 | 2.6523 | 7.0345 | 0.49185 | 0.71763 |
| 2.0 | 23.221 | 3.14508 | 2.6897 | 7.2342 | 0.45543 | 0.70257 |
| 2.1 | 26.587 | 3.28040 | 2.7227 | | 0.42156 | |
| 2.2 | 30.487 | 3.41729 | 2.7520 | | 0.39011 | |
| 2.3 | 35.007 | 3.55555 | 2.7779 | | 0.36091 | |
| 2.4 | 40.247 | 3.69503 | 2.8010 | | 0.33382 | 0.62576 |
| 2.5 | 46.322 | 3.83561 | 2.8215 | | 0.30871 | |
| 2.6 | 53.364 | 3.97714 | 2.8398 | | 0.28543 | |
| 2.7 | 61.532 | 4.11955 | 2.8561 | | 0.26386 | |
| 2.8 | 71.003 | 4.26272 | 2.8706 | | 0.24386 | |
| 2.9 | 81.989 | 4.40659 | 2.8836 | | 0.22534 | |
| 3.0 | 94.733 | 4.55106 | 2.8953 | | 0.20817 | 0.49539 |
| 3.1 | 109.52 | 4.69609 | 2.9057 | | 0.19228 | |
| 3.2 | 126.67 | 4.84161 | 2.9150 | | 0.17756 | |
| 3.3 | 146.58 | 4.98758 | 2.9234 | | 0.16393 | |
| 3.4 | 169.68 | 5.13394 | 2.9310 | | 0.15131 | |
| 3.5 | 196.50 | 5.28066 | 2.9377 | | 0.13963 | |
| 3.6 | 227.63 | 5.42770 | 2.9438 | | 0.12882 | |
| 3.7 | 263.76 | 5.57504 | 2.9493 | | 0.11882 | |
| 3.8 | 305.71 | 5.72262 | 2.9542 | | 0.10957 | |
| 3.9 | 354.41 | 5.87045 | 2.9587 | | 0.10102 | |
| 4.0 | 410.96 | 6.01849 | 2.9627 | | 0.09311 | |
| 4.2 | 552.86 | 6.31511 | 2.9696 | | 0.07904 | |
| 4.4 | 744.23 | 6.61235 | 2.9751 | | 0.06705 | |
| 4.6 | 1002.4 | 6.91010 | 2.9797 | | 0.05681 | |
| 4.8 | 1350.5 | 7.20826 | 2.9834 | | 0.04809 | |
| 5.0 | 1820.3 | 7.50676 | 2.9864 | | 0.04068 | |
| 5.2 | 2454.1 | 7.80553 | 2.9889 | | 0.03438 | |
| 5.4 | 3309.4 | 8.10453 | 2.9909 | | 0.02903 | |
| 5.6 | 4463.6 | 8.40371 | 2.9926 | | 0.02449 | |
| 5.8 | 6021.1 | 8.70303 | 2.9939 | | 0.02064 | |
| 6.0 | 8123.2 | 9.00248 | 2.9950 | | 0.01739 | |

## I. DIRECT PARTITION FUNCTION METHOD

The partition function $Q$ has already been defined as

$$\sum_{m=-j}^{j} e^{mx}, \quad \text{where} \quad x=g\mu H/kT,$$

$g$ is the Landé splitting factor, and $\mu$ is the Bohr magneton. The thermodynamic functions for a gram ion are obtained from $Q$ as follows: the free energy $F=-RT\ln Q$; the entropy $S=-\partial F/\partial T$, which is identical with $R(\ln Q-Q^{-1}xdQ/dx)$; the magnetization $M=RT\partial(\ln Q)/\partial H$, which is identical with $N\mu 2Q^{-1}dQ/dx$; the derivative $(-xdS/dx)$. It should be noted that $(-xdS/dx)=T(\partial S/\partial T)_H=H(\partial S/\partial H)_T$, where $T(\partial S/\partial T)_H$ is, of course, the specific heat in a magnetic field; and it is sometimes convenient to use the fact that $d(S/R)/dx=\frac{1}{2}xd(M/N\mu)/dx$. The total energy $U$ can be obtained immediately from the relation $U=F+TS$. The tables of these functions have been arranged separately according to the value of $j$ (see Table I). As regards numerical values, $g$ has the value 2 for the paramagnetic substances most commonly used, which depend on the paramagnetism of the free electron spin in

Ti, Cr, Mn and Fe ions. The values of the other necessary constants according to the most reliable data at present available are:

$$N=6.024 \quad 10^{23}$$
$$k=1.380 \quad 10^{-16} \text{ erg/deg.}$$
$$R=8.302 \quad 10^{7} \text{ erg/deg.}$$
$$\mu=9.28 \quad 10^{-21} \text{ erg/gauss.}$$

From these values it follows that if $H$ is expressed in kilogauss, then $x=0.134_5 H/T$.

## Uses

It may be of interest to mention some of the uses to which these tables can be put, particularly in connection with the demagnetization technique. The value of $M$, for instance, is used when computing the reduction in the effective applied magnetic field caused by the demagnetizing effect of the substance in question. The value of $S$ in terms of $H$ for a given $T$ is required for the interpretation of the resulting low temperature obtained by adiabatic demagnetization from various values of $H$; for the entropy at this low temperature in field zero is the same as the value of $S$ in field $H$ at the initial temperature $T$. The quantity $(-xdS/dx)$, being in the nature of a specific heat, can be used to interpret the experimentally determined specific heat.

It is also possible to use the tables to get some idea of the variation with temperature of the entropy and specific heat in zero field of an actual paramagnetic substance, at temperatures so low that it is no longer ideal. Namely, one may assume as a rough approximation, as did Kurti and Simon,[1] that the ground state of such a substance is split into $2j+1$ equidistant levels separated by an energy $k\theta$, where $\theta$ is a characteristic temperature for the substance. The entropy and specific heat are thus given by putting $x=\theta/T$ in the tables of $S$ and $(-xdS/dx)$. By using the approximation formulae given later, it is seen that at temperatures high compared with $\theta$ (i.e., $x$ small), the specific heat is inversely proportional to $T^2$ and the entropy defect, reckoned from the entropy when $x$ is zero, is also inversely proportional to $T^2$.

[1] N. Kurti and F. Simon, Proc. Roy. Soc. **149**, 152 (1935).

## Range of values

These tables were calculated for their utilitarian value in work with the magnetic method. The values of $j$ were therefore confined to ½ (for $Ti^{+++}$), ⅜ (for $Cr^{+++}$), and ⅝ (for $Mn^{++}$ and $Fe^{+++}$). This choice includes the substances most frequently used with this technique. At some later date[1a] it may be possible to extend them to ⅞ for Gd (whose salts are not likely to

TABLE I.—*Continued.*

| $x$ | $Q$ | $\ln Q$ | $M/N\mu$ | $(M/N\mu)^2$ | $S/R$ | $(-xdS/dx)/R$ |
|---|---|---|---|---|---|---|
| | | | j=5/2 | | | |
| 0 | 6 | 1.79176 | 0 | 0 | 1.79176 | 0 |
| 0.02 | 6.0035 | 1.79234 | 0.11664 | 0.01360 | 1.79118 | 0.00117 |
| 0.04 | 6.0140 | 1.79409 | 0.23310 | 0.05434 | 1.78943 | 0.00465 |
| 0.06 | 6.0315 | 1.79700 | 0.34923 | 0.12196 | 1.78653 | 0.01043 |
| 0.08 | 6.0562 | 1.80107 | 0.46484 | 0.21607 | 1.78248 | 0.01845 |
| 0.10 | 6.0879 | 1.80630 | 0.57977 | 0.33613 | 1.77731 | 0.02864 |
| 0.12 | 6.1268 | 1.81267 | 0.69386 | 0.48144 | 1.77103 | 0.04090 |
| 0.14 | 6.1729 | 1.82017 | 0.80696 | 0.65118 | 1.76368 | 0.05515 |
| 0.16 | 6.2264 | 1.82880 | 0.91892 | 0.84441 | 1.75528 | 0.07126 |
| 0.18 | 6.2874 | 1.83855 | 1.0296 | 1.0601 | 1.74589 | 0.08909 |
| 0.20 | 6.3559 | 1.84939 | 1.1388 | 1.2970 | 1.73550 | 0.10850 |
| 0.24 | 6.5164 | 1.87432 | 1.3526 | 1.8296 | 1.71200 | 0.15147 |
| 0.28 | 6.7090 | 1.90345 | 1.5593 | 2.4315 | 1.68514 | 0.19888 |
| 0.30 | 6.8178 | 1.91954 | 1.6598 | 2.7550 | 1.67057 | 0.22384 |
| 0.32 | 6.9354 | 1.93664 | 1.7583 | 3.0915 | 1.65531 | 0.24942 |
| 0.36 | 7.1794 | 1.97372 | 1.9489 | 3.7981 | 1.62293 | 0.30178 |
| 0.40 | 7.4972 | 2.01453 | 2.1307 | 4.5400 | 1.58838 | 0.35477 |
| 0.50 | 8.4290 | 2.13168 | 2.5458 | 6.4809 | 1.49524 | 0.48316 |
| 0.60 | 9.6617 | 2.26817 | 2.9044 | 8.4353 | 1.39686 | 0.59625 |
| 0.70 | 11.260 | 2.42123 | 3.2098 | 10.303 | 1.29780 | 0.68751 |
| 0.80 | 13.308 | 2.58835 | 3.4677 | 12.025 | 1.20130 | 0.75556 |
| 0.90 | 15.916 | 2.76731 | 3.6842 | 13.573 | 1.10941 | 0.80223 |
| 1.0 | 19.225 | 2.95619 | 3.8659 | 14.945 | 1.02326 | 0.83099 |
| 1.1 | 23.416 | 3.15341 | 4.0184 | 16.148 | 0.94328 | 0.84557 |
| 1.2 | 28.721 | 3.35764 | 4.1469 | 17.197 | 0.86947 | 0.84941 |
| 1.3 | 35.438 | 3.56777 | 4.2557 | 18.111 | 0.80160 | 0.84536 |
| 1.4 | 43.945 | 3.78293 | 4.3481 | 18.906 | 0.73928 | 0.83563 |
| 1.5 | 54.727 | 4.00236 | 4.4270 | 19.599 | 0.68207 | 0.82184 |
| 1.6 | 68.405 | 4.22545 | 4.4949 | 20.204 | 0.62955 | 0.80519 |
| 1.7 | 85.772 | 4.45169 | 4.5534 | 20.734 | 0.58129 | 0.78648 |
| 1.8 | 107.84 | 4.68066 | 4.6042 | 21.198 | 0.53690 | 0.76630 |
| 1.9 | 135.91 | 4.91200 | 4.6484 | 21.608 | 0.49603 | 0.74510 |
| 2.0 | 171.64 | 5.14541 | 4.6870 | 21.968 | 0.45837 | 0.72318 |
| 2.1 | 217.16 | 5.38063 | 4.7209 | | 0.42362 | |
| 2.2 | 275.18 | 5.61743 | 4.7508 | | 0.39155 | |
| 2.3 | 349.20 | 5.85565 | 4.7772 | | 0.36193 | |
| 2.4 | 443.68 | 6.09510 | 4.8005 | | 0.33454 | |
| 2.5 | 564.34 | 6.33565 | 4.8211 | | 0.30921 | |
| 2.6 | 718.51 | 6.57718 | 4.8395 | | 0.28578 | |
| 2.7 | 915.59 | 6.81957 | 4.8559 | | 0.26410 | |
| 2.8 | 1167.6 | 7.06274 | 4.8705 | | 0.24404 | |
| 2.9 | 1490.1 | 7.30659 | 4.8836 | | 0.22546 | |
| 3.0 | 1902.8 | 7.55107 | 4.8952 | | 0.20826 | |
| 3.1 | 2431.1 | 7.79609 | 4.9057 | | 0.19233 | |
| 3.2 | 3107.6 | 8.04162 | 4.9150 | | 0.17760 | |
| 3.3 | 3974.2 | 8.28758 | 4.9234 | | 0.16396 | |
| 3.4 | 5084.5 | 8.53394 | 4.9310 | | 0.15133 | |
| 3.5 | 6507.2 | 8.78066 | 4.9377 | | 0.13964 | |
| 3.6 | 8330.7 | 9.02770 | 4.9438 | | 0.12884 | |
| 3.7 | 10668 | 9.27504 | 4.9493 | | 0.11883 | |
| 3.8 | 13665 | 9.52262 | 4.9542 | | 0.10958 | |
| 3.9 | 17509 | 9.77045 | 4.9587 | | 0.10103 | |
| 4.0 | 22437 | 10.01849 | 4.9627 | | 0.09311 | |
| 4.2 | 36868 | 10.51511 | 4.9696 | | 0.07905 | |
| 4.4 | 60618 | 11.01235 | 4.9751 | | 0.06705 | |
| 4.6 | 99718 | 11.51010 | 4.9797 | | 0.05681 | |
| 4.8 | 164110 | 12.00826 | 4.9834 | | 0.04809 | |
| 5.0 | 270160 | 12.50676 | 4.9864 | | 0.04068 | |
| 5.2 | 444870 | 13.00553 | 4.9889 | | 0.03438 | |
| 5.4 | 732730 | 13.50453 | 4.9909 | | 0.02903 | |
| 5.6 | 1207100 | 14.00370 | 4.9926 | | 0.02449 | |
| 5.8 | 1988800 | 14.50303 | 4.9939 | | 0.02064 | |
| 6.0 | 3277100 | 15.00248 | 4.9950 | | 0.01739 | |

[1a] *Note added in proof.*—A table of the magnetization and entropy appropriate to $j=7/2$ has just been published by Giauque in the February, 1941 issue of the *Journal of the American Chemical Society.*

TABLE II. *Einstein functions.*

| $z$ | $\frac{z}{e^z-1}$ | $\ln(e^z-1)$ | $S_E/R$ | $\frac{z^2e^z}{(e^z-1)}$ |
|---|---|---|---|---|
| 0 | 1 | $-\infty$ | $\infty$ | 1 |
| 0.02 | 0.99003 | −3.90201 | 4.91204 | 0.99997 |
| 0.04 | 0.98013 | −3.19881 | 4.21894 | 0.99987 |
| 0.06 | 0.97030 | −2.78326 | 3.81356 | 0.99970 |
| 0.08 | 0.96053 | −2.48546 | 3.52600 | 0.99947 |
| 0.10 | 0.95083 | −2.25217 | 3.30300 | 0.99917 |
| 0.12 | 0.94120 | −2.05966 | 3.12086 | 0.99880 |
| 0.14 | 0.93163 | −1.89530 | 2.96693 | 0.99837 |
| 0.16 | 0.92213 | −1.75151 | 2.83365 | 0.99787 |
| 0.18 | 0.91270 | −1.62345 | 2.71615 | 0.99731 |
| 0.20 | 0.90333 | −1.50777 | 2.61110 | 0.99667 |
| 0.24 | 0.88480 | −1.30472 | 2.42951 | 0.99522 |
| 0.28 | 0.86652 | −1.12970 | 2.27622 | 0.99349 |
| 0.30 | 0.85749 | −1.05023 | 2.20771 | 0.99253 |
| 0.32 | 0.84852 | −0.97517 | 2.14369 | 0.99151 |
| 0.36 | 0.83078 | −0.83626 | 2.02704 | 0.98927 |
| 0.40 | 0.81330 | −0.70963 | 1.92293 | 0.98677 |
| 0.48 | 0.77913 | −0.48439 | 1.74352 | 0.98102 |
| 0.50 | 0.77075 | −0.43275 | 1.70350 | 0.97942 |
| 0.56 | 0.74600 | −0.28679 | 1.59278 | 0.97427 |
| 0.60 | 0.72982 | −0.19587 | 1.52569 | 0.97053 |
| 0.64 | 0.71390 | −0.10928 | 1.46318 | 0.96655 |
| 0.70 | 0.69050 | 0.01366 | 1.37684 | 0.96014 |
| 0.72 | 0.68283 | 0.05300 | 1.34983 | 0.95790 |
| 0.80 | 0.65277 | 0.20338 | 1.24939 | 0.94833 |
| 0.84 | 0.63812 | 0.27488 | 1.20324 | 0.94322 |
| 0.90 | 0.61661 | 0.37817 | 1.13844 | 0.93515 |
| 0.96 | 0.59565 | 0.47728 | 1.07836 | 0.92661 |
| 1.00 | 0.58198 | 0.54133 | 1.04065 | 0.92068 |
| 1.08 | 0.55536 | 0.66510 | 0.97026 | 0.90822 |
| 1.10 | 0.54886 | 0.69523 | 0.95363 | 0.90499 |
| 1.12 | 0.54241 | 0.72506 | 0.93735 | 0.90171 |
| 1.20 | 0.51722 | 0.84162 | 0.87560 | 0.88817 |
| 1.28 | 0.49295 | 0.95422 | 0.81873 | 0.87397 |
| 1.30 | 0.48702 | 0.98182 | 0.80521 | 0.87032 |
| 1.40 | 0.45824 | 1.11685 | 0.74139 | 0.85151 |
| 1.44 | 0.44711 | 1.16960 | 0.71751 | 0.84374 |
| 1.50 | 0.43083 | 1.24752 | 0.68331 | 0.83185 |
| 1.60 | 0.40475 | 1.37448 | 0.63027 | 0.81143 |
| 1.68 | 0.38483 | 1.47375 | 0.59109 | 0.79461 |
| 1.70 | 0.37998 | 1.49827 | 0.58171 | 0.79034 |
| 1.80 | 0.35646 | 1.61932 | 0.53714 | 0.76869 |
| 1.90 | 0.33416 | 1.73799 | 0.49617 | 0.74657 |
| 1.92 | 0.32984 | 1.76147 | 0.48838 | 0.74210 |
| 2.00 | 0.31304 | 1.85459 | 0.45845 | 0.72406 |
| 2.10 | 0.29304 | 1.96937 | 0.42367 | |
| 2.16 | 0.28158 | 2.03747 | 0.40411 | 0.68749 |
| 2.2 | 0.27414 | 2.08256 | 0.39158 | 0.67827 |
| 2.3 | 0.25629 | 2.19435 | 0.36194 | |
| 2.4 | 0.23945 | 2.30490 | 0.33455 | 0.63200 |
| 2.5 | 0.22356 | 2.41435 | 0.30921 | |
| 2.6 | 0.20861 | 2.52282 | 0.28578 | 0.58589 |
| 2.7 | 0.19453 | 2.63043 | 0.26410 | |
| 2.8 | 0.18129 | 2.73725 | 0.24404 | 0.54049 |
| 2.9 | 0.16886 | 2.84340 | 0.22546 | |
| 3.0 | 0.15719 | 2.94893 | 0.20826 | 0.49627 |
| 3.1 | 0.14624 | 3.05391 | 0.19233 | |
| 3.2 | 0.13598 | 3.15838 | 0.17760 | 0.45363 |
| 3.3 | 0.12638 | 3.26242 | 0.16396 | |
| 3.4 | 0.11739 | 3.36606 | 0.15133 | 0.41290 |
| 3.5 | 0.10898 | 3.46934 | 0.13964 | |
| 3.6 | 0.10113 | 3.57230 | 0.12883 | 0.37429 |
| 3.7 | 0.09380 | 3.67497 | 0.11883 | |
| 3.8 | 0.08695 | 3.77738 | 0.10958 | 0.33799 |
| 3.9 | 0.08058 | 3.87955 | 0.10103 | |
| 4.0 | 0.07463 | 3.98152 | 0.09311 | 0.30408 |
| 4.2 | 0.06394 | 4.18489 | 0.07905 | 0.27264 |
| 4.4 | 0.05469 | 4.38765 | 0.06705 | 0.24364 |
| 4.6 | 0.04671 | 4.58990 | 0.05681 | |
| 4.8 | 0.03983 | 4.79174 | 0.04809 | 0.19277 |
| 5.0 | 0.03392 | 4.99324 | 0.04068 | |
| 5.2 | 0.02885 | 5.19447 | 0.03438 | 0.15083 |
| 5.4 | 0.02450 | 5.39547 | 0.02903 | 0.13292 |
| 5.6 | 0.02079 | 5.59630 | 0.02449 | 0.11683 |
| 5.8 | 0.01761 | 5.79697 | 0.02065 | |
| 6.0 | 0.01491 | 5.99752 | 0.01739 | 0.08967 |
| 6.2 | 0.01261 | 6.19797 | 0.01464 | |
| 6.4 | 0.01065 | 6.39834 | 0.01232 | 0.06829 |
| 6.6 | 0.00899 | 6.59864 | 0.01035 | 0.05942 |
| 6.8 | 0.00758 | 6.79889 | 0.00870 | 0.05162 |
| 7.0 | 0.00639 | 6.99909 | 0.00730 | |
| 7.2 | 0.00538 | 7.19925 | 0.00613 | 0.03876 |
| 7.4 | 0.00453 | 7.39939 | 0.00514 | |
| 7.6 | 0.00381 | 7.59950 | 0.00431 | 0.02893 |
| 7.8 | 0.00320 | 7.79959 | 0.00361 | 0.02495 |
| 8.0 | 0.00268 | 7.99967 | 0.00302 | 0.02148 |
| 8.4 | 0.00189 | 8.39978 | 0.00211 | 0.01587 |
| 8.8 | 0.00133 | 8.79985 | 0.00148 | |
| 9.0 | 0.00111 | 8.99988 | 0.00123 | 0.01000 |
| 9.2 | 0.00093 | 9.19990 | 0.00103 | |
| 9.6 | 0.00065 | 9.59993 | 0.00072 | 0.00624 |
| 10.0 | 0.00045 | 9.99996 | 0.00050 | |
| 10.2 | 0.00038 | 10.19996 | 0.00042 | 0.00387 |
| 10.4 | 0.00032 | 10.39997 | 0.00035 | |
| 10.8 | 0.00022 | 10.79998 | 0.00024 | 0.00238 |
| 11.2 | 0.00015 | 11.19999 | 0.00017 | |
| 11.4 | 0.00013 | 11.39999 | 0.00014 | 0.00145 |
| 11.6 | 0.00011 | 11.59999 | 0.00012 | |
| 12.0 | 0.00007 | 11.99999 | 0.00008 | 0.00088 |
| 12.4 | 0.00005 | 12.4 | 0.00006 | |
| 12.6 | 0.00004 | 12.6 | 0.00005 | |
| 12.8 | 0.00004 | 12.8 | 0.00004 | |
| 13.2 | 0.00002 | 13.2 | 0.00003 | |
| 13.6 | 0.00002 | 13.6 | 0.00002 | |
| 14.4 | 0.00001 | 14.4 | 0.00001 | |

be used so much in the future) and to $\frac{9}{2}$ corresponding to certain nuclear spins.[2]

Similarly the range of values of $x$ is that likely to be useful in practice. For $M$ and $S$, the range of $x$ extends up to 6.0, corresponding to fields of 44 kilogauss at 1°K; for still higher values of $x$ the approximation formulae given below will usually be sufficient. In the tables of $(-xdS/dx)$, $x$ extends only to 2.0, as in this work the calculations involving $(-xdS/dx)$ are usually confined to small fields. For $j=\frac{1}{2}$ and $\frac{3}{2}$, however, the tables show $(-xdS/dx)$ at some values of $x$ higher than 2. These have been obtained from the table of Einstein functions (see Table II). For example, $(-zdS_E/dz)$ with $z=2.2$ was one of the quantities calculated to check $(-xdS/dx)$ for $j=\frac{1}{2}$ with $x=1.1$; it is now used as one of the quantities to give $(-xdS/dx)$ for $j=\frac{1}{2}$ with $x=2.2$.[3]

## APPROXIMATION FORMULAE

For small $x$ one has the developments

$$M/N\mu g=\tfrac{1}{3}xj(j+1)$$
$$-(1/720)[(2j+1)^4-1]x^3+\cdots, \quad (1)$$

$$S/R=\ln(2j+1)-\tfrac{1}{6}x^2j(j+1)$$
$$+(1/960)[(2j+1)^4-1]x^4+\cdots. \quad (2)$$

[2] The unit of nuclear magnetic moment is 1/1840 times the Bohr magneton; it is not possible to give any general rule for the nuclear $g$ value.

[3] If still further values of $(-xdS/dx)$ are required, to an accuracy greater than that obtainable by graphical differentiation of $S$, the Einstein function method given later is by far the shortest and most convenient.

For large $x$ one may use the relations

$$M/N\mu g = j - e^{-x} \pm e^{-2x}, \quad (3)$$

$$S/R = (x+1)e^{-x} \mp (x+\tfrac{1}{2})e^{-2x}. \quad (4)$$

Here the upper or lower sign choice is to be employed, according as $j=\frac{1}{2}$ or $j \geqq 1$.

If an accuracy of 1 percent is desired it suffices to use merely the first term of (1) or (4), and two terms of (2) or (3), provided $x$ has the following range of values: $<0.32$, 0.24, 0.12 in (1), $>2.8$, 2.2, 2.0 in (3), $<0.80$, 0.40, 0.32 in (2) and $>4.8$, 4.4, 4.4 in (4). Here the first, second, and third choices apply according as $j=\frac{1}{2}, \frac{3}{2}, \frac{5}{2}$. The first term of the formulas for $xdS/dx$ obtained by differentiating (2) and (4) is enough to give one-percent accuracy if $x<0.20$, 0.12, 0.06 or $x>6.0$, 5.4, 5.4.

## II. Einstein Function Method

For an Einstein oscillator of frequency $\nu$ the thermodynamic functions are again derived from the appropriate partition function; the free energy and total energy are, however, slightly different according as the energy of the lowest quantum state is taken as being $h\nu/2$ or zero. In the following treatment we consider always $N$ oscillators. If the energy states are $\frac{1}{2}h\nu$, $\frac{3}{2}h\nu \cdots$ etc., then the partition function is

$$Q_E = e^{-h\nu/2kT} + e^{-3h\nu/2kT} + e^{-5h\nu/2kT} + \cdots$$

$$= e^{z/2}/(e^z - 1) \quad \text{where} \quad z = h\nu/kT.$$

The free energy is

$$F = RT \cdot [\ln(e^z - 1) - \tfrac{1}{2}z],$$

while the total energy is

$$U = RT \cdot \left[\frac{z}{2} + \frac{z}{e^z - 1}\right].$$

If the energy states are 0, $h\nu$, $2h\nu$, $\cdots$ etc., i.e., if there is no zero-point energy, then the expressions for the free and total energy are obviously diminished by $\frac{1}{2}h\nu$ as compared with the above values. The entropy $S_E$ is given by $R[\ln Q - Q^{-1}xdQ/dx]$, and is thus $R[z + z(e^z-1)^{-1} - \ln(e^z-1)]$ regardless of whether there is a zero-point energy and $(-zdS_E/dz)$ is $Rz^2e^z/(e^z-1)^2$. The accompanying tables show $S_E/R$ and $(-zdS_E/dz)/R$, also $z/(e^z-1)$ and $\ln(e^z-1)$ so that the free energy and total energy are easily obtained for either partition function.

The importance of the Einstein functions for our particular purpose lies in the fact that the partition function

$$\sum_{m=-j}^{j} e^{mx}$$

for a paramagnetic substance is the ratio of two Einstein functions $e^{z/2}/(e^z-1)$, where $z$ has the values $x$ and $(2j+1)x$, respectively. Since $S$ is given by $R[\ln Q - xd(\ln Q)/dx]$, it is seen that $S/R$ for the paramagnetic substance is obtained as the difference between the two quantities $S_E/R$ for Einstein oscillators with $z$ equal to $x$ and $(2j+1)x$, respectively. In other words

$$S = S_E(z=x) - S_E \ (z=2jx+x).$$

Analogous relations apply to $-xdS/dx$. This useful property has been pointed out by Kurti and Simon.[1]

The selection of values of $z$ in the tables, which seems somewhat arbitrary at the higher values, is just that required to cover the same range of $S$ and $(-xdS/dx)$ as in the direct partition function method. The resulting values of $S$ and $(-xdS/dx)$ have not been tabulated again, as they are identical with those already obtained. As already mentioned, this agreement serves as a partial check on the numerical accuracy of our calculations.

### Accuracy

While making the calculations six significant figures were used, and the results have since been rounded off to five figures. The calculations were made as far as possible on an electrical machine, which accounts for this large number of significant figures compared with the intervals in the series of $x$ and $z$ values. There may, however, be occasions when it will be useful to have available the five significant figures, and it is hoped that the error is nowhere greater than one in the last figure.

We wish to record our indebtedness to Dr. N. Kurti for many helpful discussions.

# High Rotational Levels and the Partition Function for Hydrogen

HAROLD W. WOOLLEY
*National Bureau of Standards, Washington, D. C.*
(Received April 14, 1941)

The ordinary formula for the rotational energy of a simple rotating vibrator, when applied to a diatomic molecule, consists of the first few terms of a series that becomes poorly convergent for levels of high rotational energy. Inversion of the series results in a better approximation. An illustration is given using the results of calculations for the normal state of hydrogen. The inverted series is especially suited to derivation of approximation formulas for the partition function. Such an approximation formula should not be carried to powers of $T$ so high that lack of coefficients for the ordinary formula introduces significant error.

IN the course of some calculations of thermodynamic properties of hydrogen[1] from spectroscopic data, a difficulty was encountered arising from the form of the expression for the rotational energy of a diatomic molecule. In ordinary spectroscopic work with heavy diatomic molecules the formula

$$E_v = B_v K(K+1) + D_v K^2(K+1)^2 \qquad (1)$$

is fully adequate since the second term is very small. For hydrogen and for large energies this is no longer the case. A third term is in use in spectroscopic work on hydrogen and, to extend the application to higher energies, a fourth can be evaluated using relations from the theory of the simple rotating vibrator. The resulting formula for the rotational energy,

$$E_v = B_v K(K+1) + D_v K^2(K+1)^2 + F_v K^3(K+1)^3 + H_v K^4(K+1)^4, \qquad (2)$$

while adequate for a somewhat greater range, is still not satisfactory since it is the beginning of a series that is too slowly convergent or even divergent for large but possible values of rotational quantum number, $K$. The formula is, in fact, not very suitable for calculating thermodynamic properties of hydrogen above 2000 degrees K. Some other treatment is therefore necessary.

Using a modification of the Klein-Rydberg method,[2] the molecular potential energy for the ground state of hydrogen was determined as a function of internuclear distance and with this the quantum integral was evaluated numerically for several combinations of large rotational quantum number and total energy. The results indicated that, at least for the particular spectroscopic constants employed, the formula became adequate for the purpose when continued indefinitely as a geometric series with the ratio given by the last two terms of formula (2) and with the added part summed with the usual formula. Figure 1 shows, for $v=0$, the estimates which would be made for $E_v$ as a function of $K$, using: for curve 1, the first term of formula (2); for curve 2, the first two terms; for curve 3, the first three terms; for curve 4, the first four terms; for curve 5, the sum including the continuation as a geometric series; and for curve 6, the

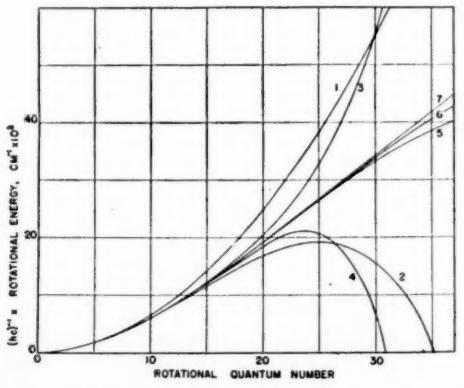


FIG. 1. Various estimates for the rotational energy of the hydrogen molecule as a function of rotational quantum number for the lowest vibrational state. Curves 1, 2, 3 and 4: Formula (2) evaluated to 1, 2, 3 and 4 terms, respectively. Curve 5: 4 terms of formula (2) with a geometric series continuation. Curve 6: Result of detailed numerical investigation. Curve 7: Formula (3) evaluated to 4 terms.

[1] A project of the National Research Council Committee on Thermodynamic Data for Chemical Industries, Dr. F. R. Bichowsky, Chairman.

[2] R. Rydberg, Zeits. f. Physik **73**, 376 (1931); O. Klein, Zeits. f. Physik **76**, 226 (1932).

interpolated results of the numerical evaluation of the quantum integral previously mentioned.

Several other usable methods of representing the relation between $E_v$ and $K$ have been suggested to the writer. One of the most interesting of these is the inversion of the series of formula (2). This leads to

$$K(K+1)=\frac{1}{B_v}E_v-\frac{D_v}{B_v^3}E_v^2+\frac{(2D_v^2-B_vF_v)}{B_v^5}E_v^3 + \frac{(5B_vD_vF_v-B_v^2H_v-5D_v^3)}{B_v^7}E_v^4+\cdots. \quad (3)$$

In using this, the total rotational and vibrational energy is to be $G_v+E_v$ where $G_v$ is the purely vibrational energy. In contrast to formula (2), in which the terms alternate in sign, formula (3) as far as evaluated is rapidly convergent, with all terms positive, for all values which $E_v$ can properly assume. In Fig. 1, curve 7 shows the result given by the first four terms of formula (3) for $v=0$. Comparison of this with curve 4 shows that, without including any estimates of remainders, formula (3) is definitely superior to formula (2) for large values of $K$ and $E_v$.

Formula (3) is particularly adapted to use in deriving one type of approximation formula for the partition function.[3] In the customary derivation, the summation

$$\sum_K \{\exp(-c_2(G_v+E_v)/T)\}(2K+1)$$

is represented in accordance with the Euler-Maclaurin summation formula as the sum of the integral

$$\int_{K_{\min}}^{K_{\max}} \{\exp(-c_2(G_v+E_v)/T)\}(2K+1)dK$$

and other terms, known in this application as the Mulholland correction,[4] and obtained from the integrand and its derivatives. In treating the integral it is preferable not to break up part of

$$\exp(-c_2E_v/T)$$

into a power series expansion in $K(K+1)$ but rather to use the transformations:

$$\int_{K_{\min}}^{K_{\max}}\left\{\exp\left(-\frac{c_2(G_v+E_v)}{T}\right)\right\}(2K+1)dK=\int_{K=K_{\min}}^{K=K_{\max}}\left\{\exp\left(-\frac{c_2(G_v+E_v)}{T}\right)\right\}d[K(K+1)]$$

$$=\left\{\exp\left(-\frac{c_2G_v}{T}\right)\right\}\int_{(E_v)_{\min}}^{(E_v)_{\max}}\left\{\exp\left(-\frac{c_2E_v}{T}\right)\right\}\frac{d[K(K+1)]}{dE_v}dE_v.$$

Continued integration by parts gives for this

$$-\left\{\exp\left(-\frac{c_2(G_v+E_v)}{T}\right)\right\}\left[\frac{T}{c_2}\frac{d[K(K+1)]}{dE_v}+\left(\frac{T}{c_2}\right)^2\frac{d^2[K(K+1)]}{dE_v^2}+\left(\frac{T}{c_2}\right)^3\frac{d^3[K(K+1)]}{dE_v^3} + \left(\frac{T}{c_2}\right)^4\frac{d^4[K(K+1)]}{dE_v^4}+\cdots\right]\Bigg|_{(E_v)_{\min}}^{(E_v)_{\max}}.$$

If $(E_v)_{\max}$ is great enough so that

$$\exp(-c_2(G_v+E_v)/T)$$

makes the contribution of the upper limit negligible and if $(E_v)_{\min}=0$, this becomes, by formula (3),

$$\left\{\exp\left(-\frac{c_2G_v}{T}\right)\right\}\left[\frac{T}{c_2}\frac{1}{B_v}+\frac{T^2}{c_2^2}\left(-\frac{2D_v}{B_v^3}\right)+\frac{T^3}{c_2^3}\frac{12D_v^2-6B_vF_v}{B_v^5}+\frac{T^4}{c_2^4}\frac{120B_vD_vF_v-24B_v^2H_v-120D_v^3}{B_v^7}+\cdots\right] \quad (4)$$

[3] W. F. Giauque and R. Overstreet, J. Am. Chem. Soc. **54**, 1731 (1932); L. S. Kassel, J. Chem. Phys. **1**, 576 (1933); H. L. Johnston and C. O. Davis, J. Am. Chem. Soc. **56**, 271 (1934).

[4] H. P. Mulholland, Proc. Camb. Phil. Soc. **24**, 280 (1928).

It must be pointed out that evaluation of formula (4) cannot be extended to higher powers of $T$ without first evaluating additional coefficients of formula (2).[5] For example, the coefficient of $T^4$ in formula (4) is thrown off by several hundred percent by setting $H_v=0$. In addition to the numerical error which would be introduced, this could lead to the inference that the series is somewhat less convergent and hence less adapted for calculation than is in fact the case.

With $g$ representing the average statistical weight due to nuclear spin degeneracy and with the zero of the energy scale chosen so that $G_0=0$, the internal partition function is the sum over $v$ of

$$Q_v=g\sum_K\left\{\exp\left(-\frac{c_2(G_v+E_v)}{T}\right)\right\}(2K+1)=g\left\{\exp\left(-\frac{c_2G_v}{T}\right)\right\}\left[\frac{T}{c_2}\frac{1}{B_v}+\frac{T^2}{c_2^2}\left(-\frac{2D_v}{B_v^3}\right)+\frac{T^3}{c_2^3}\right.$$
$$\left.\times\frac{12D_v^2-6B_vF_v}{B_v^5}+\frac{T^4}{c_2^4}\frac{120B_vD_vF_v-24B_v^2H_v-120D_v^3}{B_v^7}+\cdots+\frac{1}{3}+\frac{1}{15}\frac{c_2B_v}{T}+\frac{4}{315}\frac{c_2^2B_v^2}{T^2}+\cdots\right].$$

A few terms of the Mulholland correction have been included in the formula. They are to be used with caution since the true correction is not properly developable in powers of $T^{-1}$ and the apparent convergence is too optimistic an indication of the closeness of the approximation, especially with $T$ small. As is well known, this correction does not distinguish between sums over even and over odd values of $K$.

It is desired to acknowledge the encouragement by Dr. F. G. Brickwedde of the calculation of thermodynamic properties of hydrogen at high temperatures from spectroscopic data. Several suggestions made by Professor David M. Dennison have been very helpful in leading to this paper.

[5] For the simple rotating vibrator, see J. L. Dunham, Phys. Rev. **41**, 721 (1932); I. Sandeman, Proc. Roy. Soc. Edinburgh **60**, 210 (1940).

---

JUNE, 1941 JOURNAL OF CHEMICAL PHYSICS VOLUME 9

# On Some Properties of Bose-Einstein Gases

LOUIS GOLDSTEIN
*New York, New York*

(Received March 13, 1941)

The condition which has to be fulfilled in order that the Bose-Einstein condensation be accompanied by a discontinuity of the heat capacity at the condensation temperature is discussed. The nature of the transition depends on the distribution of the energy levels of the individual particles forming the gas. The condensation is studied for several types of individual energy spectra. It is shown that all those Bose-Einstein (B.E.) assemblies which admit a non-ambiguous definition of the statistical distribution function present, beside interesting analogies, a qualitatively different behavior from that observed in liquid helium. It appears that as long as the transition in momentum space of non-ideal B.E. systems is not understood, the possibility of connection between B.E. condensation and the transition observed in liquid helium remains an open problem.

IN a previous paper[1] we have discussed the condensation of B.E. ideal gases in presence of conservative force fields which acted directly on the motion of the center of gravity of the gas atoms. It has been assumed there that the classical Hamilton function could be used for the description of the motion of the individual gas atoms. This was equivalent to the assumption that practically no serious error was introduced by leaving aside the quantization of the motion of the individual atoms in those fields. The modification brought about by the field in the properties of the gas around the condensation

[1] L. Goldstein, J. Chem. Phys. **9**, 273 (1941).

temperature concerned uniquely this last quantity. The presence of the field increases the transition temperature above that of the free gas with the same concentration. The condensation remained a phase transition of the third order, since energy and heat capacity at constant volume were continuous at the transition temperature, the discontinuity presenting itself was that of the derivative, with respect to the temperature, of the heat capacity. Apart from the intrinsic interest in the study of the peculiar B.E. condensation under different conditions, it seemed that the eventual possibilities of connection between this effect and the well-known transition effect occurring in liquid helium[2] justify a more general discussion of some of the properties in thermal equilibrium of B.E. gases than that made on a classical basis. We will be concerned here mainly with the conditions which assure the reduction of the order of B.E. transitions and introduce, therefore, a discontinuity in the heat capacity at constant volume of the system at the transition temperature. Such B.E. systems presenting a transition of the second order seem to provide quite an attractive picture of what may eventually happen in liquid helium. However, beside the apparent analogies between B.E. condensation and some features of the transition in liquid helium there is also an important difference of a qualitative nature which will be discussed below. Evidently, no secure model of liquid helium can be based on ideal B.E. systems or B.E. systems under appropriate fields, self-consistent fields included. The internal field of non-ideal B.E. assemblies might modify considerably the transition in phase space. The study of the eventual connection between the B.E. transition and that observed in liquid helium should be based on the analysis of the thermal properties of non-ideal B.E. fluids.

## I.

We have to recall briefly some properties of the ideal B.E. gas in absence of any force field.

The average energies, at temperatures $T$, below and above the transition temperature $T_0$, are given, respectively, $k$ denoting Boltzmann's constant, by

$$E_-=\tfrac{3}{2}NkT(T/T_0)^{\frac{3}{2}}G(0)/F(0), \tag{1}$$

$$E_+=\tfrac{3}{2}NkTG(\alpha)/F(\alpha); \quad F(x)=\sum_{\lambda=1}^{\infty} e^{-\lambda x}/\lambda^{\frac{3}{2}}; \quad G(x)=\sum_{\lambda=1}^{\infty} e^{-\lambda x}/\lambda^{5/2}; \tag{2}$$

where the always positive fundamental parameter $\alpha$ is defined by the total number $N$ of spinless atoms of mass $m$ in the volume $V$ through the equation

$$N=(V/h^3)(2\pi mkT)^{\frac{3}{2}}F(\alpha). \tag{3}$$

The heat capacities at constant volume are, respectively,

$$dE_-/dT=\frac{15}{4}Nk(T/T_0)^{\frac{3}{2}}G(0)/F(0), \tag{4}$$

$$dE_+/dT=\frac{3}{2}Nk\left[G(\alpha)/F(\alpha)+T\frac{d}{d\alpha}(G/F)\frac{d\alpha}{dT}\right]. \tag{5}$$

Since, from (3),

$$d\alpha/dT=-\frac{3}{2}\frac{1}{T}F(\alpha)/F'(\alpha); \quad F'(\alpha)=\frac{dF}{d\alpha}=-\sum_{\lambda=1}^{\infty} e^{-\lambda\alpha}/\lambda^{\frac{3}{2}} \tag{6}$$

one gets

$$\frac{dE_+}{dT}=\frac{3}{2}Nk\left[\frac{5}{2}G(\alpha)/F(\alpha)+\frac{3}{2}F(\alpha)/F'(\alpha)\right]. \tag{7}$$

At high temperatures the series $G(\alpha)$, $F(\alpha)$ and $F'(\alpha)$ reduce, practically, to their first term $e^{-\alpha}$ and

[2] F. London, Nature **141**, 643 (1938); Phys. Rev. **54**, 947 (1938).

$-e^{-\alpha}$, respectively, because $\alpha$ is large. The heat capacity decreases and tends asymptotically toward the classical value $1.5Nk$. At low temperatures, just above the transition temperature, $\alpha \sim 0$, and the first term on the right-hand side of (7) tends toward $15/4NkG(0)/F(0)$ as does $(dE_-/dT)_{T_0}$. The second term on the right-hand side of (7) tends toward zero since the series $F'(0)$ or

$$-\sum_{\lambda=1}^{\infty} 1/\lambda^{\frac{1}{2}}$$

diverges. Therefore, following (6),

$$(d\alpha/dT)_{T_0}=0; \quad (d\alpha/dT)_{T>T_0} \gtrless 0. \tag{8}$$

It is instructive to write $dE_+/dT$ in the following form

$$\frac{dE_+}{dT}=\frac{15}{4}NkG(\alpha)/F(\alpha)-\frac{3}{2}NkT\frac{d\alpha}{dT}, \tag{9}$$

which shows clearly, with (4), that the continuity of the heat capacity at constant volume of ideal B.E. gases at the transition temperature is due to the fact that the derivative of the fundamental parameter $\alpha$ with respect to the temperature vanishes at the transition point.

The second derivative of the average energy of the gas is, below $T_0$,

$$\frac{d^2E_-}{dT^2}=\frac{45}{8}\frac{Nk}{T_0}\left(\frac{T}{T_0}\right)^{\frac{1}{2}} G(0)/F(0), \tag{10}$$

which is always positive. The heat capacity at constant volume increases until, approximately, $1.92Nk$ at $T_0$. Above the transition temperature the heat capacity decreases monotonously from the preceding value and tends to $1.5Nk$. An elementary calculation gives

$$\frac{d^2E_+}{dT^2}=\frac{45}{8}\frac{Nk}{T}\frac{G(\alpha)}{F(\alpha)}+\frac{9}{4}\frac{Nk}{T}\frac{F(\alpha)}{F'(\alpha)}+\frac{27}{8}\frac{Nk}{T}\frac{[F(\alpha)]^2F''(\alpha)}{[F'(\alpha)]^3}; \quad F''=\frac{d^2F}{d\alpha^2}. \tag{11}$$

At high temperatures $G(\alpha)$, $F(\alpha)$ and $F''(\alpha)$ reduce practically to $e^{-\alpha}$, $F'(\alpha)$ to $-e^{-\alpha}$ and $\lim_{T \text{ large}} d^2E_+/dT^2$ vanishes. The discontinuity of the derivative, with respect to the temperature, of the heat capacity at constant volume at the transition temperature is, with (10) and (11),

$$\begin{aligned}\Delta\left(\frac{d^2E}{dT^2}\right)_{T_0} &= \left(\frac{d^2E_+}{dT^2}\right)_{T_0}-\left(\frac{d^2E_-}{dT^2}\right)_{T_0} \\ &= \frac{27}{8}\frac{Nk}{T}\lim_{\alpha=0}\frac{[F(\alpha)]^2F''(\alpha)}{[F'(\alpha)]^3},\end{aligned} \tag{12}$$

which is negative.

Our main problem is to find under which conditions the phase transition of the third order as defined by (12) is reduced to a phase transition of the second order, i.e., with a discontinuity of the heat capacity at constant volume at the transition temperature.

It is clear from what precedes that the B.E. ideal gas cannot present a discontinuity of the heat capacity at its condensation temperature unless the derivative $d\alpha/dT$ of the fundamental parameter is finite at that temperature. It is therefore necessary to investigate the B.E. gas under such conditions which assure a finite value for $d\alpha/dT$ at the transition temperature.

We must remember here that $\alpha$ is defined at temperature $T$ by the total number $N$ of the gas atoms through

$$\begin{aligned}N &= \sum_i n_i \\ &= \sum_i g_i/\exp(\alpha+\beta W_i)-1,\end{aligned} \tag{13}$$

where $n_i$ is the average number of atoms in the state of energy $W_i$, $g_i$ is the weight of this state, $\beta$ is $1/kT$ and the summation extends over all the states $W_i$ of the energy spectrum of the individual atoms. It will be assumed throughout this paper that under all circumstances the possibility of the non-ambiguous definition of the $n_i$ or the distribution function $n_i/g_i$ is maintained. Therefore, the only way to modify the function $\alpha(N, T)$ is to introduce or impose new energy spectra $(W_i, g_i)$ for the motion of the individual gas atoms. This can be achieved by assuming the application of external fields or by allowing the existence of self-consistent fields arising from the interaction of the atoms of the system. In any of these imposed fields, the motion of the individual atoms and therefore their energy spectrum will be supposed to be known completely. We will discuss now several types of individual energy spectra which in some cases will assure a B.E. condensation accompanied by a discontinuity of the heat capacity at constant volume at the transition point.

## II.

Consider the case where the individual atoms of the system have a series of $l$ discrete stable levels of energy $-E_0, -E_1, \cdots, -E_i, \cdots, -E_l$, followed by a continuous spectrum of positive energy levels corresponding to practically free atoms. We are not concerned here with the actual existence of the type of fields which give rise to the preceding level spectrum or similar spectra and, therefore, no attempt will be made here to justify them. For the following discussion it is not indispensable that the positive energy levels form an entirely continuous spectrum. This may have a series of levels and bands which for sufficiently high energies would be followed necessarily by the free-particle continuous spectrum. The inclusion of such positive energy levels and bands would only complicate the calculations without increasing the generality of the discussion. Another simplification can be made without impairing the generality of the results, namely, that the discrete levels will be supposed to be nondegenerate and their number $l$ to increase eventually in such a way that $\lim l/N \to 0$ when $N \to \infty$. Under these conditions, the average number of spinless atoms of mass $m$ in one of the discrete states, say the $i$th, is, at temperature $T$, with $\beta$ denoting $1/kT$,

$$n_i = 1/\exp(\alpha - \beta E_i) - 1 \tag{14}$$

and in any one group of the continuous energy states with momentum between $p$ and $p+dp$,

$$dn(p) = g(p)dp/\exp(\alpha + \beta p^2/2m) - 1, \tag{15}$$

$g(p)$ being the level density in the level group in question. If there be $N$ atoms in the volume $V$ the parameter $\alpha$ is defined by

$$N = \sum_{i=0}^{l} \frac{1}{\exp(\alpha - \beta E_i) - 1} + \frac{4\pi V}{h^3} \int_0^\infty \frac{p^2 dp}{\exp(\alpha + \beta p^2/2m) - 1}. \tag{16}$$

Since no term of the right-hand side of (16) can become negative, one must have $\alpha \geqslant \beta E_0$ at any $T$. With

$$\alpha' = \alpha - \beta E_0 \tag{17}$$

one gets, after integration over the continuous spectrum and division by $N$,

$$1 = \frac{1/N}{\exp(\alpha') - 1} + \sum_{i=1}^{l} \frac{1/N}{\exp(\alpha' + \beta(E_0 - E_i)) - 1} + \left(\frac{T}{T_0}\right)^{\frac{3}{2}} \frac{F(\alpha' + \beta E_0)}{F(0)}, \tag{18}$$

where $T_0$ is the condensation temperature of the free gas with the same concentration $N/V$ as the gas under discussion and $F(x)$ has been defined by (2). At all temperatures $T > T_0$ where in the last term on the right-hand side $\alpha'$ must be finite in order to reduce this term to unity or less, the first two terms on the right-hand side can be neglected on account of their extremely small numerators $1/N$. $\alpha'$ is then defined by

$$1 = \left(\frac{T}{T_0}\right)^{\frac{3}{2}} \frac{F(\alpha' + E_0/kT)}{F(0)}. \tag{19}$$

This can also be written as

$$N = \frac{V}{h^3}(2\pi mkT)^{\frac{3}{2}} F\left(\alpha' + \frac{E_0}{kT}\right), \tag{19a}$$

which shows that at all these temperatures the

maximum number of atoms which the phase space can accommodate is

$$N_m=\frac{V}{h^3}(2\pi mkT)^{\frac{3}{2}}F(E_0/kT). \tag{20}$$

If supplementary particles are added to the gas they must go to those states which are not included in (19a), i.e., the stable discrete levels. In other words, with $N$ and $V$ kept constant, the root $T_f$ of the equation

$$1=\left(\frac{T_f}{T_0}\right)^{\frac{3}{2}}\frac{F(E_0/kT_f)}{F(0)} \tag{21}$$

is that temperature below which some of the atoms must condense or go over to those states which have been left out of account. It is clear that $T_f \geqslant T_0$, a result which is similar to that obtained in the semi-classical treatment of the influence of conservative force fields on the B.E. condensation. Remembering the behavior of $F(x)$ one sees clearly in (21) that the larger $E_0/k$ the larger is $T_f$, which is readily understandable. In order that condensation occur, the concentration $N/V$ being kept constant, one must decrease the temperature from regions of high temperatures $T>T_f$. At such temperatures, practically, no particles can be found in the group of stable levels: they are all empty. This means that $kT \gtrsim E_0$. Since $T_f$ is the smallest temperature at which the lowest levels remain empty, it is clear that $T_f$ has to vary in the same direction as $E_0$.

At temperatures $T<T_f$ the last term on the right-hand side of (18) is certainly smaller than unity, (21) having but one root $T_f$. The first two terms have to be large enough now in order to maintain the equality. The sum or the second term can still be neglected since the denominators of this sum are always finite whereas the numerators are extremely small, $N$ being enormous. The first term becomes of the order of unity if $\alpha' \sim N^{-1}$, i.e., extremely small. It can safely be neglected in the argument of $F(\alpha'+E_0/kT)$ and one gets, in this approximation,

$$1=\frac{1}{N\alpha'}+\left(\frac{T}{T_f}\right)^{\frac{3}{2}}\frac{F(E_0/kT)}{F(E_0/kT_f)} \tag{22}$$

by using the definition (21) of $T_f$. This gives $\alpha'$ and also the number of atoms $N_0$ which at temperature $T<T_f$ are condensed in the lowest state:

$$\frac{N_0}{N}=1-\left(\frac{T}{T_f}\right)^{\frac{3}{2}}\frac{F(E_0/kT)}{F(E_0/kT_f)}. \tag{23}$$

This shows that as long as $kT_f$ is not extremely large in comparison to the smallest separation $\delta$ of the stable levels, i.e., $\delta/kT_f > N^{-1}$, only the lowest level determines the condensation. The remaining stable states are practically always empty. If $\delta/kT_f$ were of the order of $N^{-1}$, then instead of the one lowest state a group of states would play a predominant role in the condensation.

One finds then easily for the average energy of the system

$$E_-=-\frac{E_0}{\exp(\alpha')-1}-\sum_{i=1}^{l}\frac{E_i}{\exp(\beta(E_0-E_i))-1}+\frac{3}{2}\frac{V}{h^3}(2\pi mkT)^{\frac{3}{2}}kTG(E_0/kT) \tag{24}$$

and

$$E_+=-\frac{E_0}{\exp(\alpha')-1}-\sum_{i=1}^{l}\frac{E_i}{\exp(\alpha'+\beta(E_0-E_i))-1}+\frac{3}{2}\frac{V}{h^3}(2\pi mkT)^{\frac{3}{2}}kTG\left(\alpha'+\frac{E_0}{kT}\right), \tag{25}$$

since no matter how small $\alpha'$ is below $T_f$ it must necessarily be taken into account in $N_0$. These energies are naturally continuous at $T_f$.

One gets, after a simple calculation, the following expression for the discontinuity in the heat capacity at constant volume at the transition temperature $T_f$,

$$\Delta C_v=C_{v+}-C_{v-}$$
$$=\sum_{i=1}^{l}\frac{E_i\exp((E_0-E_i)/kT_f)}{(\exp((E_0-E_i)/kT_f)-1)^2}\left(\frac{d\alpha'}{dT}\right)_{T_f}-\frac{3}{2}NkT_f\left(\frac{d\alpha'}{dT}\right)_{T_f} \tag{26}$$

by using (21) and the expression (3) for $T_0^{\frac{3}{2}}F(0)$. That the lowest level does not contribute to $\Delta C_v$ is evident since $\alpha'$ and $d\alpha'/dT$ are continuous at $T_f$, as can be proved on the basis of the exact Eq. (18). The contribution to $\Delta C_v$ of the stable states comes from $E_+$ where in the average energy of these states $\alpha'$ figures explicitly. That this contribution is smaller than that of the positive energy states can be seen easily. Therefore $\Delta C_v$ is different from zero unless $(d\alpha'/dT)_{T_f}$ is itself zero. In any case $(d\alpha'/dT) \gtrless 0$. In order to find it in the present case one has but to use (19a). One finds thus

$$T_f\left(\frac{d\alpha'}{dT}\right)_{T_f} = \frac{3}{2}\frac{F(E_0/kT_f)}{[-F'(E_0/kT_f)]} + \frac{E_0}{kT_f}, \tag{27}$$

which is finite in any case; the first term on the right-hand side is also finite since

$$-F'(x) = \sum_{\lambda=1}^{\infty} e^{-\lambda x}/\lambda^{\frac{1}{2}}; \quad x = E_0/kT_f$$

is convergent. The discontinuity $\Delta C_v$ is finally

$$\Delta C_v = \left(\frac{1}{T_f}\sum_{i=1}^{l}\frac{E_i \exp\left((E_0-E_i)/kT_f\right)}{(\exp\left((E_0-E_i)/kT_f\right)-1)^2} - \frac{3}{2}Nk\right)\left(\frac{3}{2}\frac{F(E_0/kT_f)}{[-F'(E_0/kT_f)]} + \frac{E_0}{kT_f}\right). \tag{28}$$

This discontinuity being negative is of the same type as that observed in lambda-point transitions. One may say, therefore, that as soon as the individual level spectrum of the gas atoms includes at least one discrete stable level which is followed by the free particle continuous spectrum the B.E. transition becomes that of the second order.

Beside the case just discussed, the nonvanishing of the derivative $(d\alpha'/dt)_{T_f}$, assuring thus a B.E. transition accompanied by a discontinuity of the heat capacity at the transition point, can be eventually achieved in a number of different ways corresponding to the motion of the gas atoms in appropriate fields. The modifications of the individual energy spectrum of the atoms which assure a B.E. transition of the second order are the consequences of the quantization of the motion of these atoms under given conditions. As long as the quantization is left out of account the B.E. transition is of the third order. However, the quantization does not lead necessarily to such individual energy spectra which would assure a transition of the second order, as it will be seen below.

The results of the preceding discussion may then be summarized by saying that whereas the condensation phenomenon is a direct consequence of the symmetry of the system in phase space, the nature of the transition is determined by the properties of the energy spectrum of the individual atoms.

## III.

Whereas in the preceding section we have discussed the properties of B.E. gases whose atoms were supposed to have arbitrary individual energy spectra, we should like to discuss now briefly the behavior of such gases in periodic potential fields. The internal structure of the atoms will be left aside.

We should like to consider first the case of the so-called free-particle approximation. Here the amplitudes of the field's potential are so small that the influence of the field on the motion of the particles consists essentially in the introduction of the well-known discontinuities in the energy spectrum of the individual atoms. We will hardly influence the behavior of our B.E. system by assuming that the free-particle level spectrum is realized everywhere in the interior of the permitted energy bands. The small but physically important deviations from this spectrum in the vicinity of the discontinuities will be neglected in order to simplify the calculations. We denote by $\epsilon_i$ the discontinuity in the energy of a particle when crossing the boundary between the $i$th and $(i+1)$th Brillouin zone in wave-vector space. We will have the following distribution functions for our gas occupying a volume $V$ at temperature $T$ in the periodic potential field assumed to be

simple cubic with the spatial period $d$,

$$dn_{i+1}=\frac{V}{h^3}\frac{dp_x dp_y dp_z}{\exp\left(\alpha+\beta\epsilon_i+\beta(p_x^2+p_y^2+p_z^2)/2m\right)-1} \tag{29}$$

and the parameter $\alpha$ determined through the total number $N$ of the gas atoms will be given by

$$\begin{aligned} N&=\sum_{i=0}^{\infty}\int dn_{i+1} \\ &=\frac{V}{h^3}\sum_{i=0}^{\infty}\int_v \frac{dp_x dp_y dp_z}{\exp\left(\alpha+\beta\epsilon_i+\beta(p_x^2+\cdots)/2m\right)-1}, \end{aligned} \tag{30}$$

where $v$ is the fundamental volume in momentum space associated with each Brillouin zone. It is clear that $\epsilon_0$ is zero, and that $v$ is the volume $h^3/d^3$; the volume associated with the first zone being that of a cube centered at the origin of momentum space. In order to simplify further the calculations without reducing the generality of the discussion it will be assumed that there are but two zones, the first and the second, and from then on the particles may be regarded as being completely free. A simple calculation shows then that the condensation temperature of the system in this periodic field is the root $T_f$ of the equation

$$1=\left(\frac{T_f}{T_0}\right)^{\frac{3}{2}}\frac{F(\alpha=0,\ \epsilon_1/kT_f,\ \epsilon_2/kT_f,\ h/d(2mkT_f)^{\frac{1}{2}})}{F(0)}, \tag{31}$$

where $F(\alpha, \epsilon_1/kT, \cdots)$ generalizes the often-met $F$ functions associated with the free-particle continuous spectrum, and $T_0$ is the transition temperature of the free gas with the same concentration in absence of the field. Since $F(\alpha, \epsilon_1/kT, \cdots)\lesseqgtr F(\alpha)$ for all $\alpha$, $T_f$ must be necessarily larger than $T_0$.

The average energy of the gas will now be given by

$$E_-=\frac{3}{2}\frac{V}{h^3}(2\pi mkT)^{\frac{3}{2}}kTG\left(0,\frac{\epsilon_1}{kT},\frac{\epsilon_2}{kT},\frac{h}{d(2mkT)^{\frac{1}{2}}}\right);\quad T<T_f; \tag{32}$$

$$E_+=\frac{3}{2}\frac{V}{h^3}(2\pi mkT)^{\frac{3}{2}}kTG\left(\alpha,\frac{\epsilon_1}{kT},\cdots\right);\quad T>T_f; \tag{33}$$

where $G(\alpha, \epsilon_1/kT, \cdots)$ generalizes the function $G(x)$ associated with the free-particle continuous spectrum. The explicit expressions of these more general $F$ and $G$ functions are somewhat complicated and will not be given here. A simple glance on the forms of $E_-$ and $E_+$ indicates that here too the order of the transition will depend on the value of $(d\alpha/dT)_{T_f}$ since the heat capacities $(dE_-/dT)_{T_f}$ and $(dE_+/dT)_{T_f}$ differ only by a term proportional to $(d\alpha/dT)_{T_f}$. One can show now without difficulty that this derivative and, therefore, $\Delta C_v$ vanish at the transition temperature. The band structure of the individual energy spectrum with the free-particle level density does not change the nature of the transition from that existing with the completely free B.E. gas. This result is due to the fact that around the origin of the momentum space, inside the volume corresponding to the first Brillouin zone, the atoms behave as free particles. It is clear that the approximation made in the expression of the energy and level density in the neighborhood of the energy discontinuities cannot affect qualitatively this result.

We should like finally to comment briefly on the B.E. transition in the limiting case of tight binding, i.e., of tightly bound B.E. particles in molecular periodic fields. The individual energy spectrum is formed now by a series of bands. One can show now that the condensation proceeds in this case also as in the more simple case of the free-particle approximation. However, the nature

of the transition will depend now on the level distribution near the bottom of the deepest energy band. In other words, the order of phase transition will depend now on the behavior of the bound B.E. particles around the origin of the first Brillouin zone.

## IV.

The above given discussion of B.E. systems, apart from its academic interest has been motivated by the possibility, pointed out by London,[2] that the curious transition observed in liquid helium might be connected to the B.E. condensation phenomenon. On the basis of the preceding study it appears possible to make a few remarks on any model of liquid helium founded on a B.E. assembly which admits a distribution function.

As we have seen, it seems possible eventually to define such conditions where the B.E. condensation is accompanied by a discontinuity in the heat capacity. Neither the energy nor the entropy have anomalies in the cases we have considered. The anomaly in the heat capacity is connected to the fact that the derivative, with respect to the temperature, of the fundamental parameter $\alpha$ is finite at the transition point. Those quantities which do not depend on this derivative show no anomaly at the transition temperature.

A model reproducing almost quantitatively several features of liquid helium, under its saturated vapor pressure, has been devised recently by London.[3] In order to get the observed discontinuity in the heat capacity it was assumed that the helium atoms, although having their energy proportional to the square of their momentum, had a level density which was proportional to a power of their momentum higher than two. Apart from the difficulty which might exist in any attempt to justify the association of such a level density to practically free-particle energies, there are two remarks which can be made about such models.

First, the model in question has left out of account the physical condition which must be fulfilled by any B.E. gas model, namely, that for high energies the particles will necessarily behave practically as free particles, and at such energies the level density must become equal to that of free particles.

The second remark concerns the preceding model as well as any other similar model. This can be formulated as a proposition which can be proved easily. The proposition in question is the following: Consider any B. E. system in which it is possible to define in a non-ambiguous way a distribution function. The condensation temperature of such a system will always vary in the same direction as the total number of particles, the concentration, the density or the pressure of the system. The derivative, with respect to the temperature, of the functions representing these physical quantities are always positive along the transition curve for such B.E. systems. The proof of this proposition is quite simple and will be omitted here.

This characteristic behavior of such B.E. systems contrasts strikingly with that observed in liquid helium where the mentioned physical quantities vary in opposite direction to the temperature along the transition or lambda line. One is therefore led to the conclusion that investigations of non-ideal B.E. systems are necessary. In such systems no individual level spectrum and no distribution function can be defined anymore. It seems that as long as the B.E. condensation in such non-ideal assemblies is not known, the question of the possibility of connection between the transition observed in liquid helium and the B.E. condensation phenomenon remains entirely open.

[3] F. London, J. Phys. Chem. **43**, 49 (1939).

# On the Polymerization of Ethylene and Propylene by Free Alkyl Radicals

OTTO BEECK AND F. F. RUST
*Shell Development Company, Emeryville, California*

(Received April 4, 1941)

Methyl- and ethyl-induced polymerizations of ethylene and propylene were carried out in static, as well as flow experiments. The latter allowed collection of enough reaction products for analysis by low temperature distillation. Efficiency of polymerization in propylene is much lower than in ethylene which is explained by the easy formation of allyl radicals. Analyses of the reaction products readily indicate that the polymer is formed by the successive addition of olefin molecules to radicals, that chain transfer through radical decomposition takes place, and that the chains are terminated by disproportionation or association of two radicals.

THE recent continued interest in free radical reactions[1] has prompted us to publish and discuss these data on the polymerization of ethylene and propylene by organic free radicals which were obtained several years ago and which appear to be of considerable interest in the light of recent publications in this field.

## Apparatus and Experimental Methods

Both static and flow experiments were carried out. For static experiments a bulb (100 cc) was immersed in a well-stirred molten salt bath of the required temperature, and pressure changes with respect to time were taken by means of a Bourdon gauge, the volume of which was small as compared to the volume of the bulb. To eliminate the effect of temperature changes on the gauge it was maintained at constant temperature in a glass jacket through which water was circulated. Ethylene, propylene, and all polymerizing agents were freed of dissolved oxygen by solidifying or liquefying them with liquid air, distilling off a part of the material under vacuum, and using the center cut for the experiments.

In the flow experiments the olefin was run through a flow meter, a drying tube, and into an evaporator containing either tetramethyl or tetraethyl lead. The temperature of the evaporator bath was so regulated that the desired quantity of lead alkyl was carried by the olefin into the preheater and furnace. The reactor was a Pyrex tube about 30 cm long. In preliminary runs the diameter was varied widely in order to detect possible effects of the wall but no influence was observed. The exit gases passed through tightly packed glass wool to remove lead; the polymers were condensed in traps cooled by a $CO_2$-alcohol mixture; and in most cases the remaining gases were vented.

## Experimental Results

The static method was used mainly to investigate the relative efficiency of a great number of polymerizing agents. Of particular interest is the greater ease of the free-radical-induced polymerization of ethylene as compared with that of propylene.[2] Figure 1 shows the polymerization of ethylene and propylene by lead tetramethyl in which the decrease of pressure is plotted against time. The experiments were started slightly below atmospheric pressure.

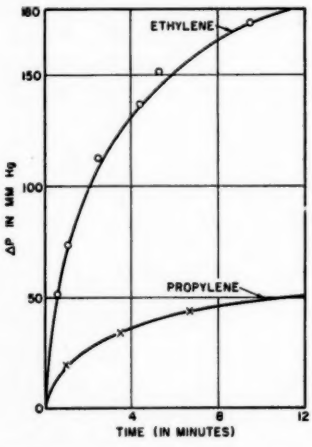


FIG. 1. Methyl-induced polymerization of ethylene and propylene (7 mole percent $Pb(CH_3)_4$ at 354°C).

[1] J. C. Jungers and L. M. Yeddanapalli, Trans. Faraday Soc. **36**, 483 (1940); H. S. Taylor and J. O. Smith, Jr., J. Chem. Phys. **8**, 543 (1940).

[2] See also F. O. Rice and E. Teller, J. Chem. Phys. **6**, 489 (1938) who mention unpublished work by D. V. Sickman.

TABLE I.

| EXP. NO. | REACTION | TEMP. °C | GAS FLOW LITERS/HR. | LEAD ALKYL MOLE % | $CH_3$ OR $C_2H_5$ CONSUMED G/HR. | WEIGHT OF PRODUCT G/HR. | MOLES OF OLEFIN COMBINED PER MOLE OF RADICAL USED |
|---|---|---|---|---|---|---|---|
| 1 | $Pb(CH_3)_4$ | 450 | 6.6 | 1.97 | 0.32 | 1.41 | 1.8 |
| 2 | in $C_2H_4$ | 450 | 6.6 | 4.06 | 0.67 | 2.17 | 1.2 |
| 3 | $Pb(C_2H_5)_4$ | 400 | 6.6 | 0.5 | 0.16 | 0.40 | 1.6 |
| 4 | in $C_2H_4$ | 400 | 6.6 | 1.5 | 0.48 | 1.04 | 1.2 |
| 5 | $Pb(C_2H_5)_4$ | 400 | 7.5 | 0.5 | 0.18 | 0.34 | 0.6 |
| 6 | in $C_3H_6$ | 400 | 7.5 | 1.6 | 0.58 | 0.82 | 0.3 |

Polymerization reactions of this type do not lend themselves readily to a theoretical treatment on the basis of experimental reaction rates and yields because the different stages in the polymerization need the postulation of hypothetical steps which, preferably, should be verified experimentally. For this reason detailed knowledge of the reaction products appears to be of interest. Since relatively large quantities of reaction products were needed for analysis by Podbielniak distillation, the flow method described above was adopted. The temperatures were chosen as low as was compatible with complete decomposition of the lead alkyls used. An analysis from an experiment using 4.06 mole percent lead tetramethyl showed 0.1 g of lead remaining in the product from 38.2 g lead alkyl consumed, showing the lead alkyl was practically completely decomposed. The conditions of this particular experiment were considered the most likely to show undecomposed lead compounds.

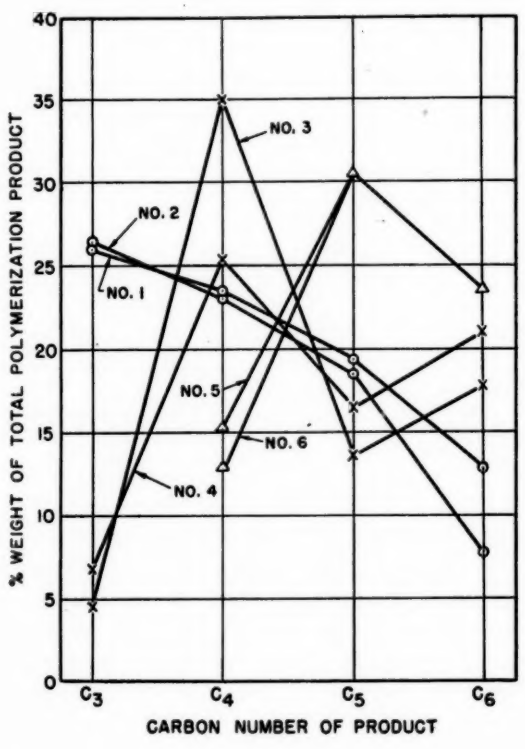


FIG. 2. Analysis of polymerization products (paraffins +olefins). For type of reaction see corresponding numbers in Table I.

Table I gives 6 representative experiments. The relative effectiveness of the lead compound in each experiment is denoted by the net moles of olefin combined per mole of radical consumed. It is seen that this yield drops off considerably for higher radical concentrations and that the yield is higher in polymerizations induced by methyl radicals than by ethyl radicals. As in the static experiments with methyl radicals the yield obtained with ethyl radicals in the polymerization of propylene is low as compared with the ethylene polymerization.

The analyses of the reaction products heavier than the gases to be polymerized are shown in Fig. 2. The fractions are plotted in percent of total polymerization product against the carbon number of the fractions. In Fig. 3 the analytical results of the methyl-induced ethylene polymerization (Exp. 1 and 2) are split up into paraffins and olefins. In Fig. 4 the same is done for the ethyl-induced ethylene polymerization (Exp. 4) and in Fig. 5 for the ethyl-induced propylene polymerization (Exp. 6). Some further segration is given in the figures. In one case—the ethyl-induced ethylene polymerization—a careful analysis of the gases not condensed in the $CO_2$ traps gave no hydrogen and only relatively small amounts of methane and ethane.

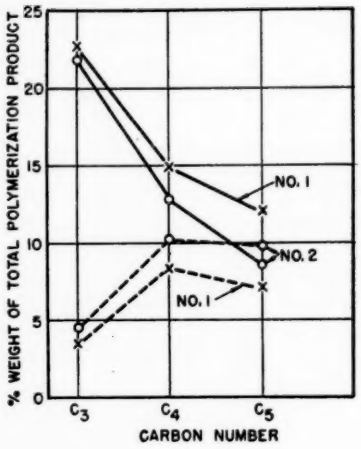


FIG. 3. Analysis of products of methyl-induced ethylene polymerization (—— olefin, - - - - - paraffin).

## DISCUSSION

The strikingly low polymerization efficiency of both methyl and ethyl radicals in propylene as compared to that in ethylene is at once explained in the light of recent experiments by H. S. Taylor and J. O. Smith.[1] These investigators have measured the methane formation in the interaction of methyl radicals with propylene and find the surprisingly low activation energy of 3.1 kcal. for this process—the lowest activation energy found in any of their studies with hydrocarbons. The relatively very low yield of methane and ethane during the ethylene polymerization in our experiments, together with earlier observations[3] that a much smaller methane formation obtains from reactions of methyl radical with ethylene than with saturated hydrocarbons, suggests strongly that in our case the polymerizing radical chain (to be discussed below) in propylene may easily be broken by methane and ethane formation leaving an allyl radical.* The allyl radical having resonance characteristics and an estimated resonance energy of 15.4 kcal. would have a long life and would mainly disappear by collision with itself or other radicals, the latter having a net effect of breaking two radical chains. It is for these reasons that the interaction of methyl and ethyl radicals with ethylene leads more easily to the formation of higher alkyl radicals. The analysis of the reaction products readily indicates that the polymer is formed by successive additions of the olefin molecule to radicals through a bimolecular reaction of the type

$$CH_3+C_2H_4\rightarrow C_3H_7,$$
$$C_3H_7+C_2H_4\rightarrow C_5H_{11}\text{ - - - -}.$$

The fact that most of the polymer is of low carbon number and that the products of low molecular weight contain more olefins than paraffins shows that the formation of larger radicals is mainly interrupted by decomposition of the radicals into olefins and smaller radicals, i.e., by chain transfer through radical decomposition. Other experimental evidence to this effect is found in a paper by Paneth and Lautsch[4] where the preparation of free propyl and free butyl were attempted by decomposition of tetra-*n*-propyl lead and tetra-isobutyl lead at 400°C and 300°C, respectively. Methyl radicals only were detected in both cases and the conclusion was drawn that free propyl and butyl were formed transiently, but very rapidly decomposed into ethylene and methyl or propylene and methyl. F. O. Rice and K. K. Rice in their monograph on free radicals[5] also assume in general that larger radicals break down very readily into smaller radicals and compounds containing a double bond. It is seen from experiments of Frey and Hepp[6] that about $\frac{3}{4}$ of the butyl radicals formed by decomposition of di-*n*-butyl mercury at 490°C decompose accord-

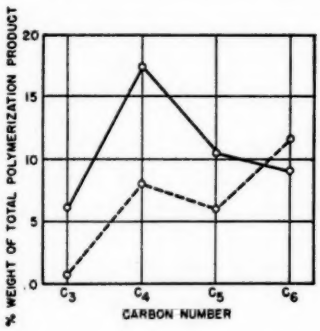


FIG. 4. Analysis of products of ethyl-induced ethylene polymerization (—— olefin, - - - - - paraffin). 17.3 percent $C_4H_8$=0.3 percent iso-$C_4H_8$+16.3 percent *n*-$C_4H_8$+0.7 percent 1,3-butadiene.

[3] H. S. Taylor and J. C. Jungers, Trans. Faraday Soc. **33**, 1353 (1937).

* Recent mass spectrographic studies in these laboratories by Mr. G. C. Eltenton on the interaction of alkyl radicals and olefins have shown the above formation of the allyl radical for the first time in a direct manner. This mass spectrographic work will be published in the near future.

[4] Paneth and Lautsch, J. Chem. Soc., p. 380 (1935).

[5] F. O. Rice and K. K. Rice, *The Aliphatic Free Radicals* (The Johns Hopkins Press, 1935).

[6] Frey and Hepp, J. Am. Chem. Soc., **55**, 3357, 1933; (see reference 5, p. 65).

ing to the equation:

$$C_4H_9 \rightarrow C_2H_4 + C_2H_5.$$

From the distribution of the products in the reaction between ethylene and ethyl radicals (Exp. 3) we must deduce that this and similar reactions leading to butylene or hexylene formation occur simultaneously with reactions leading to propylene and amylene and $CH_3$ radicals.

The paraffins must be formed either by disproportionation or by association of the radicals, i.e., by chain termination, for instance,

$$2C_4H_9 \rightarrow C_4H_8 + C_4H_{10}$$
$$2C_4H_9 \rightarrow C_8H_{18}.$$

The decomposition of an alkyl radical into a hydrogen atom and an olefin, which has been frequently suggested, does not take place since no trace of hydrogen has been found in our reaction products.

Characteristic of the three types of polymerization performed is the fact that the efficiency increases with decreasing amounts of radicals. This is easily understood because there is less chance for two radicals to be eliminated by reaction with each other to form stable molecules, a process which furthermore is energetically (dissipation of reaction energy) less favorable for methyl than for ethyl radicals. This

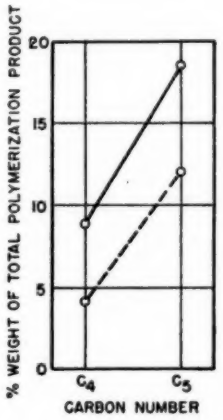


FIG. 5. Analysis of products of ethyl-induced propylene polymerization (——— olefin, – – – – paraffin). 8.9 percent $C_4H_8$ = 2.3 percent iso-$C_4H_8$ + 6.6 percent $n$-$C_4H_8$.

may account for the latter's lower efficiency. Finally, it is of interest to note that in the reaction of ethyl radicals with propylene 35 percent of the butylene formed is isobutylene. Unquestionably the only major reaction leading to its formation must be:

$$C_3H_6 + C_2H_5 \rightarrow \text{iso } C_5H_{11} \rightarrow \text{iso } C_4H_8 + CH_3.$$

This is in sharp contrast to the reaction of propylene with HBr for which a chain mechanism with bromine atom as carrier[7] has been generally accepted and where the bromine atoms almost exclusively go to the end position.

[7] M. S. Kharasch, H. Engelmann and F. R. Mayo, J. Org. Chem. **2**, 288, 400, 577 (1937); F. R. Mayo and C. Walling, Chem. Rev., **27**, 372 (1940).

# Letters to the Editor

*THIS section will accept reports of new work, provided these are terse and contain few figures, and especially few halftone cuts. The Editorial Board will not hold itself responsible for opinions expressed by the correspondents. Contributions to this section should not exceed 600 words in length and must reach the office of the Managing Editor not later than the 15th of the month preceding that of the issue in which the letter is to appear. No proof will be sent to the authors. The usual publication charge ($3.00 per page) will not be made and no reprints will be furnished free.*

## Statistical Thermodynamics of Several Halomethanes

WALTER F. EDGELL AND GEORGE GLOCKLER
*Department of Chemistry, State University of Iowa, Iowa City, Iowa*
April 16, 1941

THE heat capacities of methyl fluoride and methyl iodide at several temperatures have been calculated to the rigid rotator simple harmonic oscillator approximation in connection with another problem. Inasmuch as they do not appear elsewhere in the literature it was felt worth while to present them here.

The fundamental frequencies are well known and appear in Table I together with those of $CH_2Br_2$ as discussed below. The value 2916 $cm^{-1}$ is the mean of the resonating frequencies 2862, 2965 and 2860, 2971 appearing in methyl fluoride and methyl iodide, respectively. Linnett[1] has used the values 2862 and 2940 in calculating force constants for these molecules, but it appears more probable that the unperturbed fundamental lies closer to the mean. The heat capacities are given in Table II. Entropies at 298.1°K have also been calculated and appear in Table III. Moments of inertia used were those given by Dennison.[2] The standard state is the usual one of unit fugacity and zero pressure. Corrections to finite pressures have been adequately discussed.[3,4a]

When the heat capacities of $CH_3Cl$, $CH_2Cl_2$ and $CHCl_3$[4] (in the temperature range $T=298.1$ to 600°K) are plotted against log $T$, the resulting curves are nearly parallel. They may be brought into near superposition by shifting the temperature scale for each substance, i.e., plotting

TABLE I. *Fundamental frequencies.*

| $CH_3F$* | $CH_3I$* | $CH_2Br_2$*,‡ |
|---|---|---|
| 2987 (2)** | 3074 (2) | 3060 |
| 1476 (2) | 1445 (2) | 2988 |
| 1200 (2) | 885 (2) | 1390 |
| 2916 (1) | 2916 (1) | 1183 |
| 1460 (1) | 1252 (1) | 1090 |
| 1048 (1) | 532 (1) | 806 |
| | | 636 |
| | | 576 |
| | | 174 |

* H. Sponer, *Molekülspektren* (J. Springer, Berlin, 1935).
** Values in parenthesis are the degeneracies.
‡ See reference 6 of text.

TABLE II. $C^\circ_p$ *for several halomethanes.*

| $T$ | $CH_3F$ | $CH_3I$ | $CH_2Br_2$ |
|---|---|---|---|
| 298.1°K | 8.95* | 10.55 | 13.15 |
| 350 | 9.72 | 11.48 | 14.20 |
| 373.1 | 10.09 | 11.88 | 14.66 |
| 400 | 10.55 | 12.34 | 15.14 |
| 473.1 | 11.80 | 13.53 | 16.34 |
| 500 | 12.25 | 13.91 | 16.70 |
| 600 | 13.83 | 15.29 | 17.96 |

* Units are cal./°K/mole.

TABLE III. $S^\circ_{298.1}$ *for several halomethanes.*

| $CH_3F$ | $CH_3I$ | $CH_2Br_2$ |
|---|---|---|
| 53.30 E.U. | 60.85 E.U. | 70.16 E.U. |

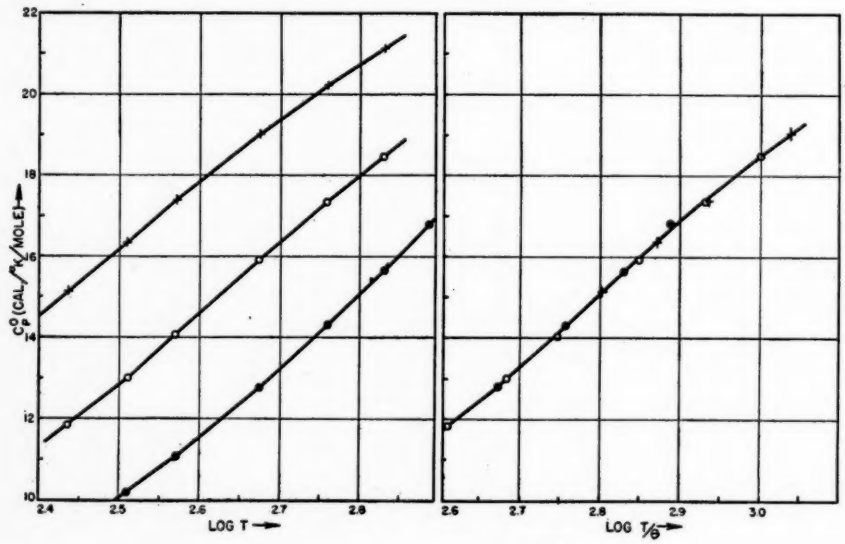


FIG. 1. Heat capacities of $CH_3Cl$, $CH_2Cl_2$, $CHCl_3$.[4a] + = $CHCl_3$; ○ = $CH_2Cl_2$; ● = $CH_3Cl$.

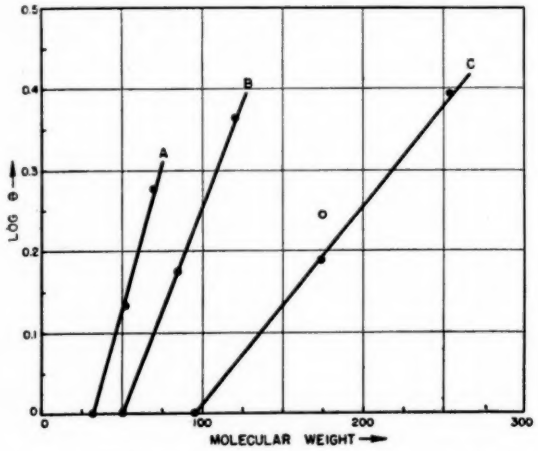


FIG. 2. Shift in temperature scale *vs.* molecular weight. *A*—$CH_3F$, $CH_2F_2$, $CHF_3$; *B*—$CH_3Cl$, $CH_2Cl_2$, $CHCl_3$; *C*—$CH_3Br$, $CH_2Br_2$, $CHBr_3$; O—$CH_2Br_2$, Stevenson and Beach.[4b]

$C^\circ_p$ against log $T/\theta$, where $\theta$ is a constant characteristic of each substance (see Fig. 1). If log $\theta$ is plotted against molecular weight, the three points lie on a straight line. This is shown in Fig. 2. The same thing is true of the corresponding fluorine compounds. However the heat capacity of $CH_2Br_2$, as calculated by Stevenson and Beach[4b] cannot be brought into superposition with that of $CH_3Br$ and $CHBr_3$—being too high at low temperatures and too low at high temperatures if the average value of $\theta$ is taken. This value of $\theta$ is designated by the clear circle in Fig. 2. Inasmuch as there is no question of the correctness of the fundamentals in these latter two molecules, it may be assumed that the fault lies with those of $CH_2Br_2$. Since the above calculations[4b] were made, Wagner's interesting normal coordinate treatment of the vibrations of the methylene halides has appeared.[5] Although this work still leaves some question as to the fundamentals in this class of compounds, it indicates that there is no room for five low-lying fundamentals in $CH_2Br_2$ as assumed by Stevenson and Beach. This is confirmed by calculations made in this laboratory. Therefore the most uncertain of these, 478 $cm^{-1}$, is deleted, and 1183 taken as the ninth fundamental. This frequency has been observed both in Raman and absorption spectra[6] and is not satisfactorily accounted for otherwise. With the fundamentals as given in Table I the calculated heat capacity of $CH_2Br_2$ is brought into superposition with those of $CH_3Br$ and $CHBr_3$ by the value of $\theta$ falling on the straight line *C* in Fig. 2. The heat capacity and entropy of methylene bromide appear in Tables II and III.

[1] J. W. Linnett, J. Chem. Phys. **8**, 91 (1940).
[2] D. M. Dennison, Rev. Mod. Phys. **12**, 175 (1940).
[3] P. Fugassi and C. Rudy, Jr., Ind. Eng. Chem. **30**, 1029 (1938).
[4] References to calculated heat capacities other than those from this note are from the following sources: (a) $CH_3Cl$, $CH_2Cl_2$, $CHCl_3$: R. D. Vold, J. Am. Chem. Soc. **57**, 1192 (1935). (b) $CH_3Br$ and $CHBr_3$: D. P. Stevenson and J. Y. Beach, J. Chem. Phys. **6**, 25 (1938). (c) $CH_2F_2$: G. R. Leader, "Studies in molecular structure," Ph.D. Thesis, University of Minnesota (1940). (d) $CHF_3$: George Glockler and W. F. Edgell, J. Chem. Phys. **9**, 224 (1941).
[5] J. Wagner, Zeits. f. physik. Chemie **B45**, 69 (1939).
[6] See references to spectra of this molecule tabulated by Ta-You Wu, *Vibrational Spectra and Structure of Polyatomic Molecules* (China Science Corp., Shanghai, 1939), p. 248.

## Thermodynamic Functions for Molecules with Internal Rotation

KENNETH S. PITZER AND WILLIAM D. GWINN
*Department of Chemistry, University of California, Berkeley, California*
April 12, 1941

SEVERAL years ago one of us[1] presented formulas and tables of thermodynamic functions for molecules with restricted internal rotation. The cosine function was assumed for the potential barrier. The treatment was based on Nielsen's[2] work on the quantum mechanics of two coaxial tops, and while not absolutely exact, it was a very good approximation for that case. It was presumed, on the basis of the classical approximation, that the results would probably be quite accurate for all molecules whose moments of inertia are independent of the angle of internal rotation. A molecule of this class may also be described as consisting of a rigid frame with an attached symmetrical top. We can now prove rigorously this more general applicability of the tables. In view of this development, we have decided to recalculate the tables with greater numerical accuracy, and to publish the new derivation with the new tables. The purpose of this communication is first to state the more general applicability of the old tables, and second to outline another, slightly less precise, derivation which is based on the detailed analysis of the quantum mechanics of such molecules presented recently by Crawford.[3]

Crawford's final formula is somewhat different from that used in computing the tables referred to above.[4] However, he introduced certain approximations which we shall attempt to remove. These approximations arose through the use, in correction terms, of quantities ($v$ and $a$ in the section "limiting values") calculated with harmonic oscillator or rigid rotation wave functions, instead of the exact Mathieu functions or linear combinations thereof. While it is not possible to obtain a simple final formula using exact correcting terms, it can be shown[5] that this final formula will depend only on the following independent variables: $T$, the potential barrier, $V$, the reduced moment of inertia $F$ or $I_r$, the number of potential peaks, $\nu$ or $n$, and the ratio of the reduced moment to top moment $\Omega$. If we can find the true partition function for some special case which includes all values of these variables we will have the problem solved simply and accurately. This is done by taking the case of two coaxial tops. Here $\Omega = I_1/(I_1+I_2)$ so that all values from 0 to 1 can be obtained. Likewise all values of the other variables are attainable in this special case. Since the tables[1] previously published were quite accurate for the case of two coaxial tops, we conclude that they are also quite accurate for the more general case of a rigid frame with an attached top. In the more general case Crawford's formula for the reduced moment of inertia should be used.

$$I_r = F = A\Omega = A\left[1 - \sum_{i=1}^{3} (A/I_i)\lambda_i^2\right].$$

Here the $I_i$'s are the three principal moments of inertia of the whole molecule, the $\lambda_i$'s are direction cosines between

the top axis and these principal axes, and $A$ is the moment of inertia of the top itself.

To summarize briefly, Crawford's analysis shows that the partition function does not change when one goes from the special case of two coaxial tops to the more general case of any rigid frame with one top. Therefore one may use the simple tables computed for the special case in the more general case. The problem of a frame with more than one attached top will be discussed in the paper to be published later.

This result affects the conclusions of a number of recent publications. The general recommendation of Wilson[6] that Crawford's formulas are more accurate is to be reversed. Insofar as the two methods differ, the new calculations of Crawford, Kistiakowsky, Rice, Wells and Wilson[7] on propylene are in error. Since we have believed that their conclusions were uncertain on other grounds,[8] we merely conclude that doubt remains. In Crawford's[9] calculations for methyl alcohol, the results based on his formulas should be discarded in favor of results from the tables which he also gives but dismisses as less accurate. This reduces, but does not remove, the discrepancy between the entropy calculated from the $470\pm40$ cm$^{-1}$ barrier proposed by Koehler and Dennison[10] and the experimental value. We may also note that Aston and Doty's[11] calculations on methyl amine may now be said to be based on accurate equations. Consequently one concludes that the torsional frequency in methyl amine is greater than the 270 cm$^{-1}$ value suggested by Owens and Barker.[12]

[1] K. S. Pitzer, J. Chem. Phys. **5**, 469 (1937).
[2] H. H. Nielsen, Phys. Rev. **40**, 445 (1932).
[3] B. L. Crawford, Jr., J. Chem. Phys. **8**, 273 (1940).
[4] For the extensively investigated case of ethane, Crawford's formula is a much poorer approximation that that used in computing the tables.
[5] This functional dependence can be verified easily for Crawford's final approximate formula, Eqs. (2–7), or for his accurate formula through the first order correction, Eqs. (41) and (42). To obtain this result accurately through the second-order correction, it is necessary to note that his quantity $(\mathbf{H}_2)^{t,\,t}$ will still be proportional to $\mathbf{p}_m^2$ but with a coefficient in general different from $-F_m/2$. This coefficient, however, will be a function of $V_m$, $\nu_m$, $F_m$, and $t$ only. One must carry out a transformation similar to that between the unnumbered equations at the top of p. 280, column 2. The desired result may then be verified without great difficulty.
[6] E. B. Wilson, Chem. Rev. **27**, 17 (1940).
[7] B. L. Crawford, Jr., G. B. Kistiakowsky, W. W. Rice, A. J. Wells and E. B. Wilson, Jr., J. Am. Chem. Soc. **61**, 2980 (1939); also J. Chem. Phys. **8**, 610, 970 (1940).
[8] K. S. Pitzer, Chem. Rev. **27**, 39 (1940).
[9] B. L. Crawford, Jr., J. Chem. Phys. **8**, 744 (1940).
[10] J. S. Koehler and D. M. Dennison, Phys. Rev. **57**, 1006 (1940).
[11] J. G. Aston and P. M. Doty, J. Chem. Phys. **8**, 743 (1940).
[12] R. G. Owens and E. F. Barker, J. Chem. Phys. **8**, 229 (1940).

## The Photovoltaic Effect

EDWARD ADLER
*Department of Chemistry, College of the City of New York, New York, New York*
April 12, 1941

THIS is in reply to a letter by H. M. Cassel about our papers[1] on this subject which appeared in the April, 1941 issue of this journal.

We do not wish to enter into a polemic on this subject, but we believe there are some statements in the letter which are not entirely valid, and which require an answer.

(1) The theory which we proposed for the photovoltaic or Becquerel effect enables one to derive a simple mathematical relation between light intensity and potential which is in agreement with the experimental light intensity/potential curve for small and medium light intensities. The term accounting for the photo-current, due to the transition of photoelectrons from the electrode to the electrolyte:

$$I_p=\epsilon k_3 J \tag{1}$$

(using our previous nomenclature) is *not* introduced *ad hoc* into an overvoltage equation, as Dr. Cassel's letter seems to imply, but follows naturally from the concept of a potential barrier.

The fact that our equations are similar to those encountered in the treatment of overvoltage means simply that similar processes are present in both phenomena, and that both problems can be treated by the method of absolute reaction rates.

(2) Our derived relation referred to above does not, indeed, without modification lead to the "saturation potential" at very high light intensities, which is experimentally found. We were, of course, well aware of this so-called "discrepancy" and suggested that it might be due to the fact that only a finite, limited number of photo-active centers were available for liberating photoelectrons.

Dr. Cassel believes that a "saturation potential" may be explained by the substitution for (1) of

$$I_p=\epsilon[A^+_{\text{ads}}]k_3' J, \tag{2}$$

and indicates that "It can easily be seen that with this correction the theory covers the whole range of the empirical curve." We do not believe that this can be at all easily seen, for if the substitution *is actually made* and the mathematical operations carried through, the result *is exactly the same* as the one which we found for medium light intensities, namely, $V_e=C+B\log J$.

(3) The fact is, of course, that the number of photo-active centers *is* finite and limited. This is not an assumption. It can be seen from data in the field of photo-conductivity, and also in dry, solid photo-cells in both of which a saturation current and a saturation photo-potential obtain. It seems to us that in the photovoltaic effect also, at very high light intensities, the limited number of photo-centers would make itself noticed in the form of a saturation effect. We might also indicate that in our paper we pointed out that a primary negative photo-e.m.f. could be explained by a mechanism into which $[A^+_{\text{ads}}]$ *does not enter* and which gives the same type of relation found for primary positive photo-e.m.f.

[1] E. Adler, "The photovoltaic effect," J. Chem. Phys. **8**, 500 (1940); "The photovoltaic effect," Trans. Electrochem. Soc. Preprint **79**, 6 (1940).